Experimental Study of the QGP with Soft Probes and Vacuum Baseline

Yen-Jie Lee

National Nuclear Physics Summer School

Institute for Nuclear Theory, Seattle, Washington

6 July 2026

MIT HIG group's work was supported by US DOE-NP

QCD Phase Diagram

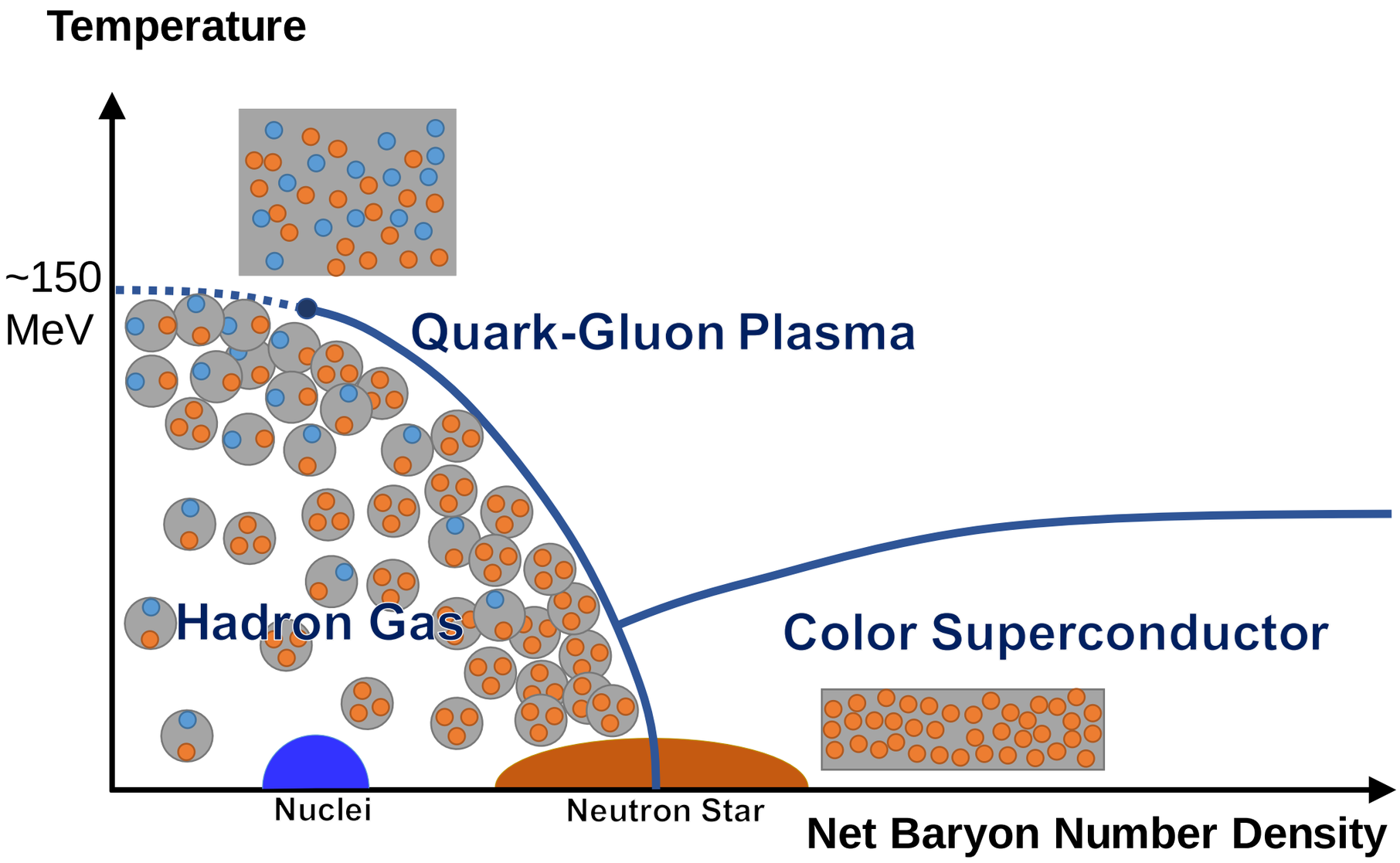

QCD Phase Diagram

Expansion of Early Universe

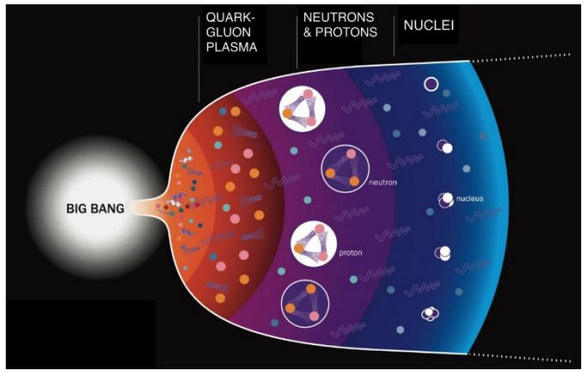

Neutron Star Formation

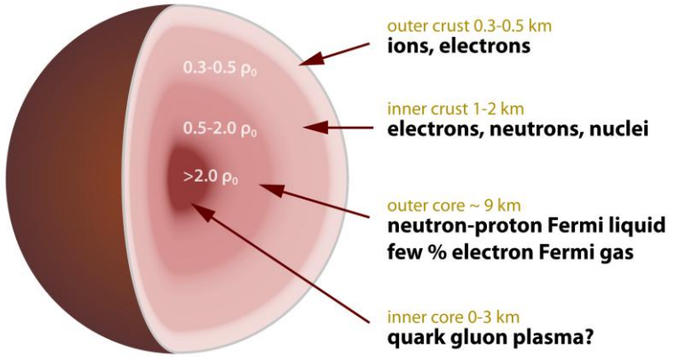

QCD Phase Diagram

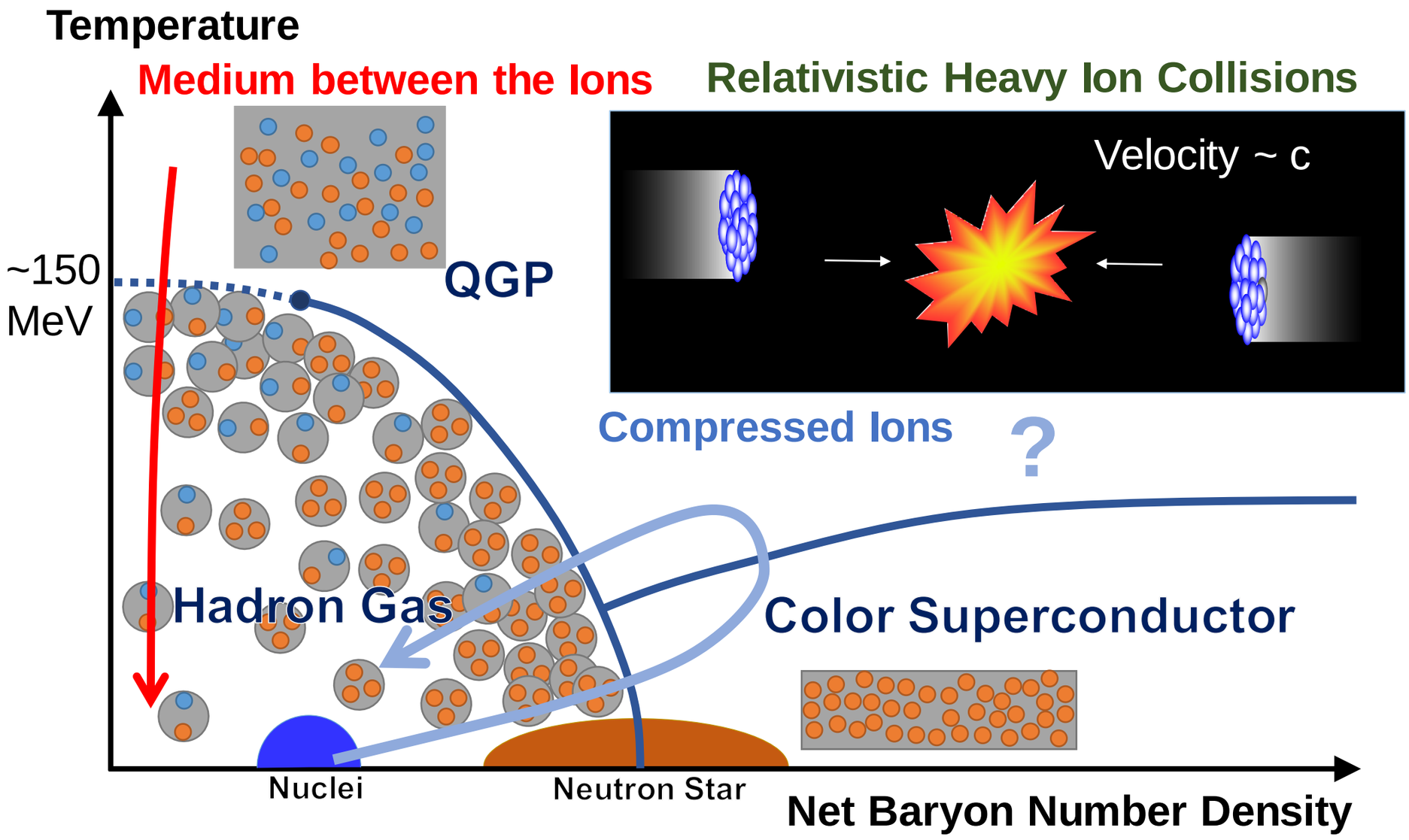

The First Dedicated Heavy Ion Collider

Relativistic Heavy Ion Collider

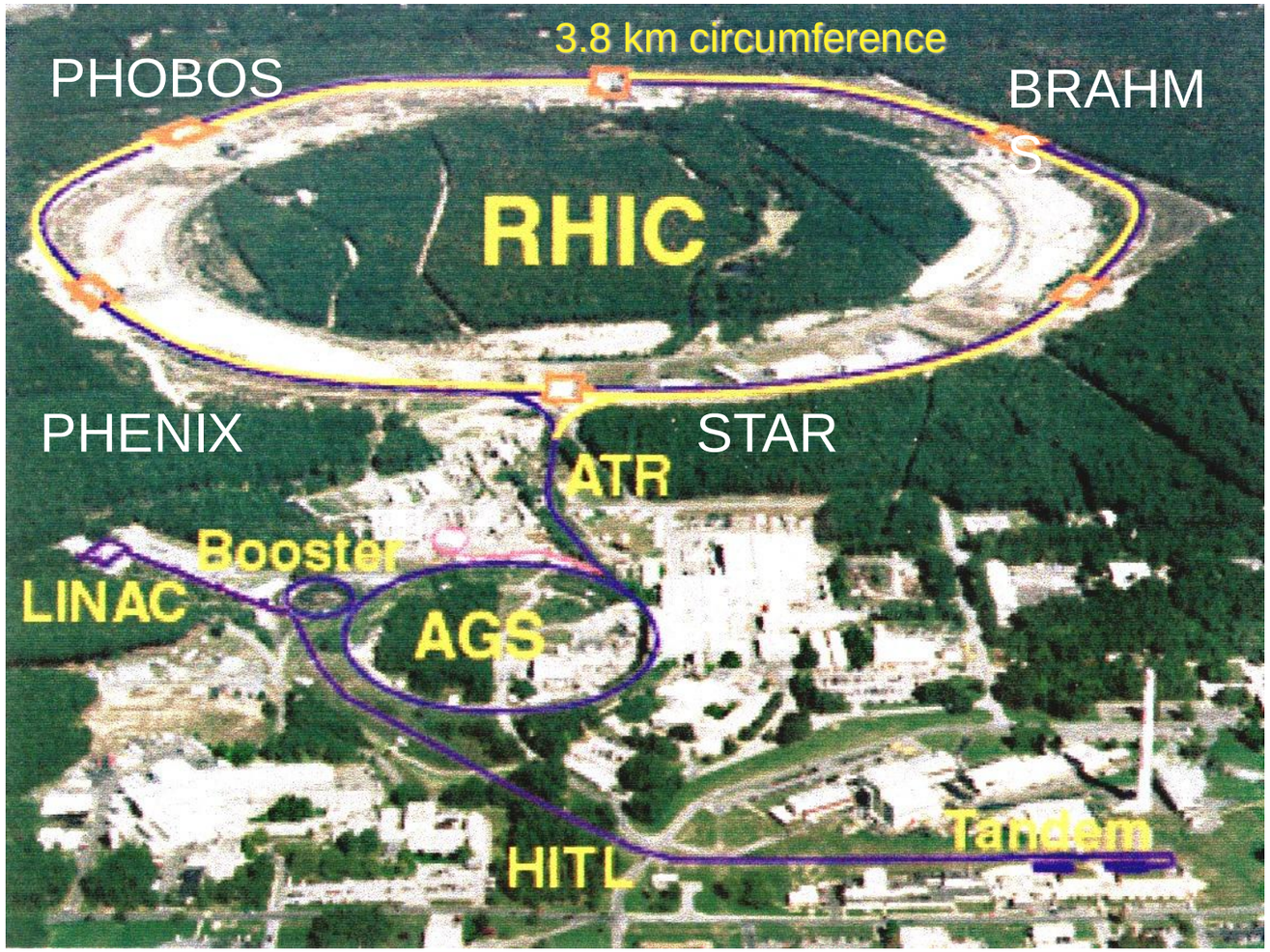

Au+Au
7.7 - 200 GeV

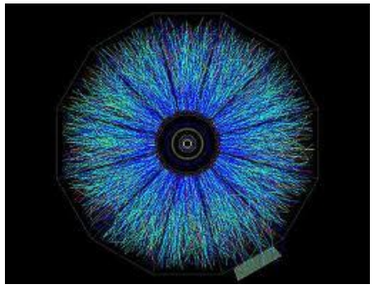

Since 2000~

sPHENIX Data-Taking 2023-26

Relativistic Heavy Ion Collider

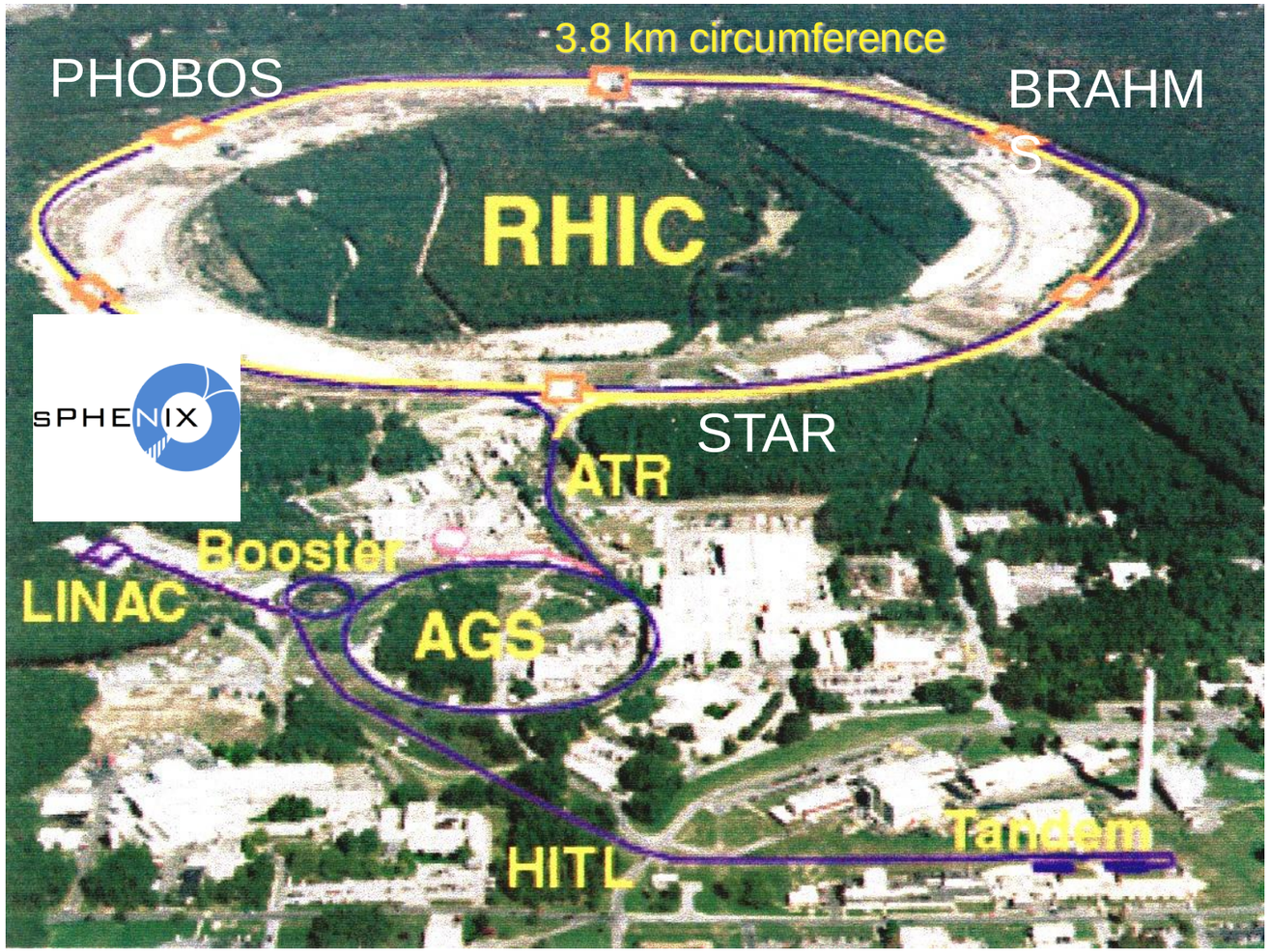

Au+Au

7.7 - 200 GeV

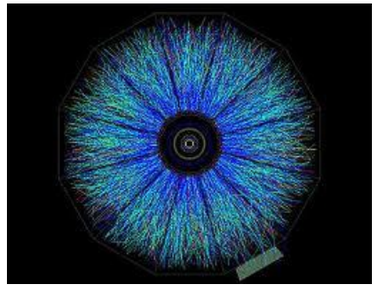

Since 2000~

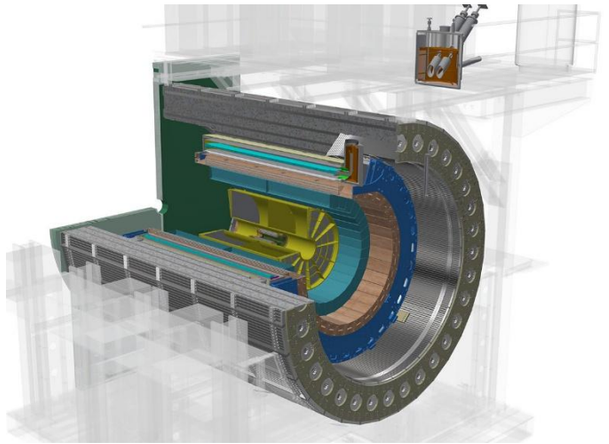

High Energy (Temperature) Frontier

Large Hadron Collider

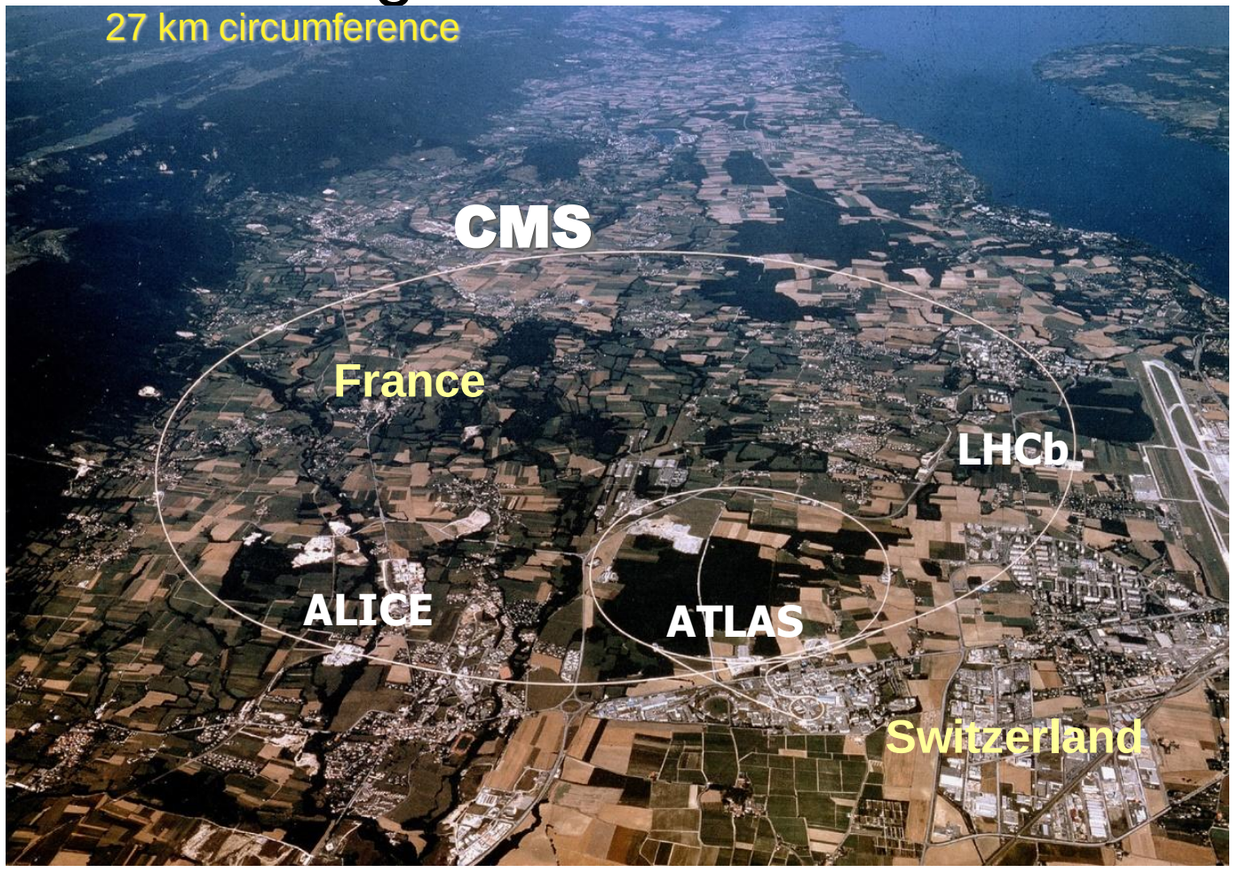

Lead-Lead (PbPb) collisions
2010-11: 2.76 TeV
2015-18: 5.02 TeV
2022-26: 5.36 TeV

ALICE

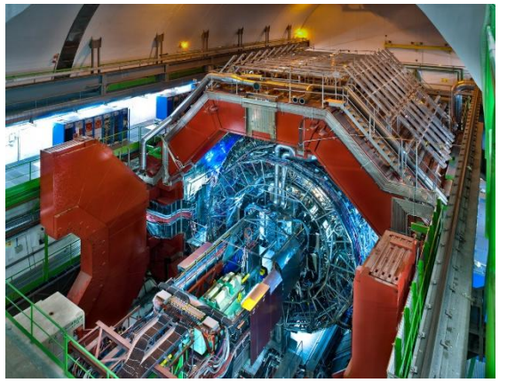

CMS

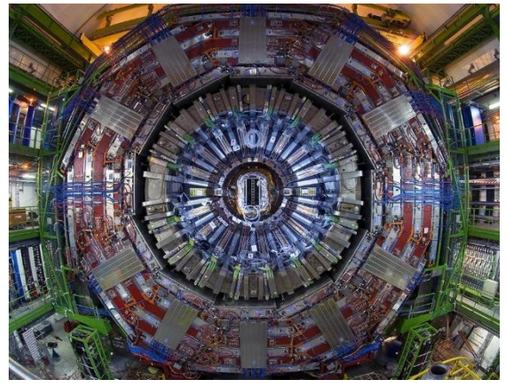

ATLAS

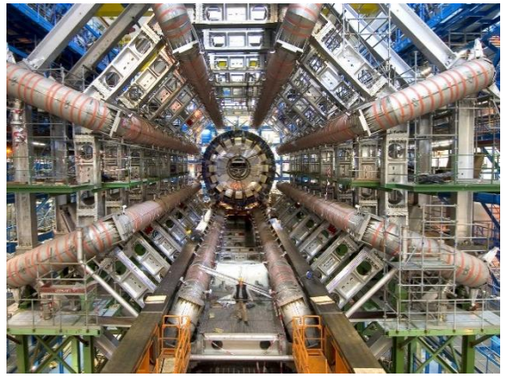

LHCb

Also smaller system data:
Proton-lead at 5.02 & 8.16 TeV
Xenon-Xenon at 5.44 TeV
Oxygen-Oxygen and **Neon-Neon** at 5.36 TeV

A flying mosquito has about 4 trillion electronvolts **(4TeV)** of energy

Particle Detection with CMS

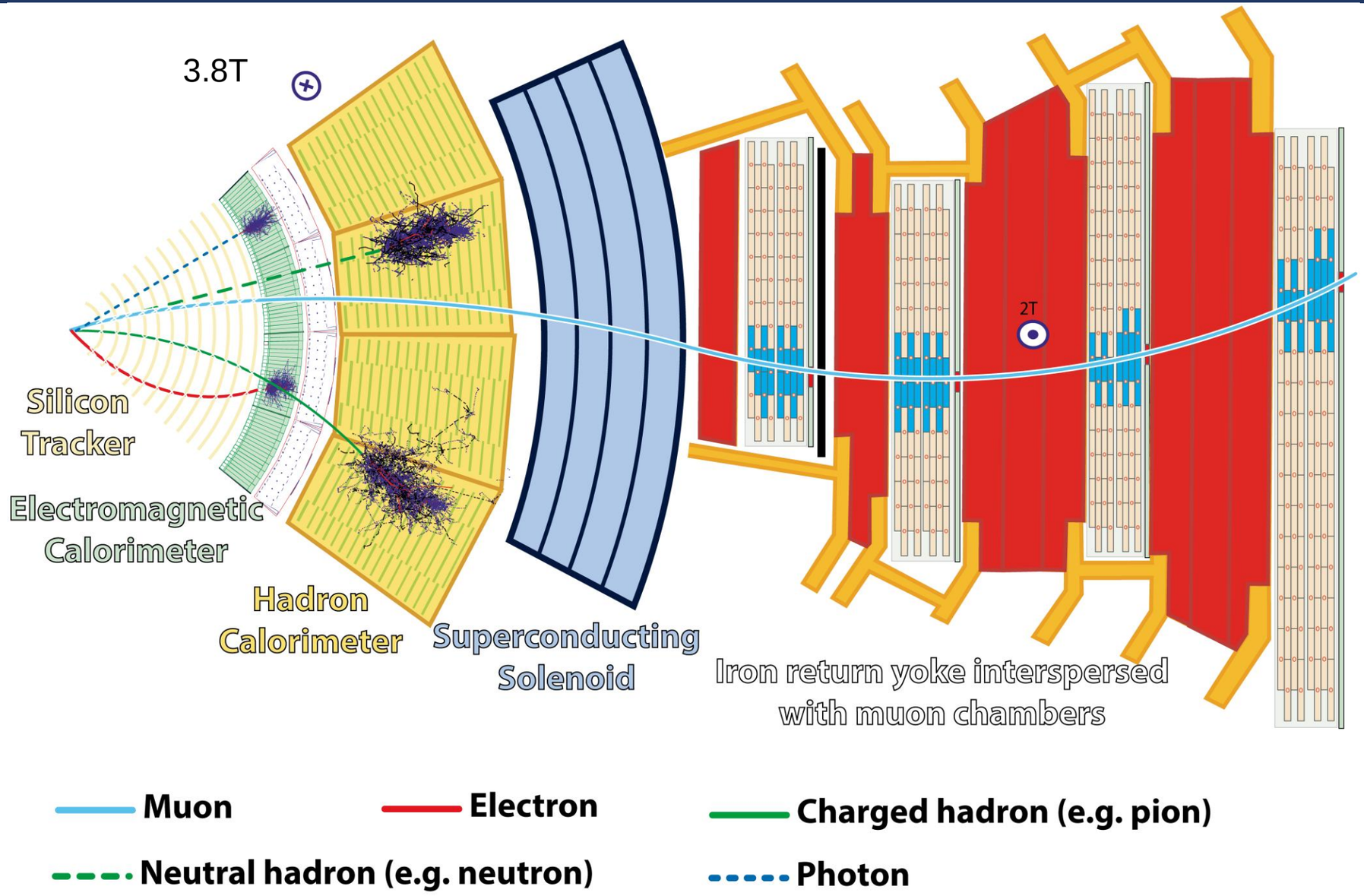

Proton-Proton Collision Recorded by CMS

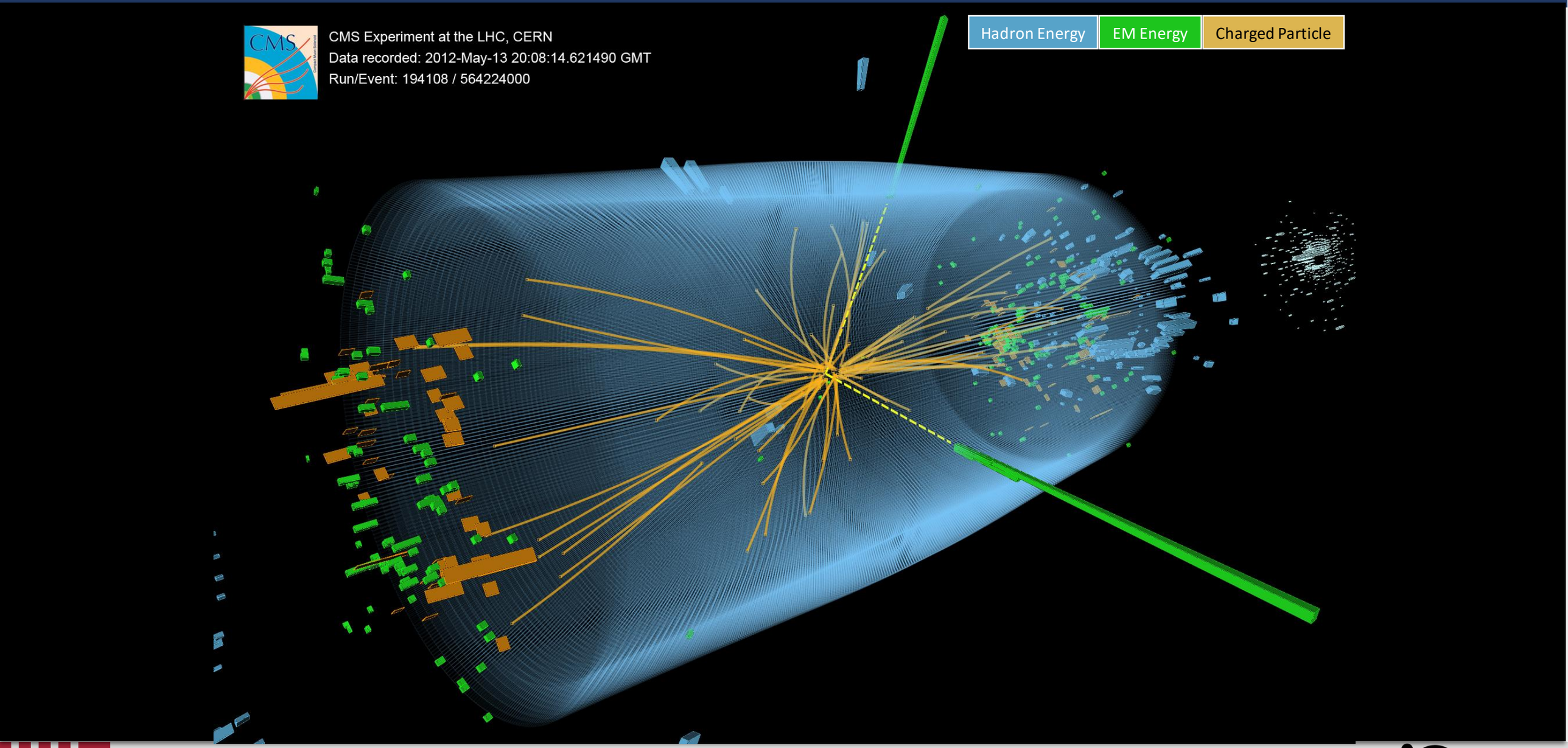

Lead-Lead Collision Recorded by CMS (2018)

CMS Experiment at the LHC, CERN
Data recorded: 2018-Nov-12 08:36:52.866176 GMT
Run / Event / LS: 326586 / 2491137 / 6

Hadron Energy | EM Energy | Charged Particle

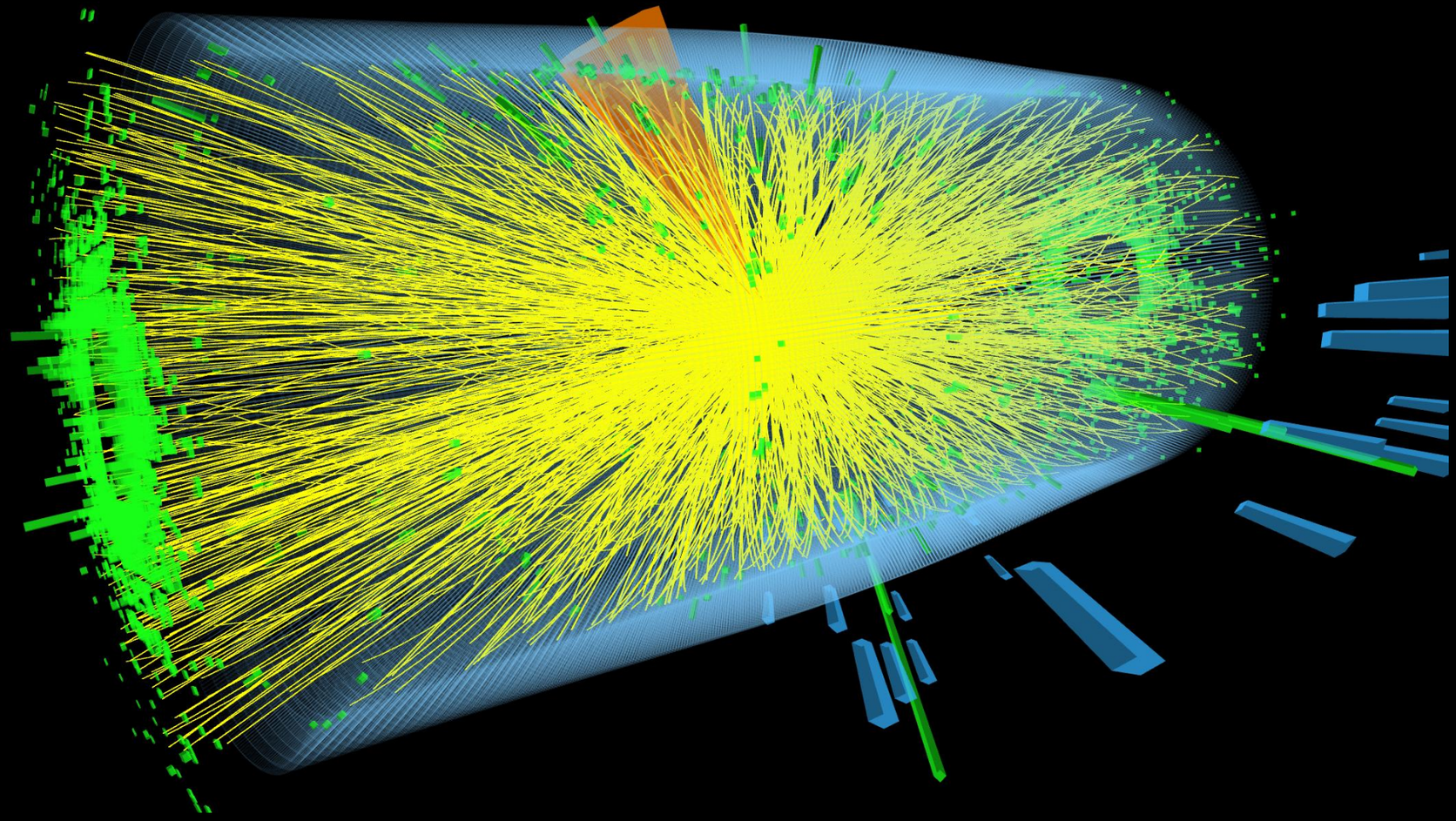

“Reconstruct” the QGP with Particle Detector

Size of the CMS detector

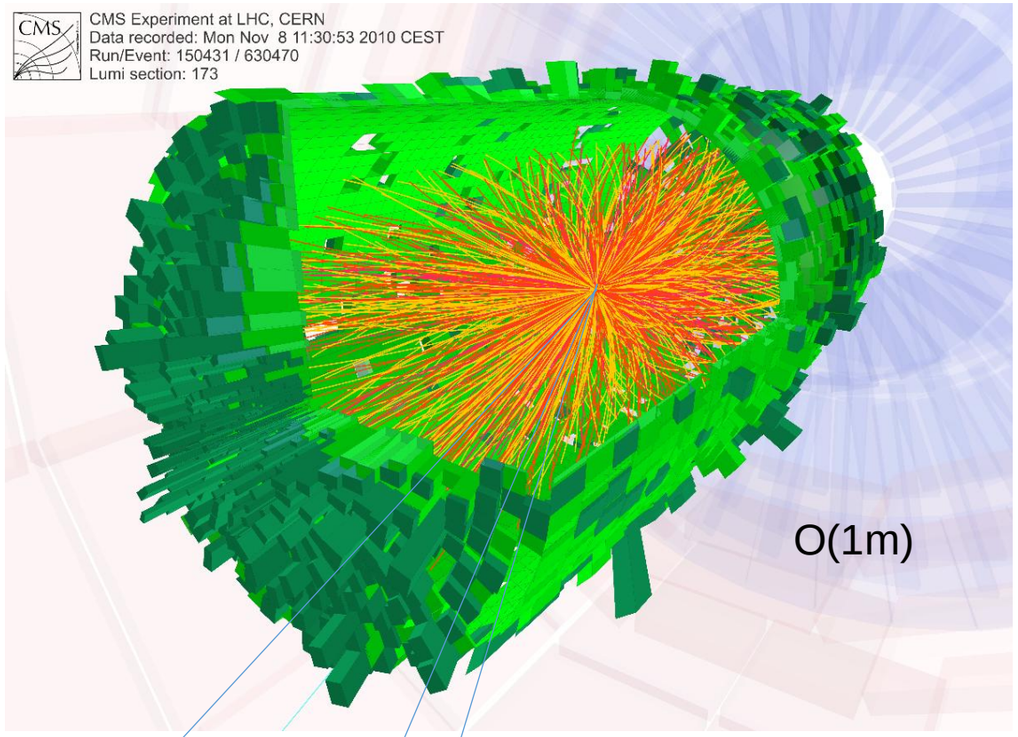

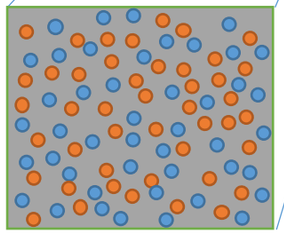

O(10^{-14} m)

Inner Structure of QGP

Size of the Universe

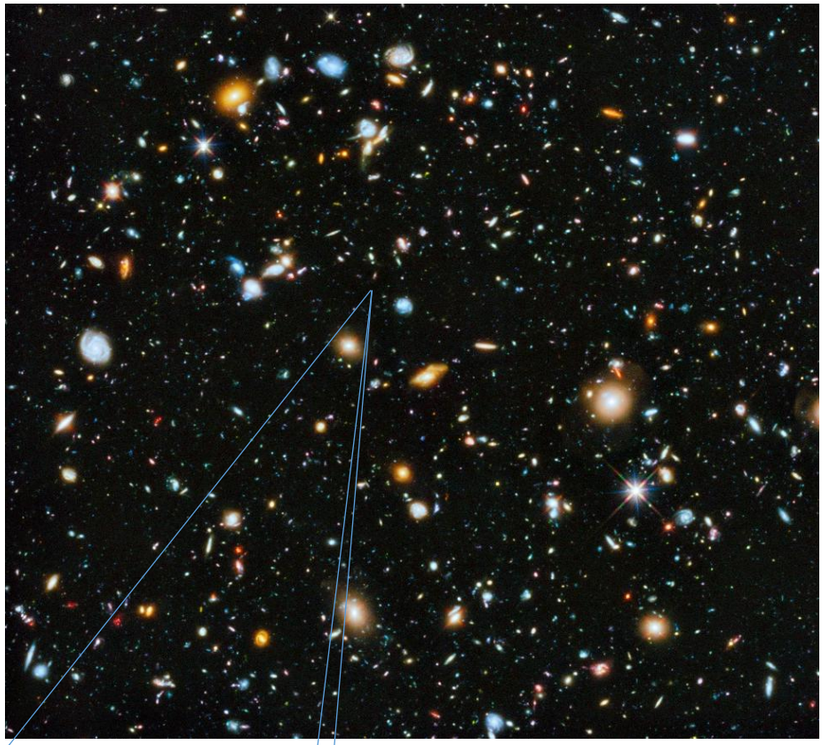

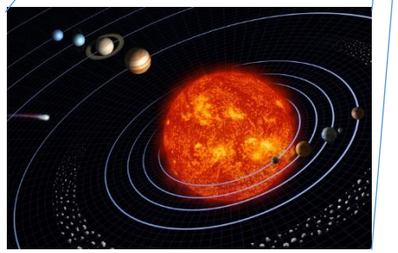

O(10^{27} m)

O(10^{13} m)

Inner Structure of Our Solar System

CMS event display

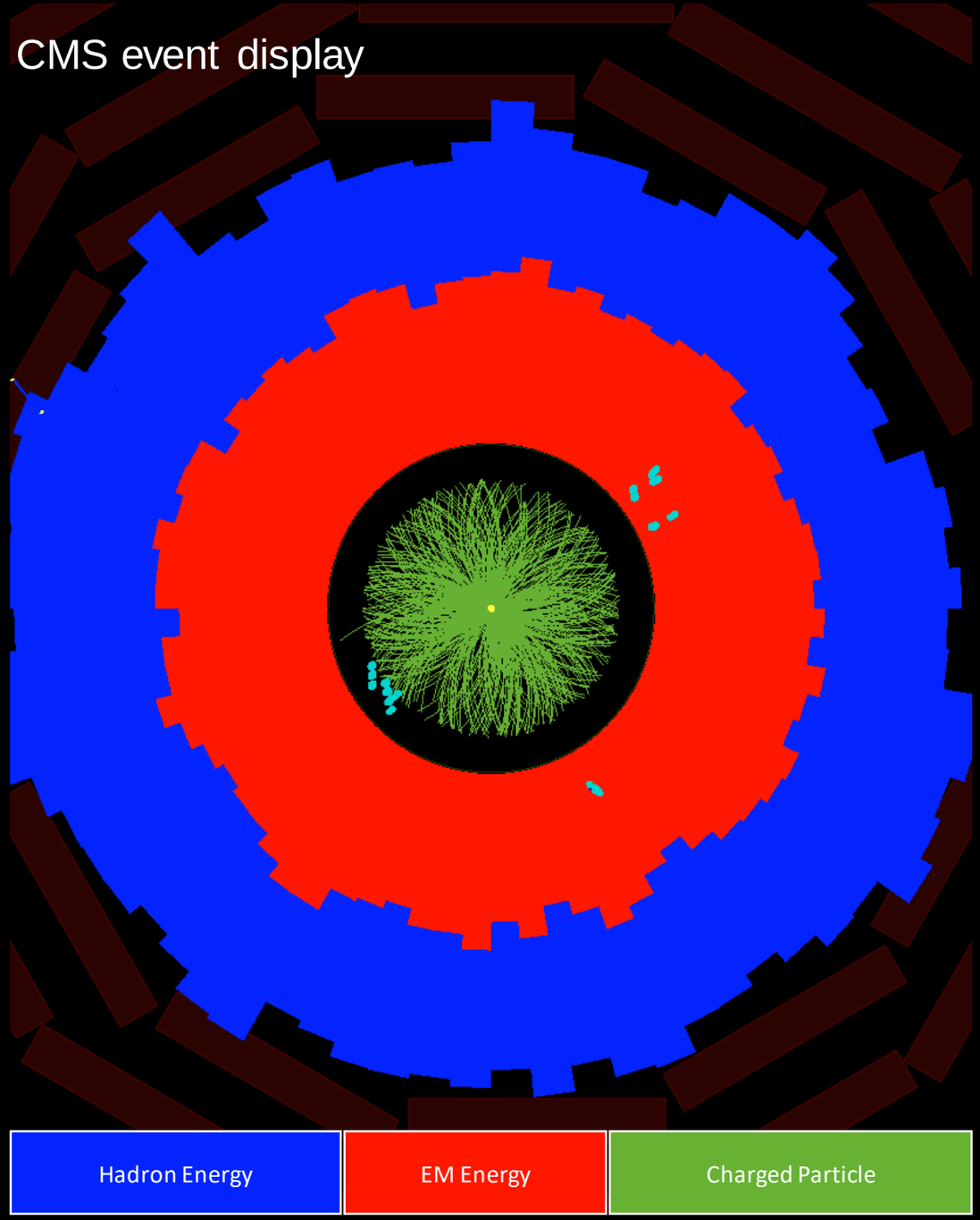

Initial Shape Before Expansion

Initial azimuthal anisotropic shape

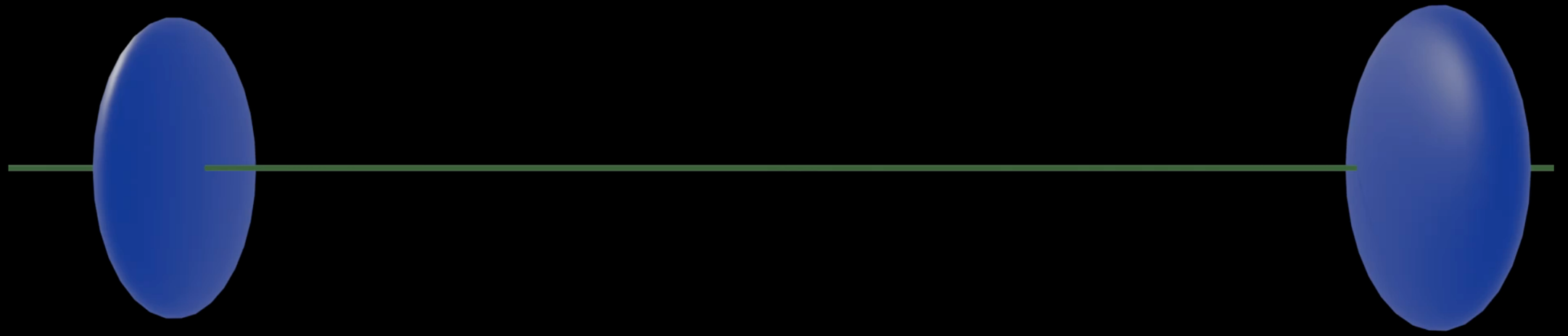

Animation from Jing Wang (MIT)

Centrality

- Need experimental access to the impact parameter **b** of the collision
- Idea: use observables that change **monotonically with b**, such as:
  - Forward calorimeter energy
  - Charged particle multiplicity (N_{ch}).
- Centrality classes: percentiles (fraction of total integral) of centrality distribution
- Convention:
  - 0% = "**most central**" (head-on!), b~0 (high N_{ch})
  - 100% = **most peripheral** (low N_{ch})

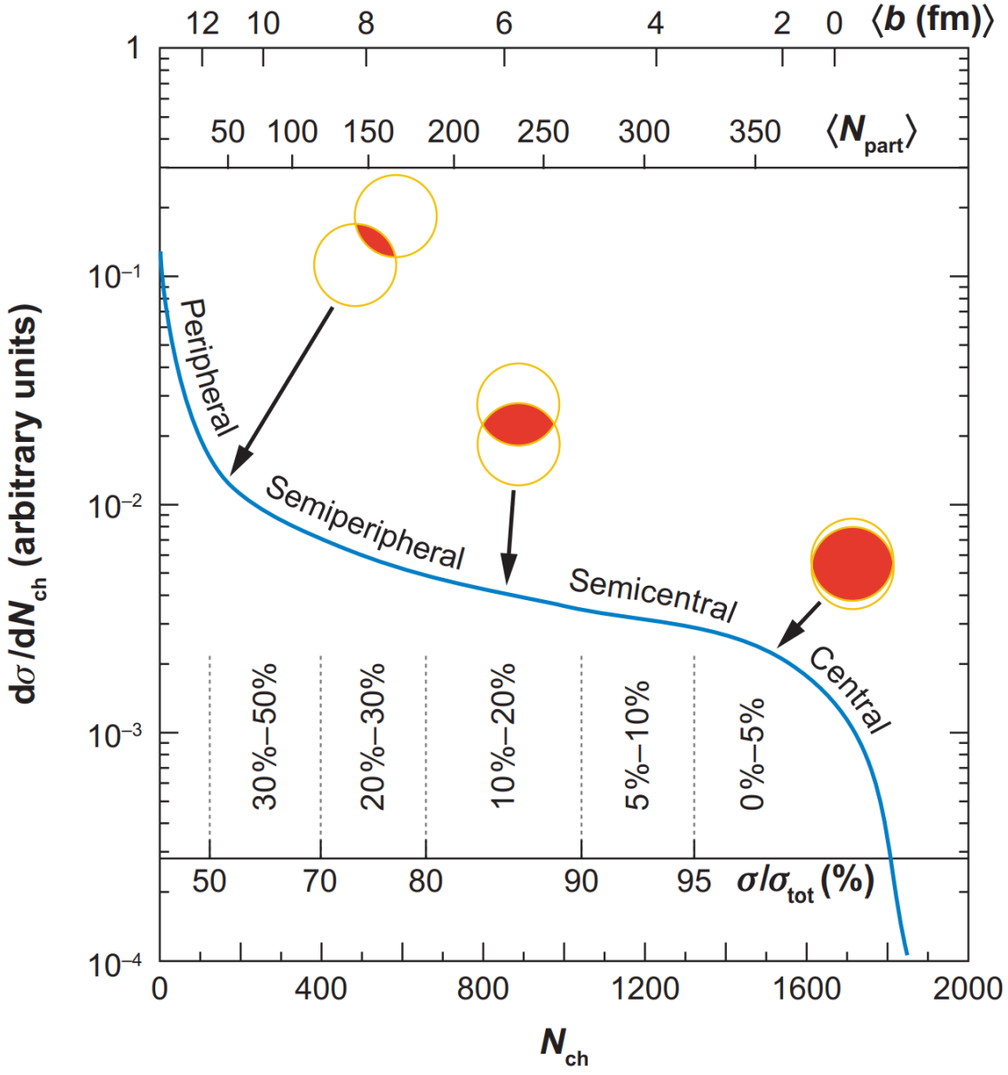

Annual Review of Nuclear and Particle Science, 57:205-243 (2007)

Monte-Carlo Glauber Model

- Randomly choose impact parameter ***b*** and nucleon distribution

- Sample the probability of nucleons to interact from interaction cross-section if they are separated by $d < \sqrt{\sigma_{NN}^{\text{inel}}/\pi}$

- Calculate the N_{part} and N_{coll}

- Map onto experimental centrality observables, such as forward calorimeter energy and particle multiplicity

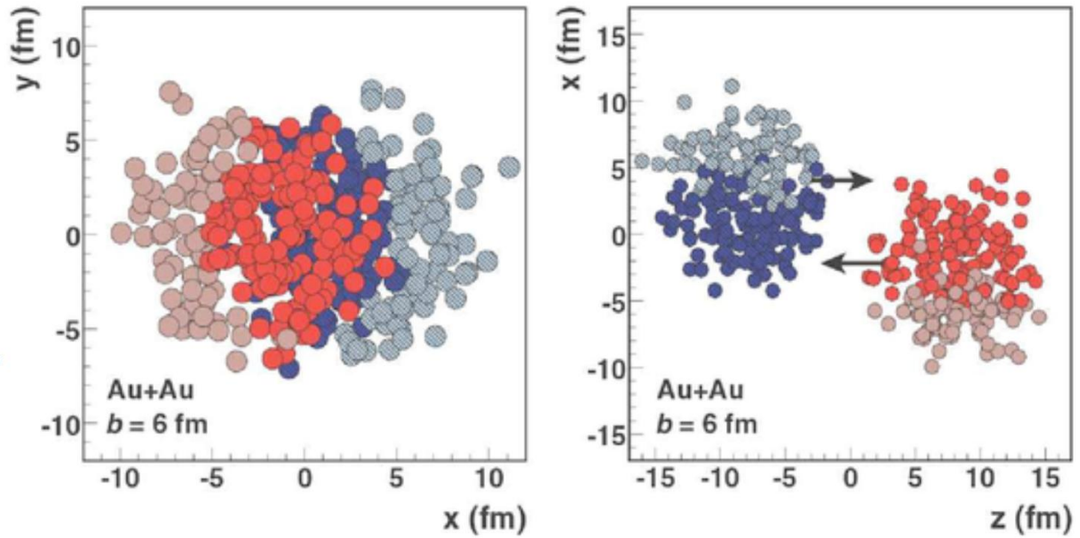

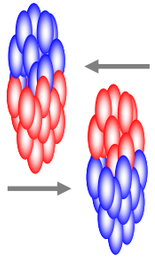

N_{part} → Number of participating nucleons

N_{coll} → Number of binary scatterings

Example:

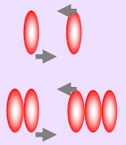

$N_{part} = 2$ $N_{coll} = 1$

$N_{part} = 5$ $N_{coll} = 6$

Density of the Quark Soup

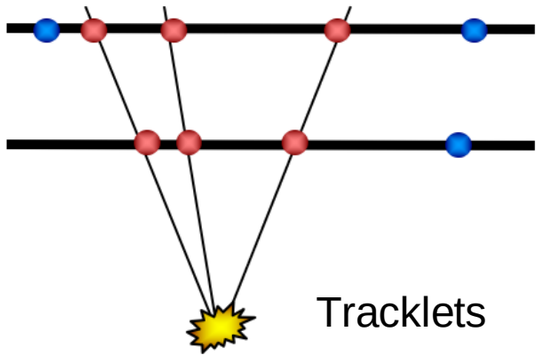

Count the number of particles produced in **head-on** collisions.
Particle density in **Lead+Lead** ~ **400x** of that in **Proton+Proton**

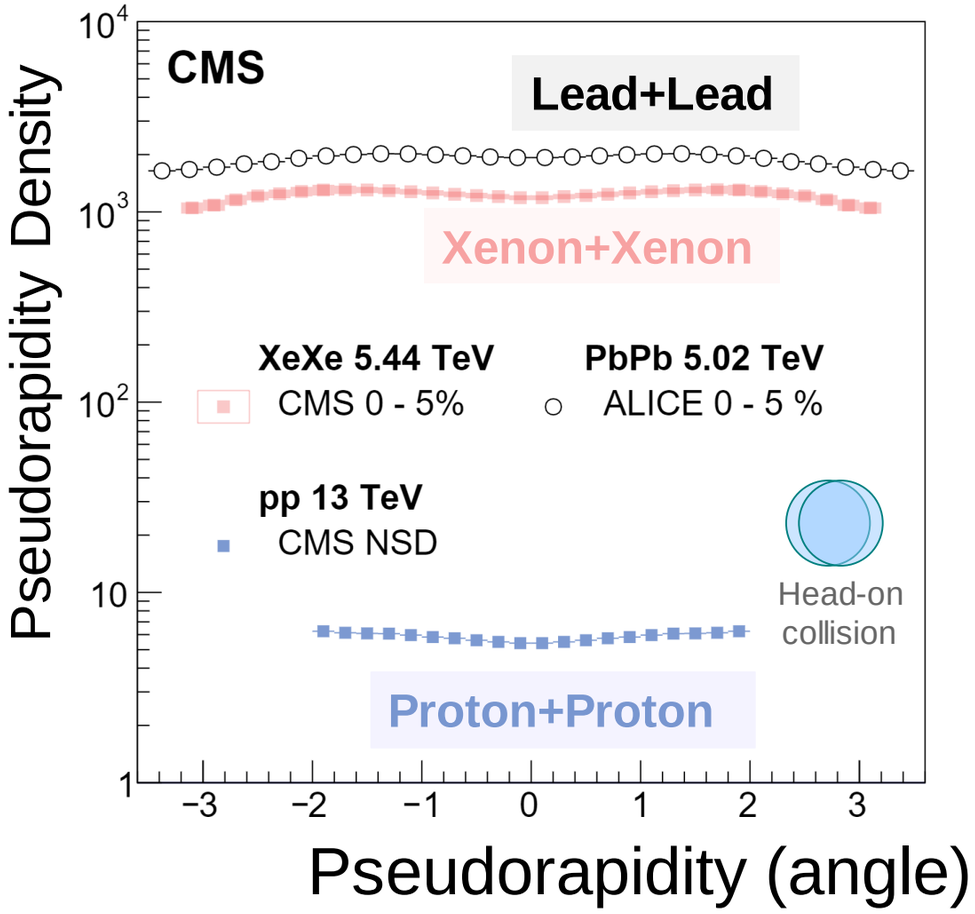

At time ~ 1 fm/c:

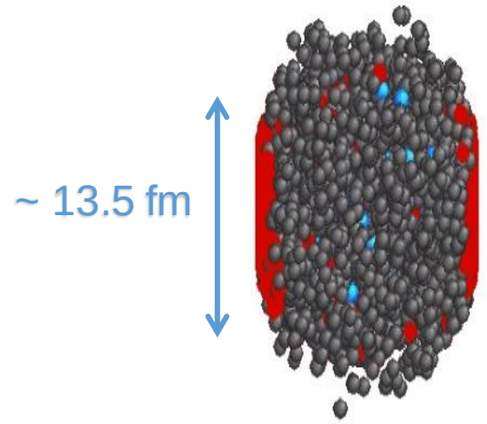

Energy density of the medium based on CMS dE/dη ~ 2 TeV:

$$\epsilon = \frac{1}{A \cdot \tau_0} \frac{dE_T}{dy}\bigg|_{y=0}$$ ~13 GeV/fm^3

> 20x denser than the proton!

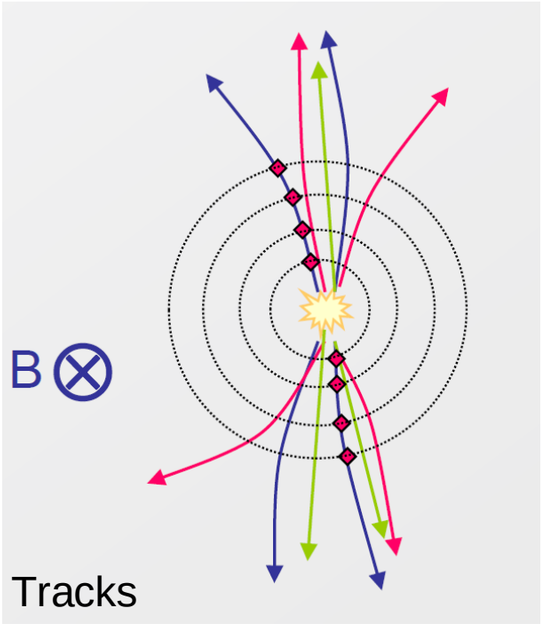

At **early time** of the collision, the system cannot be described by hadrons

Rough Estimation of QGP Temperature

At $\tau_0 \sim 1$ fm/c:

$$\epsilon = \frac{1}{A \cdot \tau_0} \frac{dE_T}{dy}\bigg|_{y=0} \approx 13 \text{ GeV/fm}^3$$

$$\approx 0.1 \text{ GeV}^4 \qquad = 47.5 \times \frac{\pi^2}{30} T^4$$

$1 \text{ fm}^{-1} = 0.1973 \text{ GeV}$

$$T \approx 0.283 \text{ GeV} = 283 \text{ MeV}$$

$$\approx 3.3 \times 10^{12} \text{ K}$$

!!!

$1 \text{ GeV} = 1.16 \times 10^{13} \text{ K}$

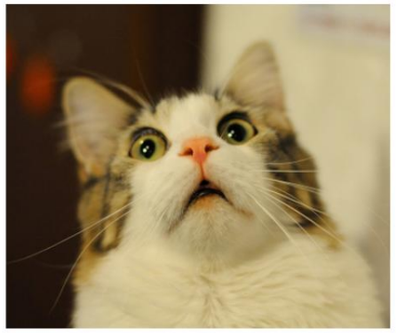

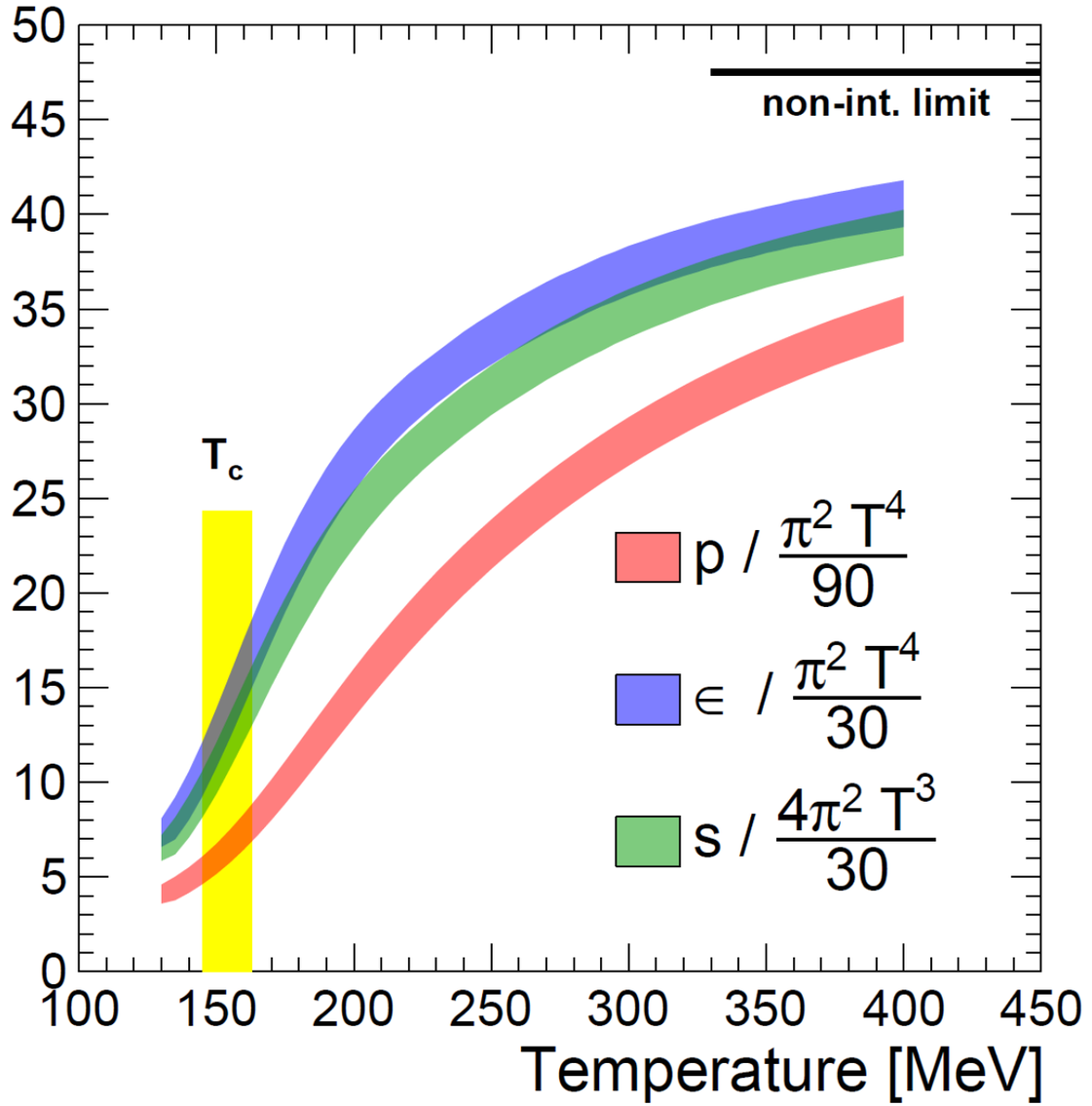

Pressure Driven Expansion of the Quark Soup

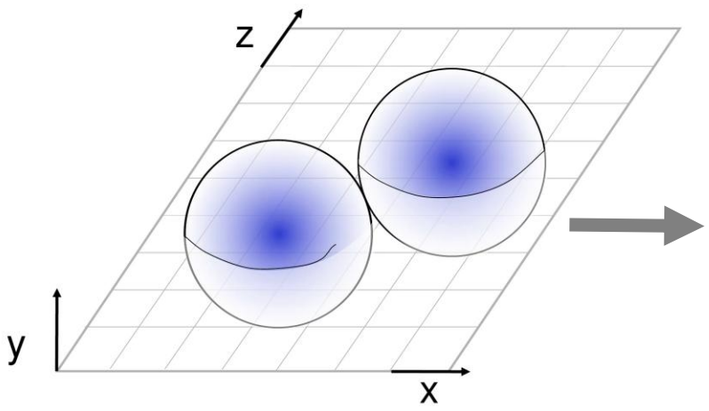

Small pressure gradient

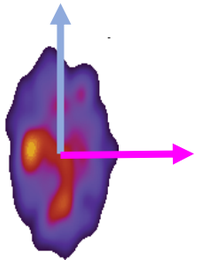

Large pressure gradient

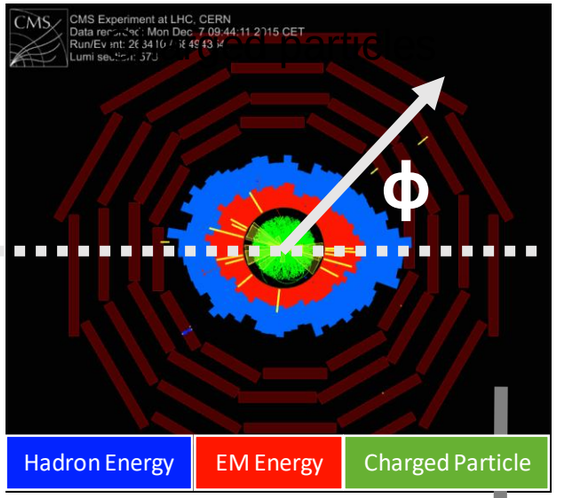

Event plane angle

Expansion of **Ultra-cold atoms (Li-6)** released from laser trap

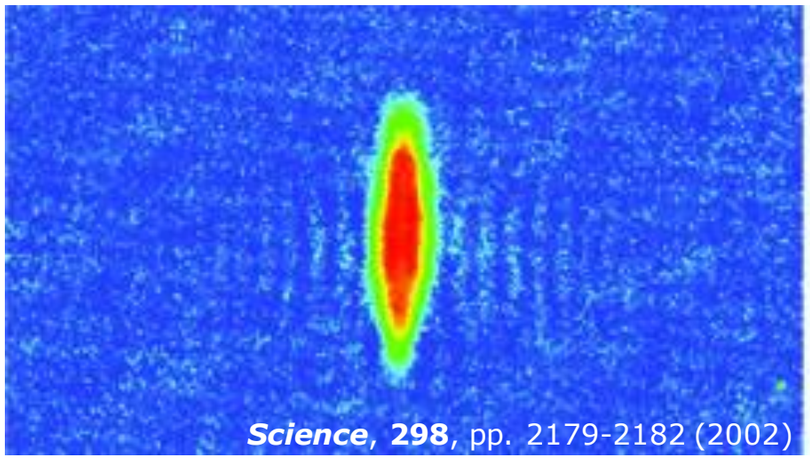

100 μs

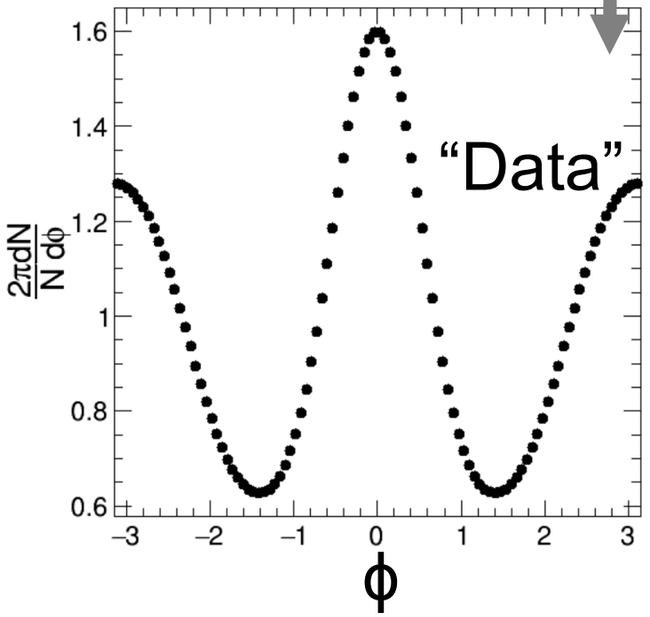

Particle Azimuth Angle Distribution

Collective motion is observed, consistent with **early hydrodynamization!**

Elliptic Flow

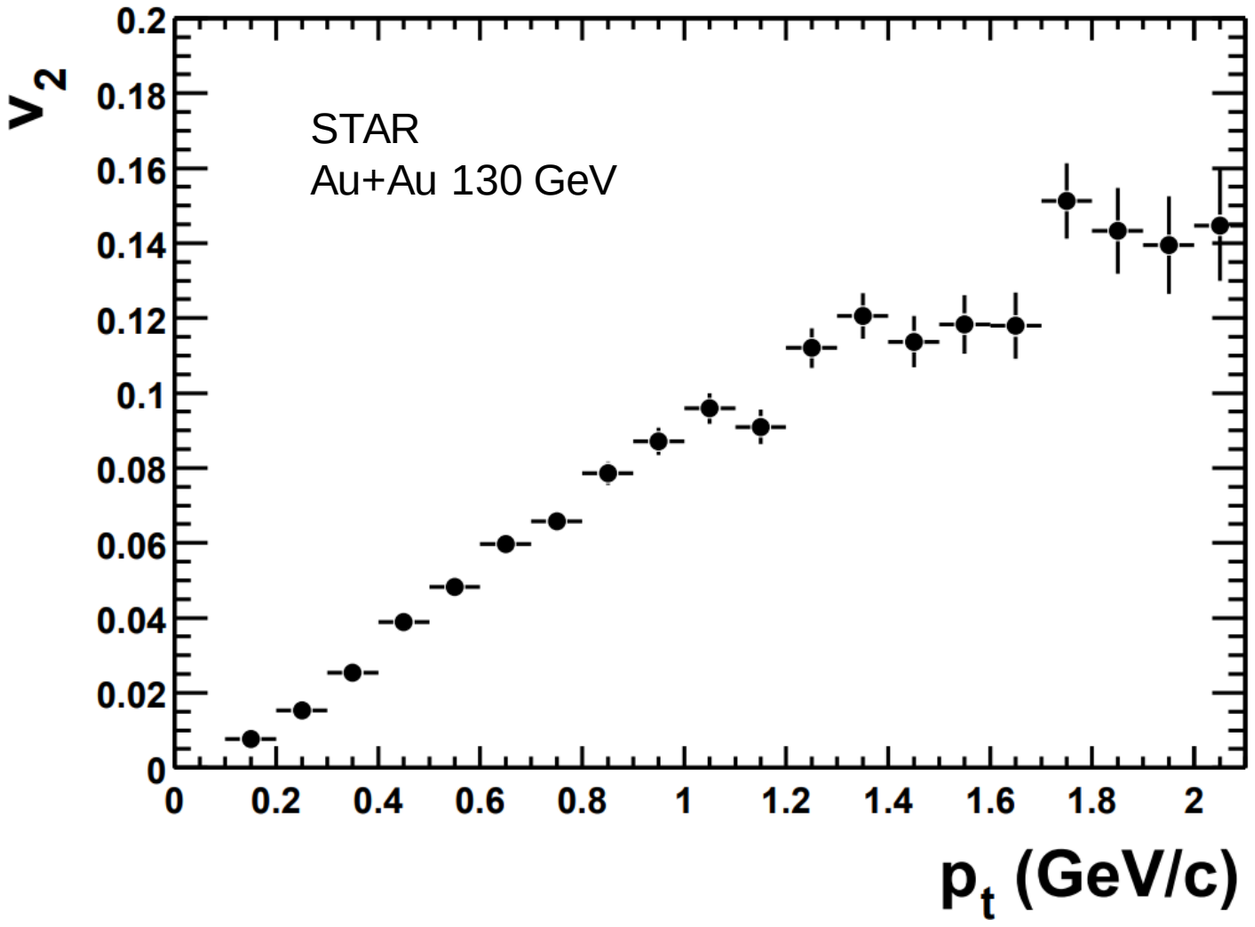

PRL 86 (2001) 402

- The first result from **STAR** at RHIC
- The extracted v_2 increases with transverse momentum

$$\frac{2\pi}{N}\frac{\mathrm{d}N}{\mathrm{d}\phi} = 1 + \sum_{n=1}^{\infty} 2v_n \cos[n(\phi - \Psi_n)]$$

Expansion of **Ultra-cold atoms (Li-6)** released from laser trap

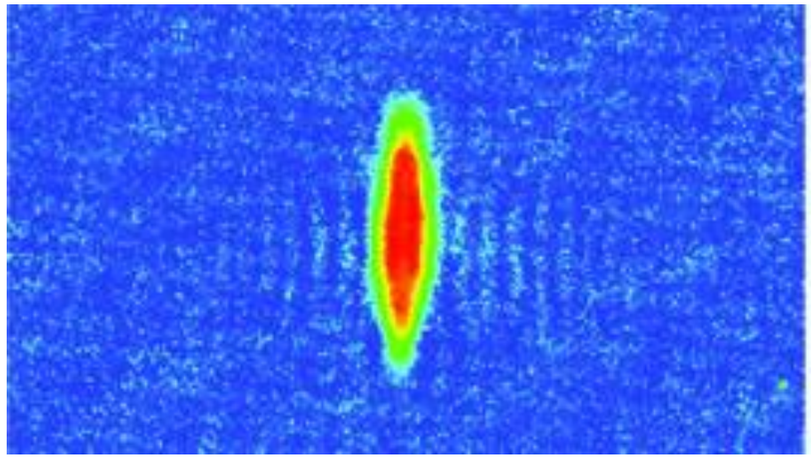

Two-Particle Correlation Function

Signal pair distribution:

same event pairs

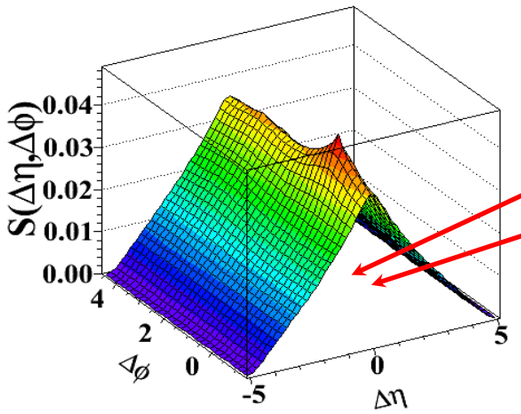

Beam Axis

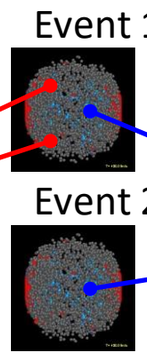

Background pair distribution:

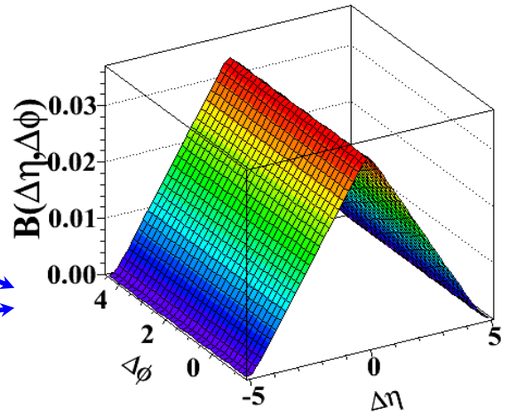

mixed event pairs

$$S(\Delta\eta,\Delta\phi) = \frac{1}{N_{trig}} \frac{d^2N^{same}}{d\Delta\eta d\Delta\phi}$$

$$B(\Delta\eta,\Delta\phi) = \frac{1}{N_{trig}} \frac{d^2N^{mix}}{d\Delta\eta d\Delta\phi}$$

$\Delta\eta = \eta_1 - \eta_2$
$\Delta\varphi = \varphi_1 - \varphi_2$

Two-Particle Correlation Function

Signal pair distribution:

Background pair distribution:

Beam Axis

Event 1

Event 2

same event pairs

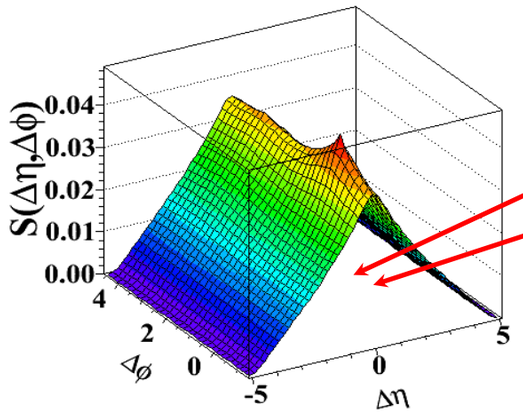

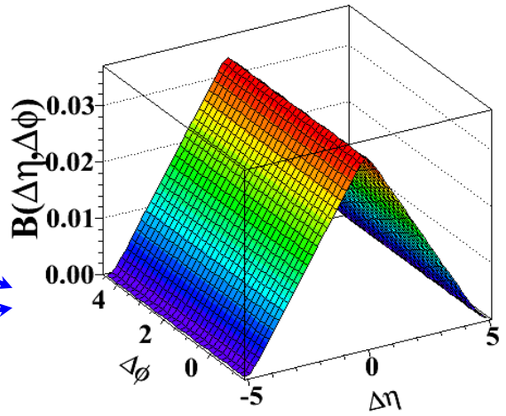

mixed event pairs

$$S\left(\Delta\eta,\Delta\phi\right)=\frac{1}{N_{trig}}\frac{d^2N^{same}}{d\Delta\eta d\Delta\phi}$$

$$B\left(\Delta\eta,\Delta\phi\right)=\frac{1}{N_{trig}}\frac{d^2N^{mix}}{d\Delta\eta d\Delta\phi}$$

CMS Preliminary

PbPb $\sqrt{s_{NN}}$ = 2.76 TeV

35-40%

PbPb

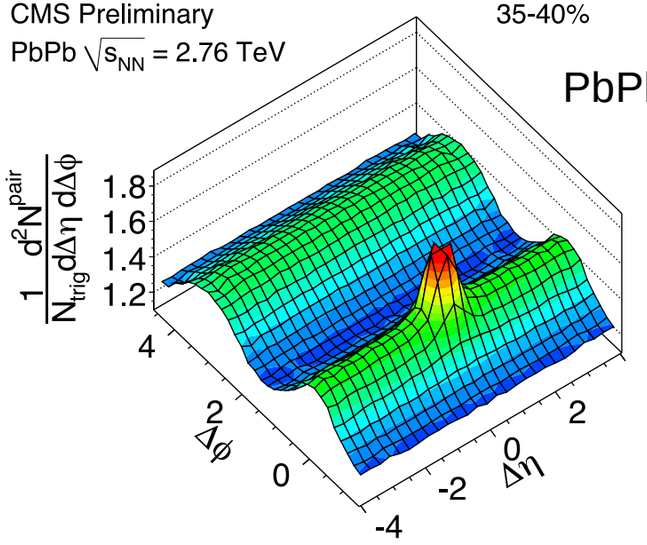

$\Delta\eta = \eta_1-\eta_2$

$\Delta\varphi = \varphi_1-\varphi_2$

Associated hadron yield per trigger:

$$\frac{1}{N_{trig}}\frac{d^2N^{pair}}{d\Delta\eta d\Delta\phi}=B\left(0,0\right)\times\frac{S(\Delta\eta,\Delta\phi)}{B(\Delta\eta,\Delta\phi)}$$

Understanding the Correlation Function

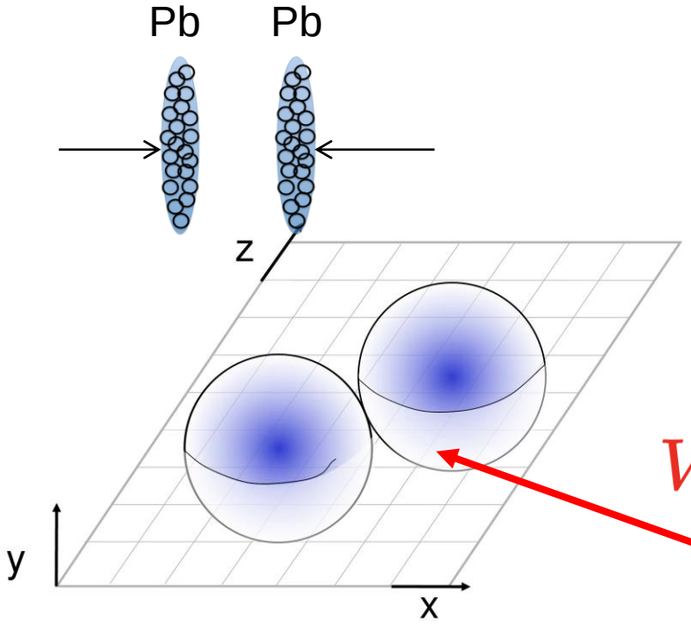

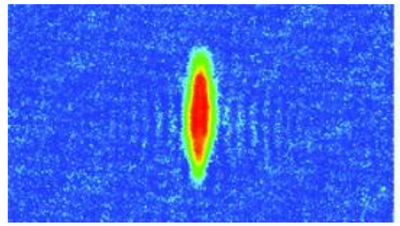

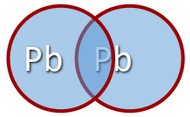

35-40% centrality

CMS PbPb 2.76 TeV

$V_{2\Delta}\cos(2\Delta\phi)$

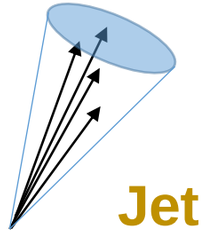

Jet

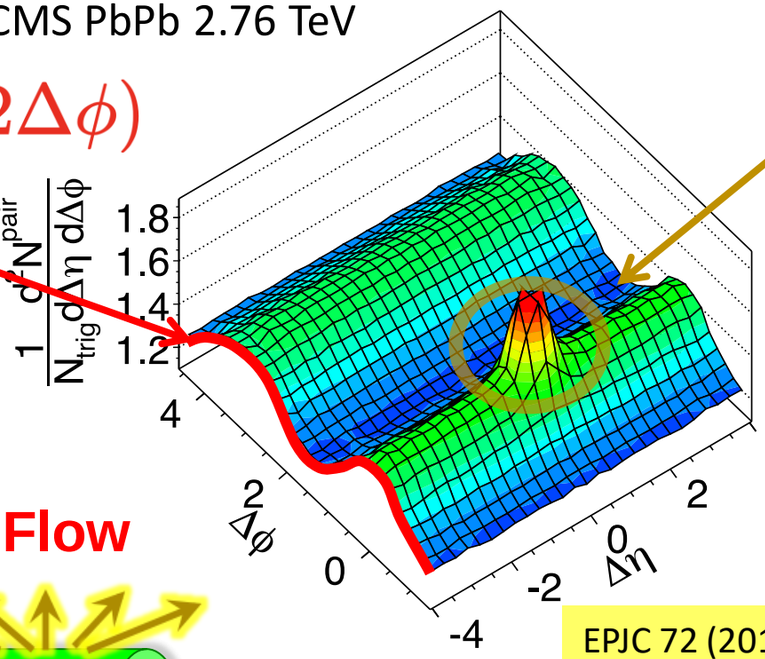

EPJC 72 (2012) 2012

p_T^{trig}: 4–6 GeV/c

p_T^{assoc}: 2–4 GeV/c

Particle azimuthal distributions:

$dN/d\phi \propto 1 + \Sigma\, 2V_n \cos(n(\phi-\phi_0))$

Assuming factorization

$$v_n = \sqrt{V_{n\Delta}}$$

Flow

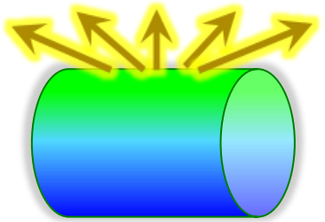

Two-Particle Angular Correlation in PbPb vs Centrality

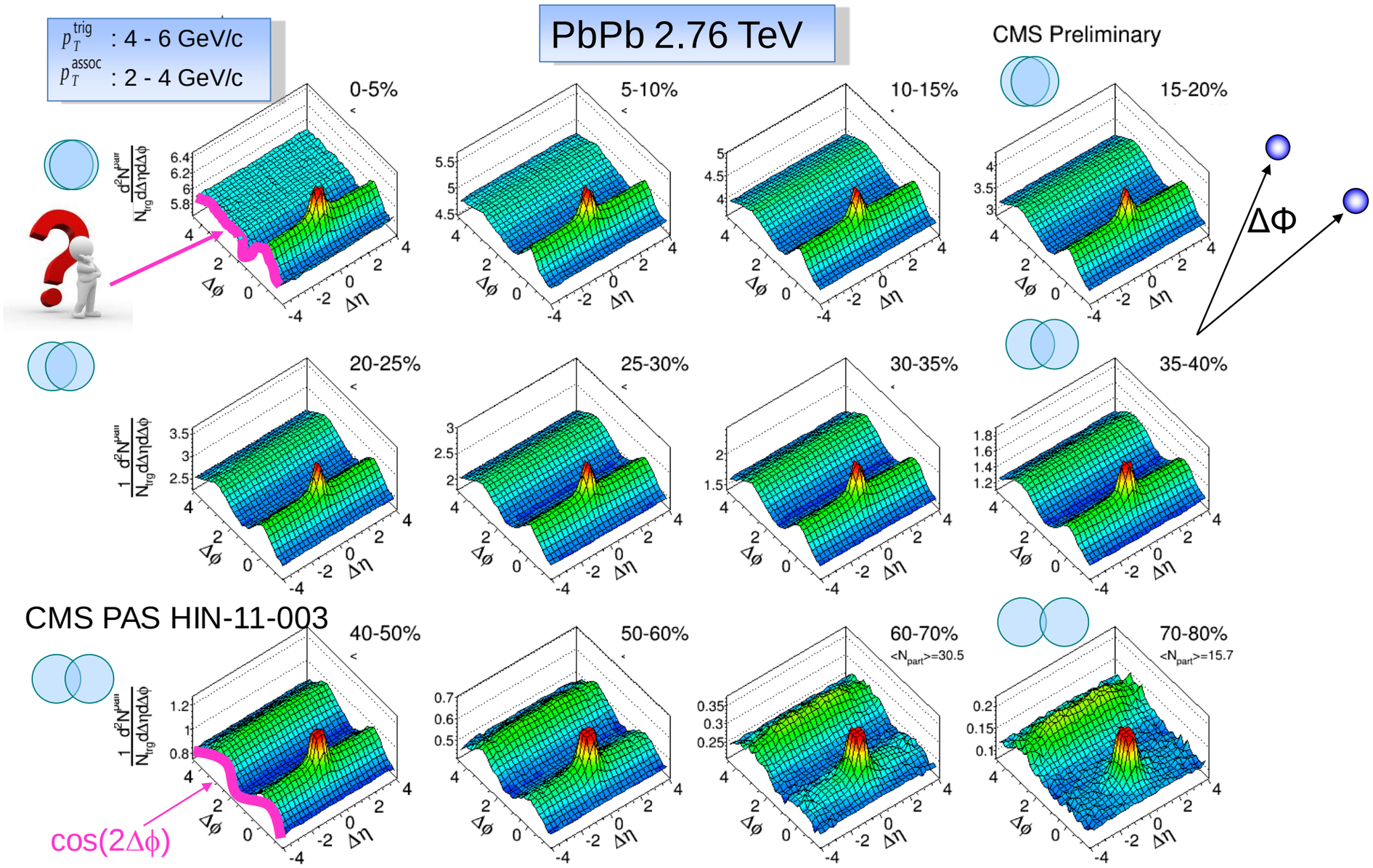

Initial Condition of the Collision

"Classic view"

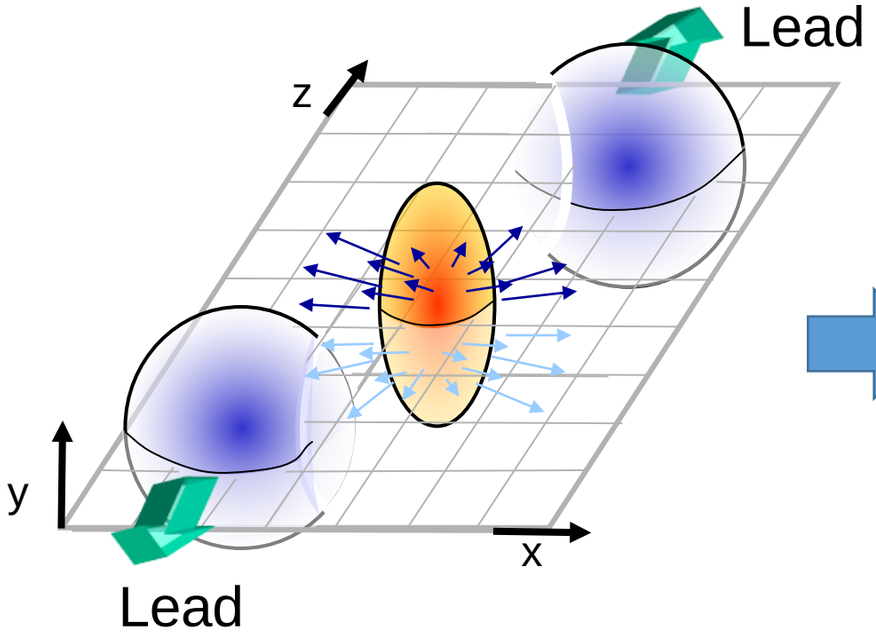

"Modern view"

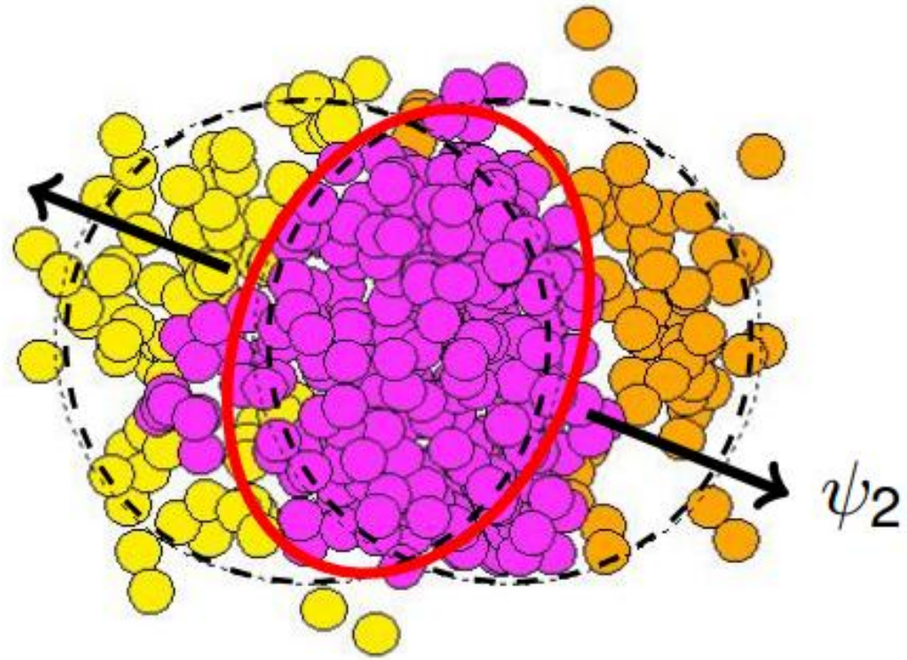

B. Alver & G. Roland *Phys. Rev. C81:054905, 2010*

Origin of the Ridge Structure

It was now understood that the ridge may be induced by higher order flow terms (v_2, v_3, v_4, v_5, …)

Elliptic flow (v_2)

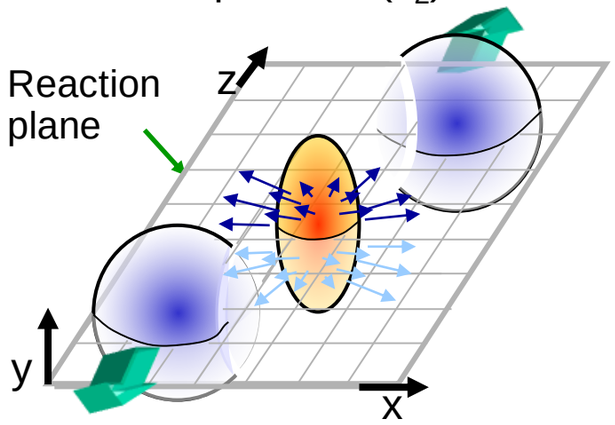

Triangular flow (v_3) from event-by-event fluctuation

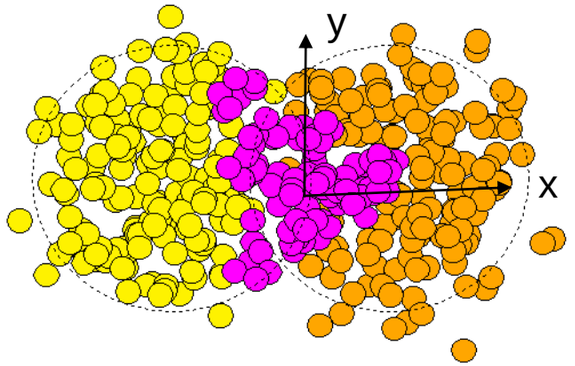

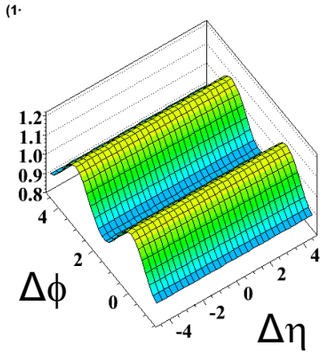

~ $V_2 \cos(2\Delta\phi)$

Add V_2 and V_3 together

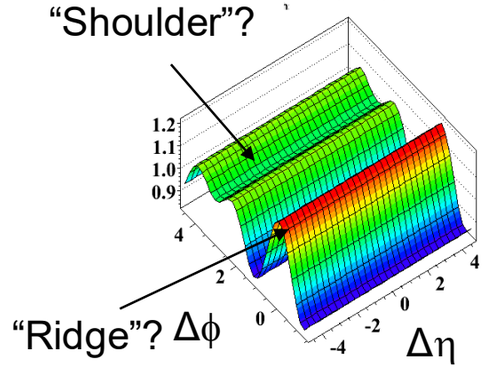

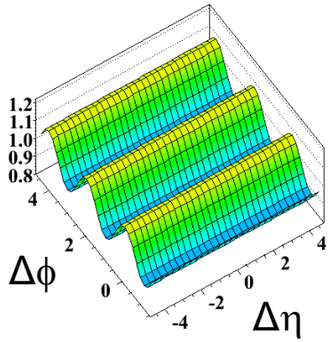

~ $V_3 \cos(3\Delta\phi)$

Particle Azimuthal Anisotropy

Magnitude

v_2 Ψ_2

+ Ψ_3

v_3

+ Ψ_4

v_4

⋮

+

v_n ...

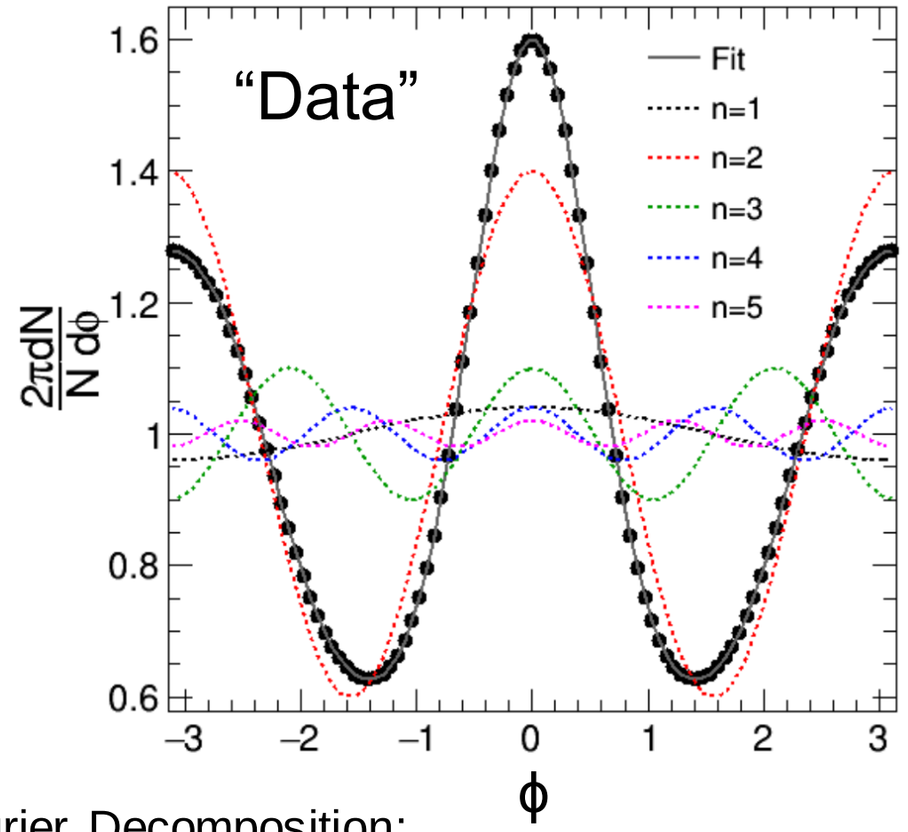

Fourier Decomposition:

$$\frac{2\pi}{N}\frac{\mathrm{d}N}{\mathrm{d}\phi} = 1 + \sum_{n=1}^{\infty} 2v_n \cos[n(\phi - \Psi_n)]$$

Alver and Roland (MITHIG)
"Collision geometry fluctuation"
PRC82 (2010) 039903

Density Fluctuation

Power spectrum of **the Big Bang**

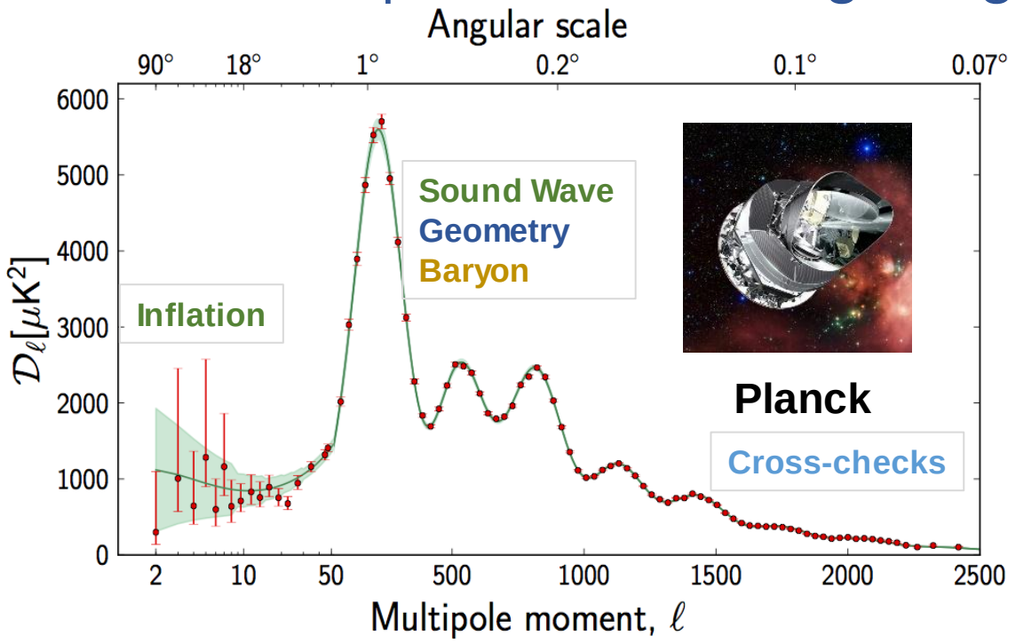

Cosmic Microwave Background (CMB)

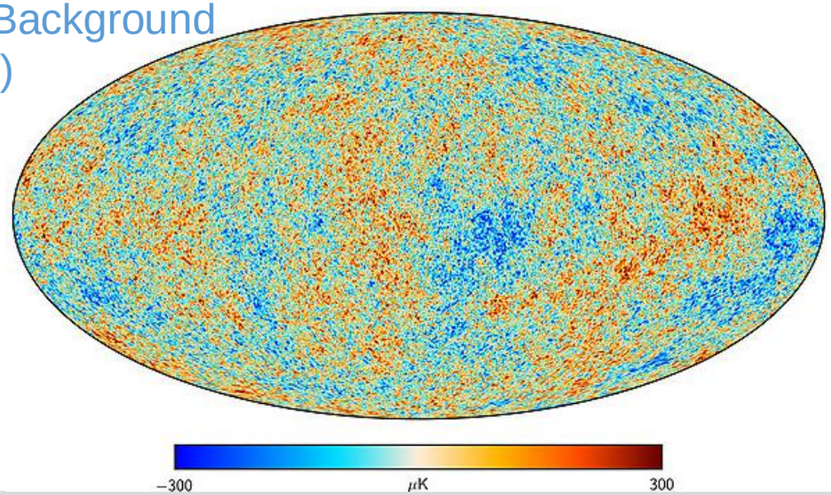

Fourier analysis of **many little bangs**

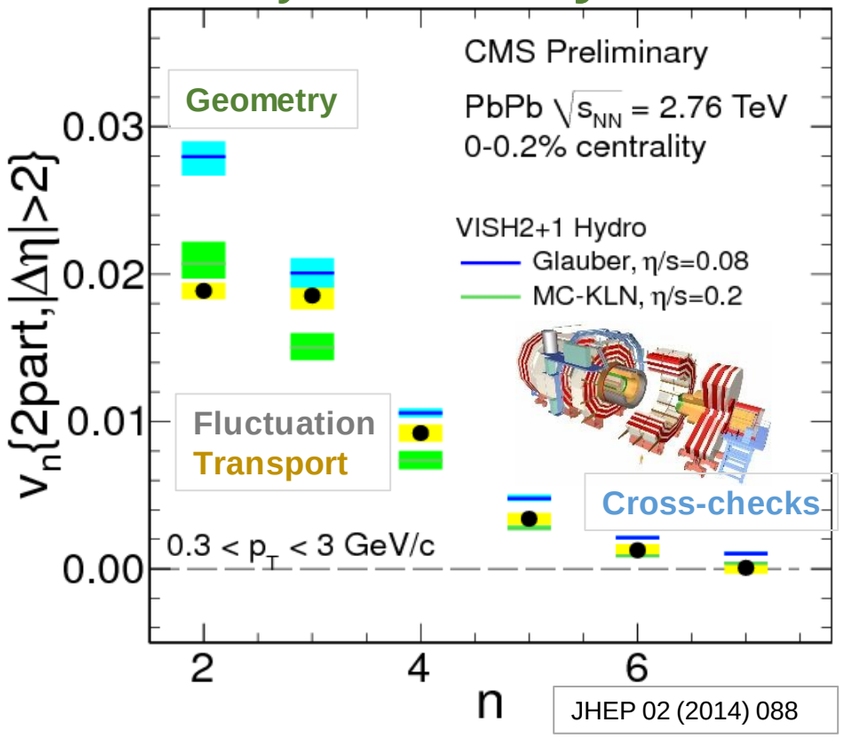

JHEP 02 (2014) 088

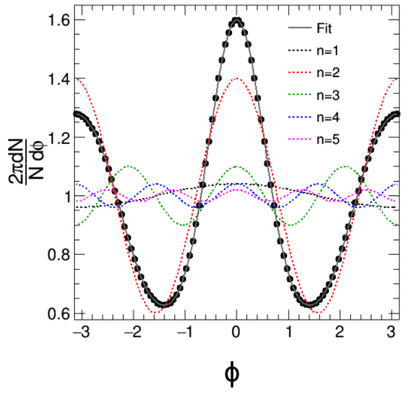

Quark Gluon Plasma (QGP)

Relativistic Hydrodynamics Calculations

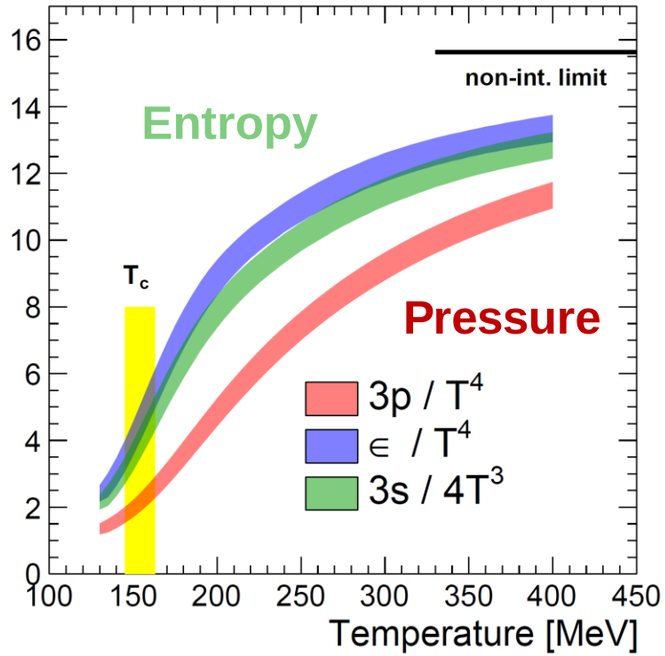

HotQCD Collaboration
PRD90 (2014) 094503

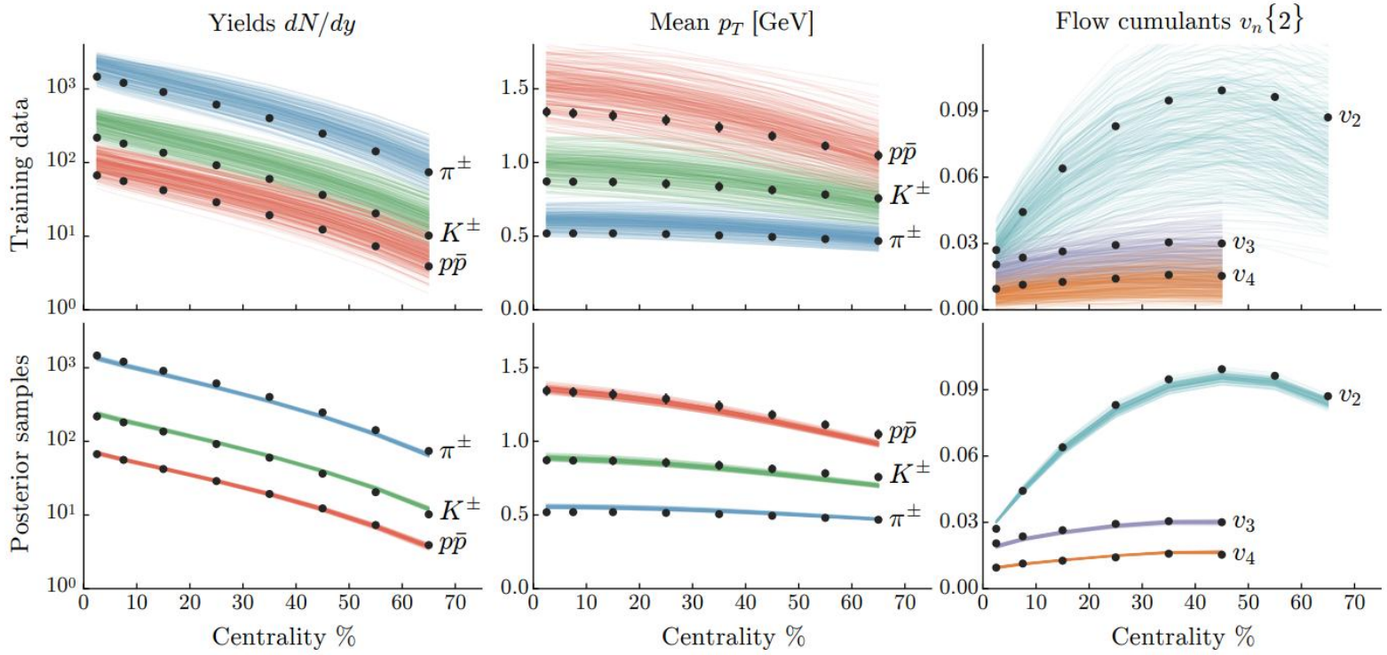

Lattice QCD based
Equation of State

Output (from Global fit)
Medium Properties

$$T_{\mu\nu} = \varepsilon u_\mu u_\nu + p[\varepsilon]\Delta_{\mu\nu} - \eta[\varepsilon]\sigma_{\mu\nu} - \zeta[\varepsilon]\Delta_{\mu\nu}\nabla_\mu u^\mu + \mathcal{O}(\partial^2),$$

$$\sigma_{\mu\nu} = \Delta_{\mu\alpha}\Delta_{\nu\beta}(\nabla^\alpha u^\beta + \nabla^\beta u^\alpha) - \frac{2}{3}\Delta_{\mu\nu}\Delta_{\alpha\beta}\nabla^\alpha u^\beta,$$

$$\Delta_{\mu\nu} = g_{\mu\nu} + u_\mu u_\nu,$$

hydrodynamic evolution equations, $\nabla_\mu T^{\mu\nu} = 0$

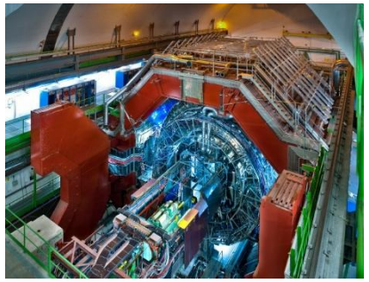

ALICE

Example:
PRC 94 (2016) 2, 024907

Effect of Shear Viscosity in Simulation

Ideal hydrodynamics

η/s = 0

Viscous hydrodynamics

η/s = 0.08

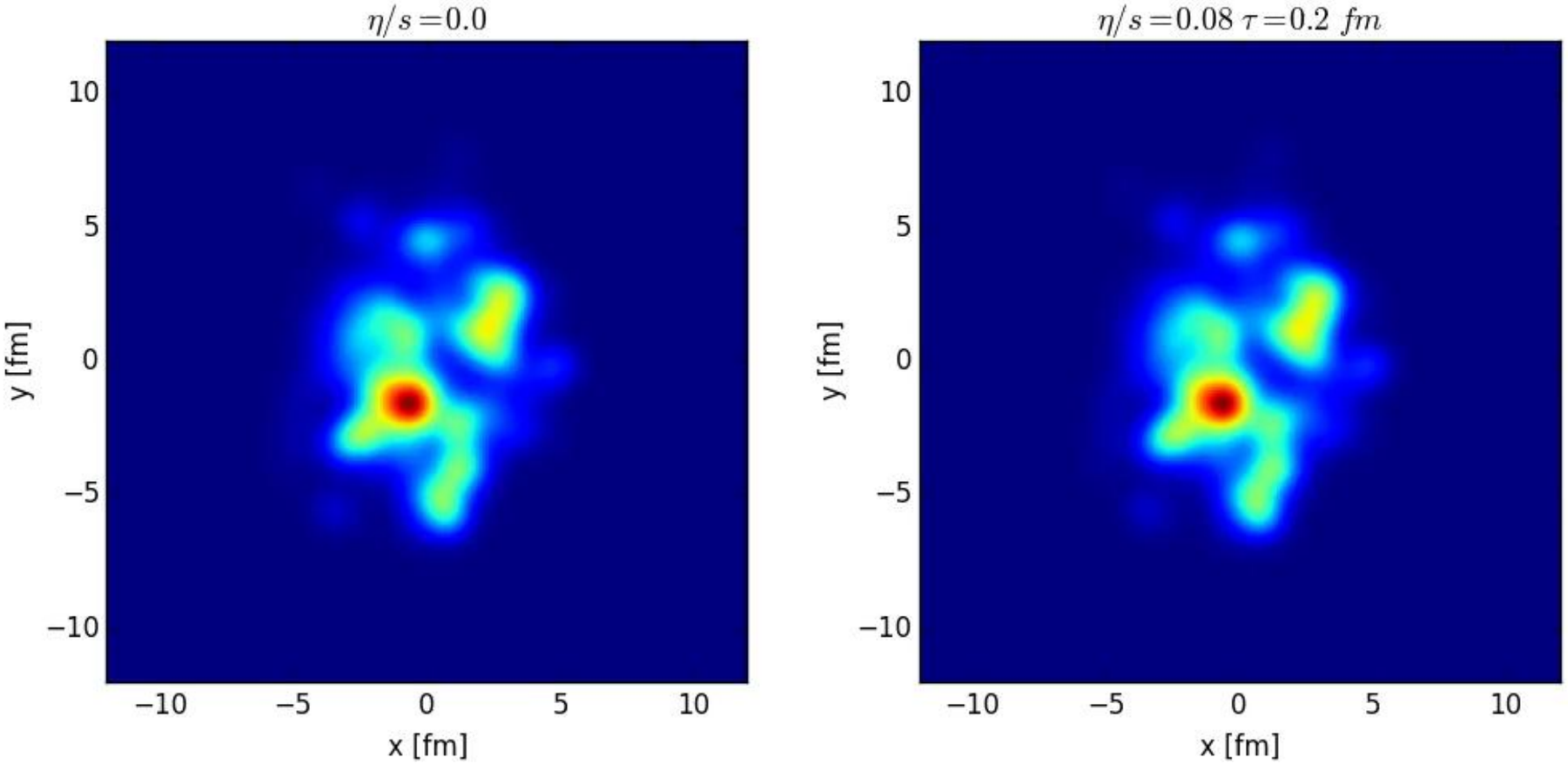

Animation from L. G. Peng

Near Perfect Fluid

Shear viscosity to entropy ratio

Electron fluid in Graphene

PRL103,025301 (2019)

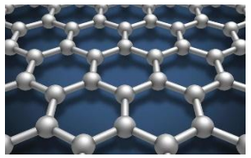

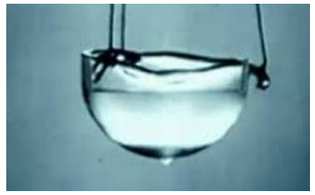

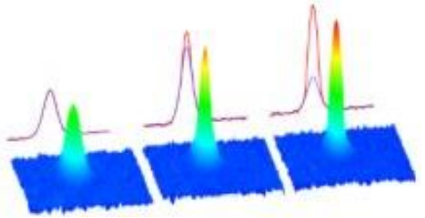

MIT cold atom group

Calculation from
Annals Phys.326:770-796,2011

Bayesian Analysis on Data (Duke)
PRC94 (2016) no.2, 024907

Evidence for Partonic Degrees of Freedom

- Suppose elliptic flow is **additive** and the flow is approximately built at the partonic level.
- The observed flow pattern in $v_2(m_T)$ could become simple at the parton level!

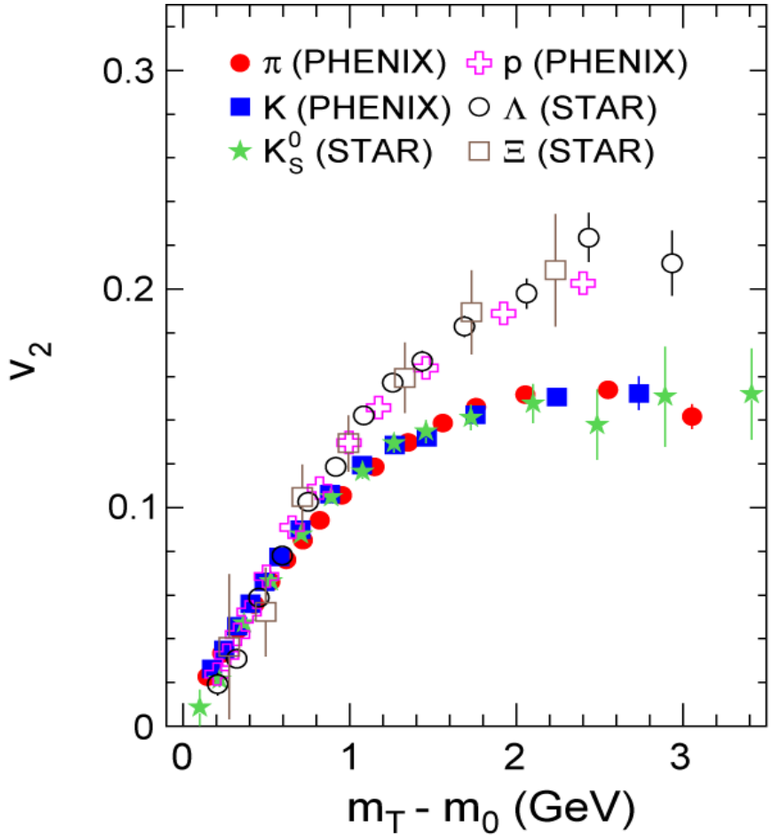

$m_T \rightarrow m_T/n$
$v_2 \rightarrow v_2/n$

n= number of quarks in the hadron

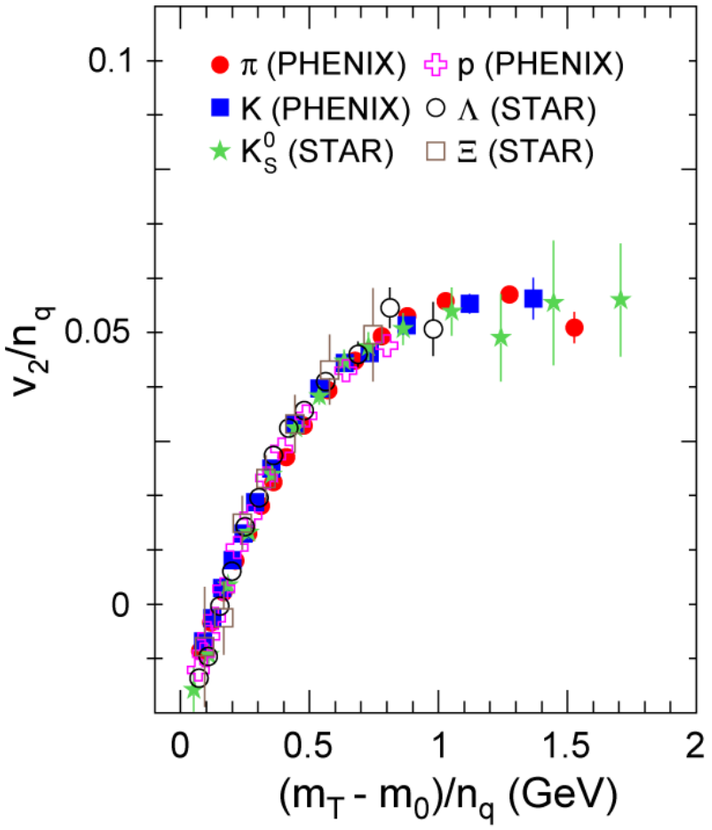

Scaling behavior: Constituents of QGP are partons

3D Structure of QGP

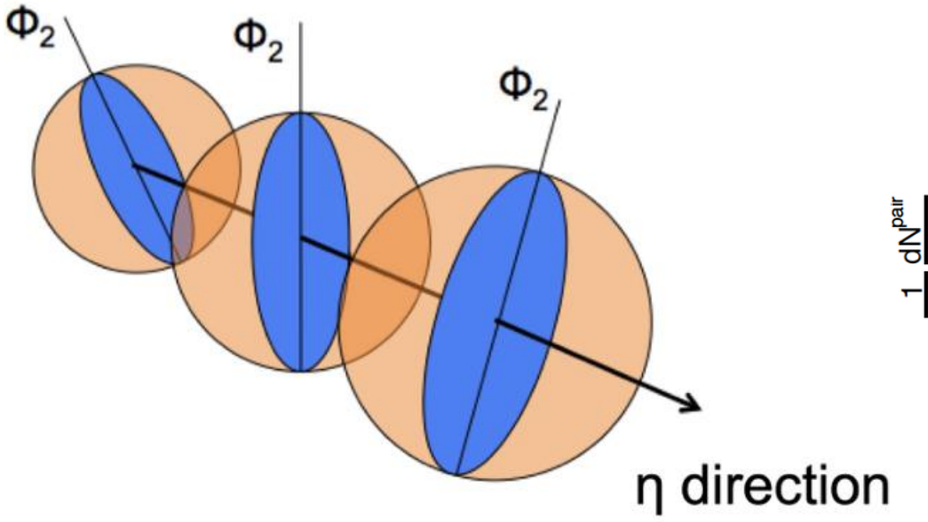

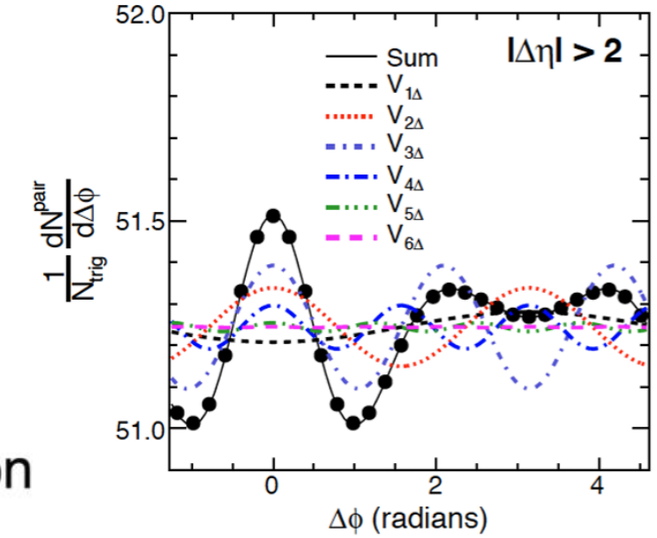

Long-range correlations (|Δη|>2)

$$\frac{dN^{pair}}{d\Delta\phi} \sim 1 + 2\sum_n V_{n\Delta}(p_T^a, p_T^b)\cos(n\Delta\phi)$$

$$r_n \equiv \frac{V_{n\Delta}(p_T^a, p_T^b)}{\sqrt{V_{n\Delta}(p_T^a, p_T^a)}\sqrt{V_{n\Delta}(p_T^b, p_T^b)}} \sim \left\langle \cos[n(\Psi_n(p_T^a) - \Psi_n(p_T^b))] \right\rangle$$

event-averaged observable

(r_n = 1 if Ψ_n is independent of p_T; Otherwise, r_n<1)

3D Structure of QGP

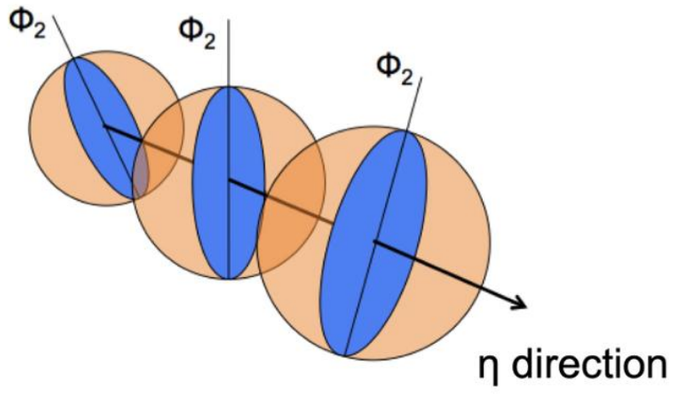

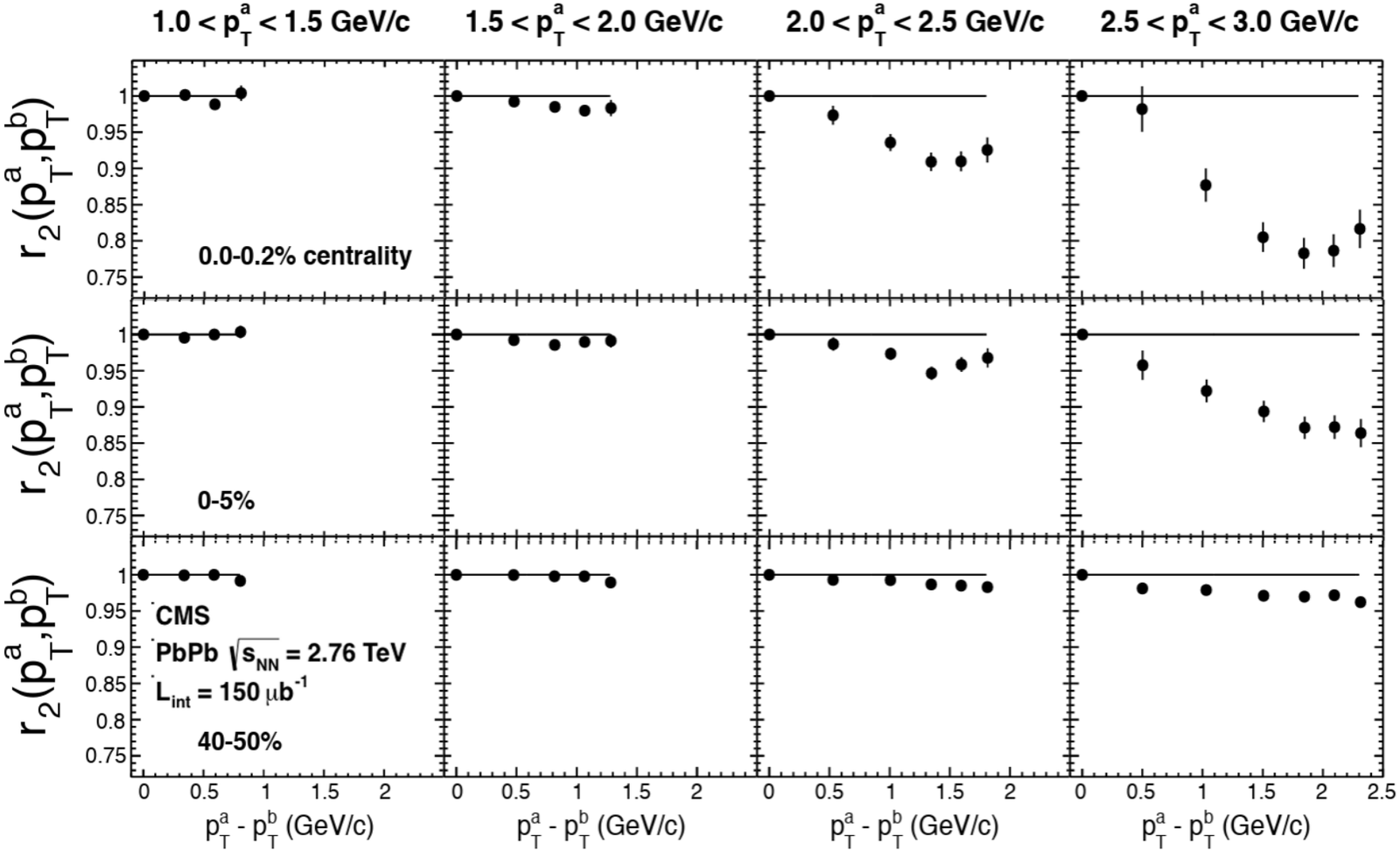

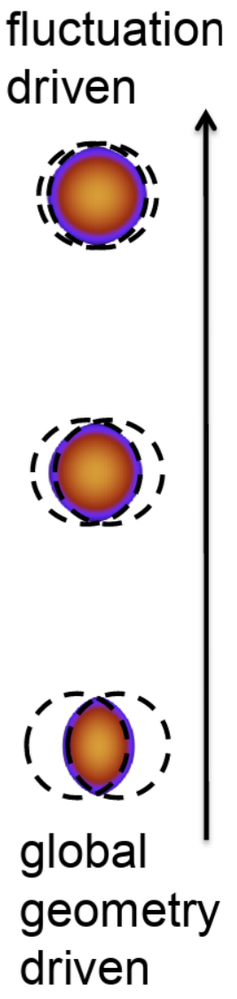

Chemical Freeze-out: Statistical Hadronization

- Hadronization process is non-perturbative
- In e^+e^- and pp: string fragmentation
- Postulate: QGP cools into an equilibrated gas of hadrons
- Particle abundance produced in QGP could be described by calculation with partition function

$$n = \int N(E) d^3p \quad \text{and} \quad N(E) = \frac{D}{(2\pi)^3} \frac{1}{e^{\frac{E-\mu}{T}} \pm 1}$$

- Conserved quantum number, such as baryon number gives a chemical potential μ_B
- Temperature at the freeze-out could be extracted

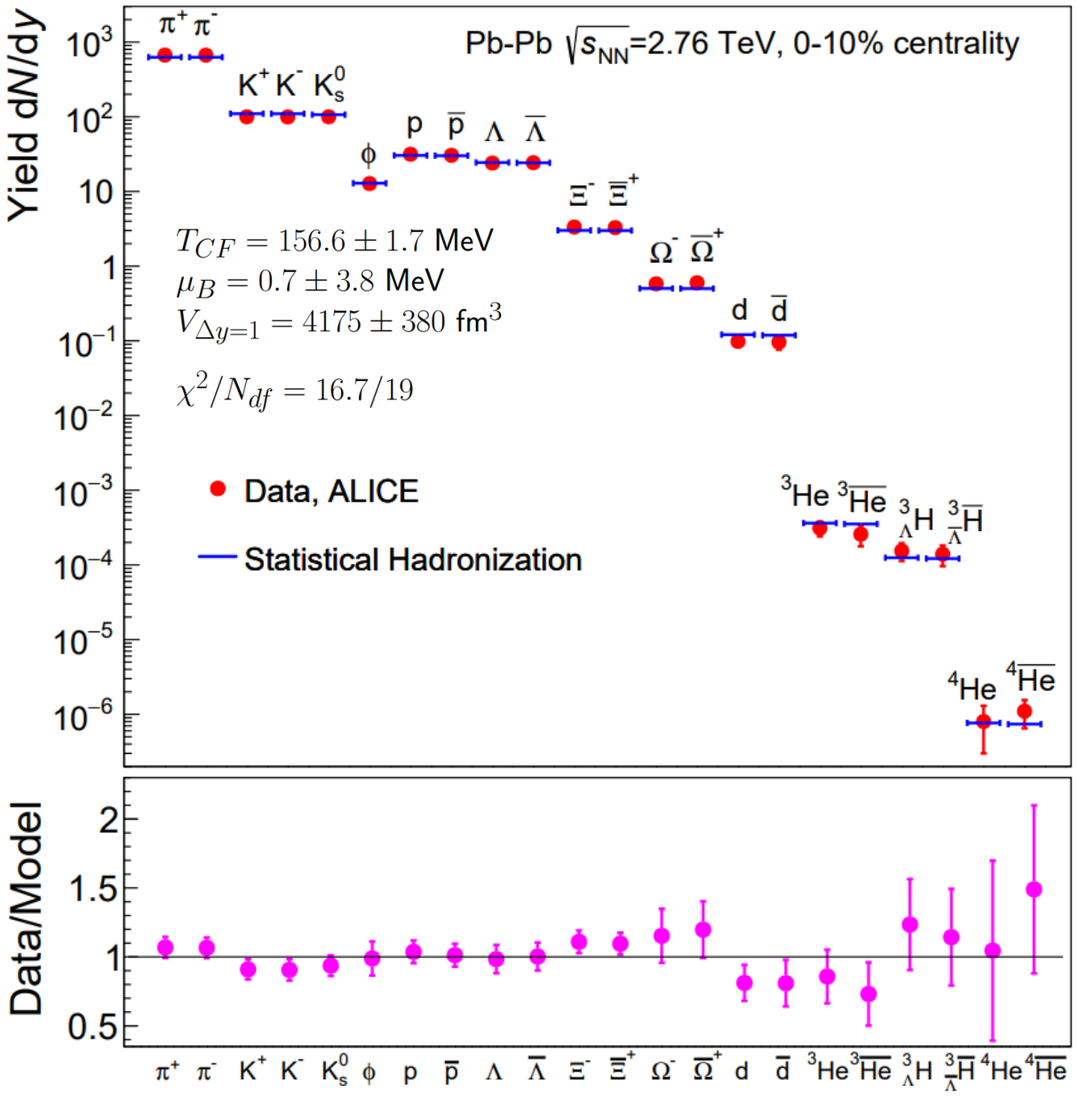

QGP Phase Diagram from Stat Hadronization Model

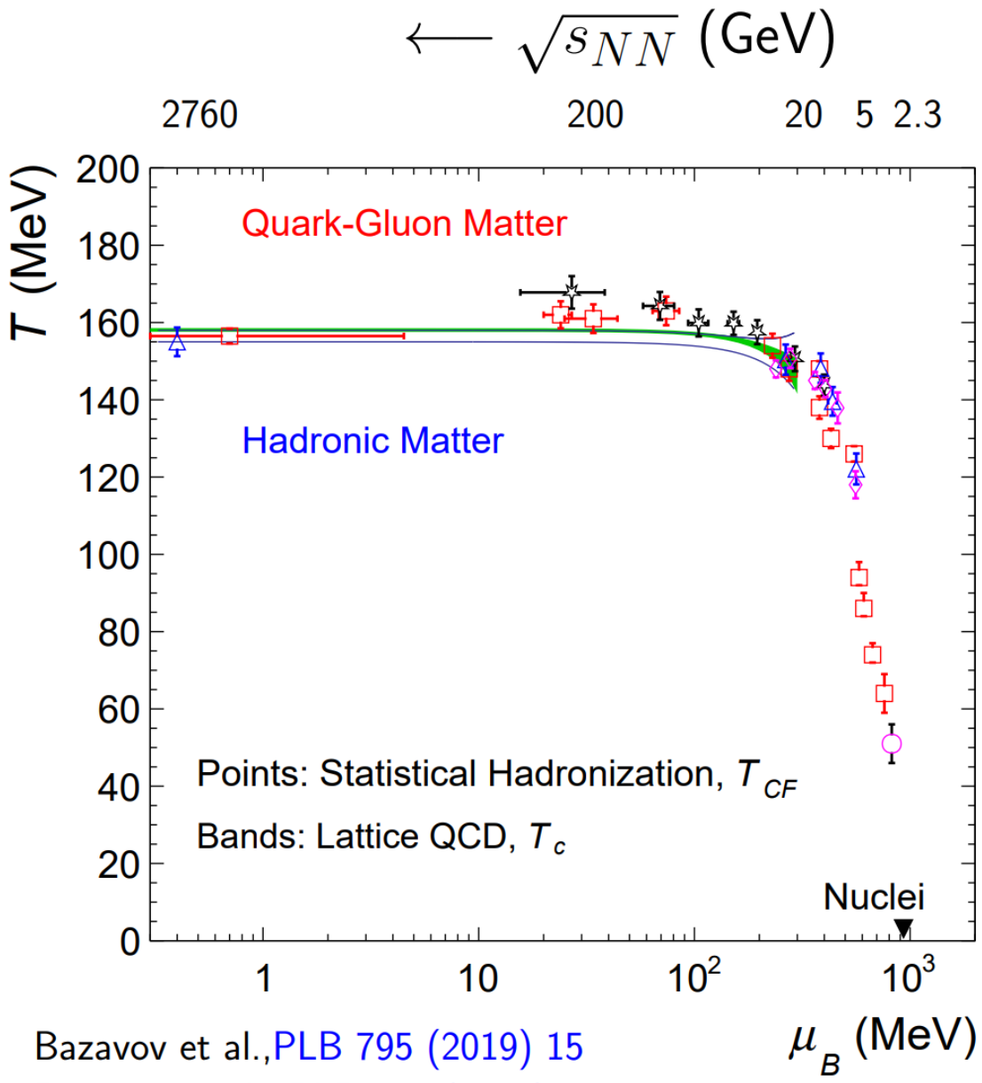

Bazavov et al.,PLB 795 (2019) 15
Borsanyi et al., PLB 370 (2014) 99

- Extracted result from LHC: remarkable coincidence with Lattice QCD results
- At LHC, baryon chemical potential $\mu_B \sim 0$: produced matter and anti-matter as in the Early Universe

  At lower collision energy: more matter from beam remnants of the colliding nuclei, larger μ_B
- Critical point: not established; search continues at large μ_B and low collision energy

Kinematics after Last Elastic Scattering

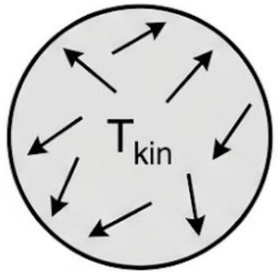

Static thermal source

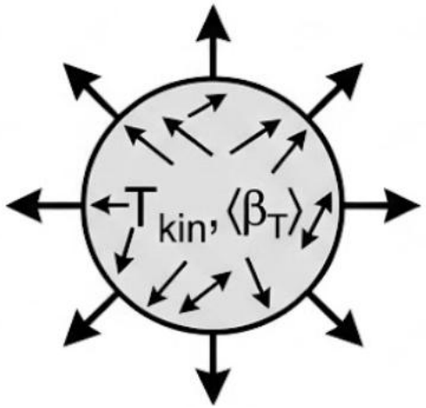

Explosive source: radial collective flow superimposed on the thermal motion

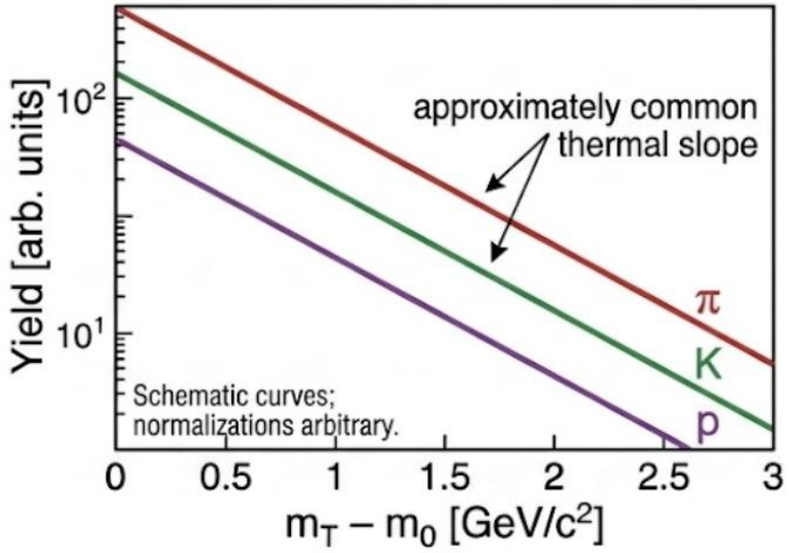

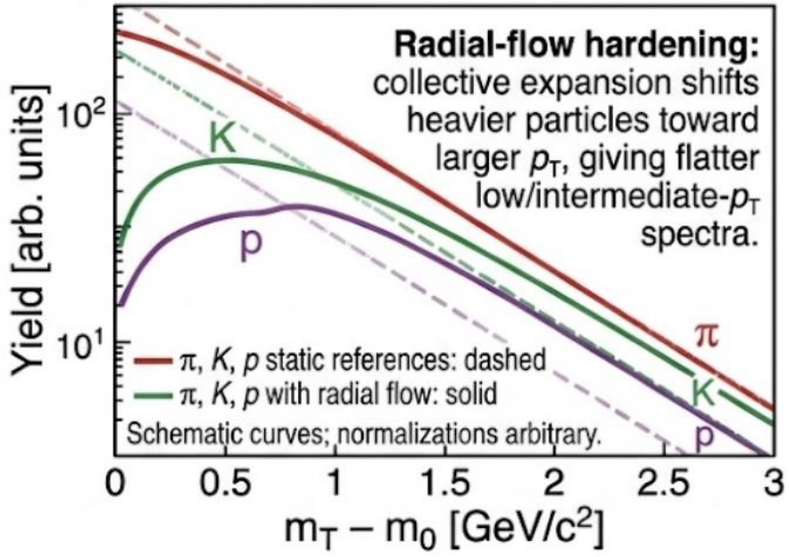

Kinematics after Last Elastic Scattering

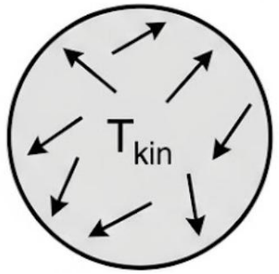

Static thermal source

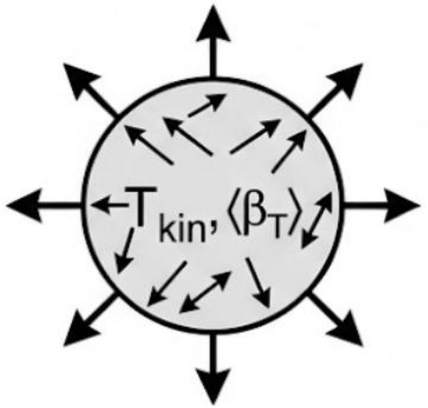

Explosive source: radial collective flow superimposed on the thermal motion

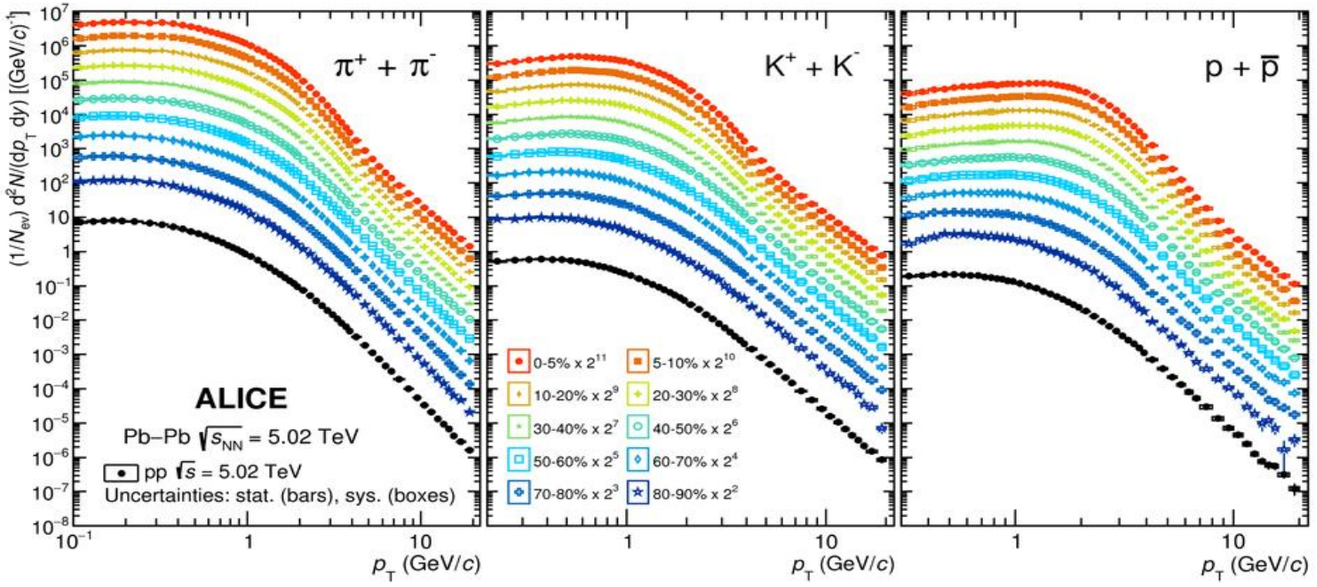

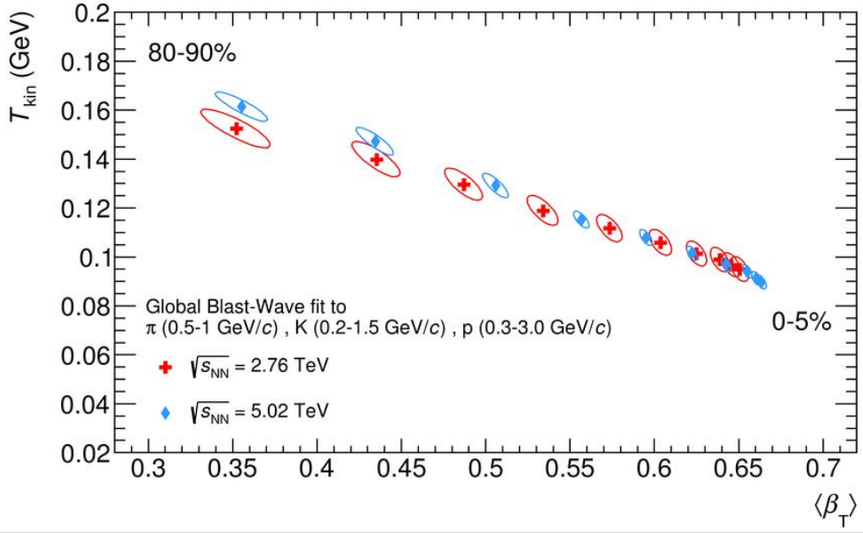

Relativistic Heavy Ion Collision Timeline

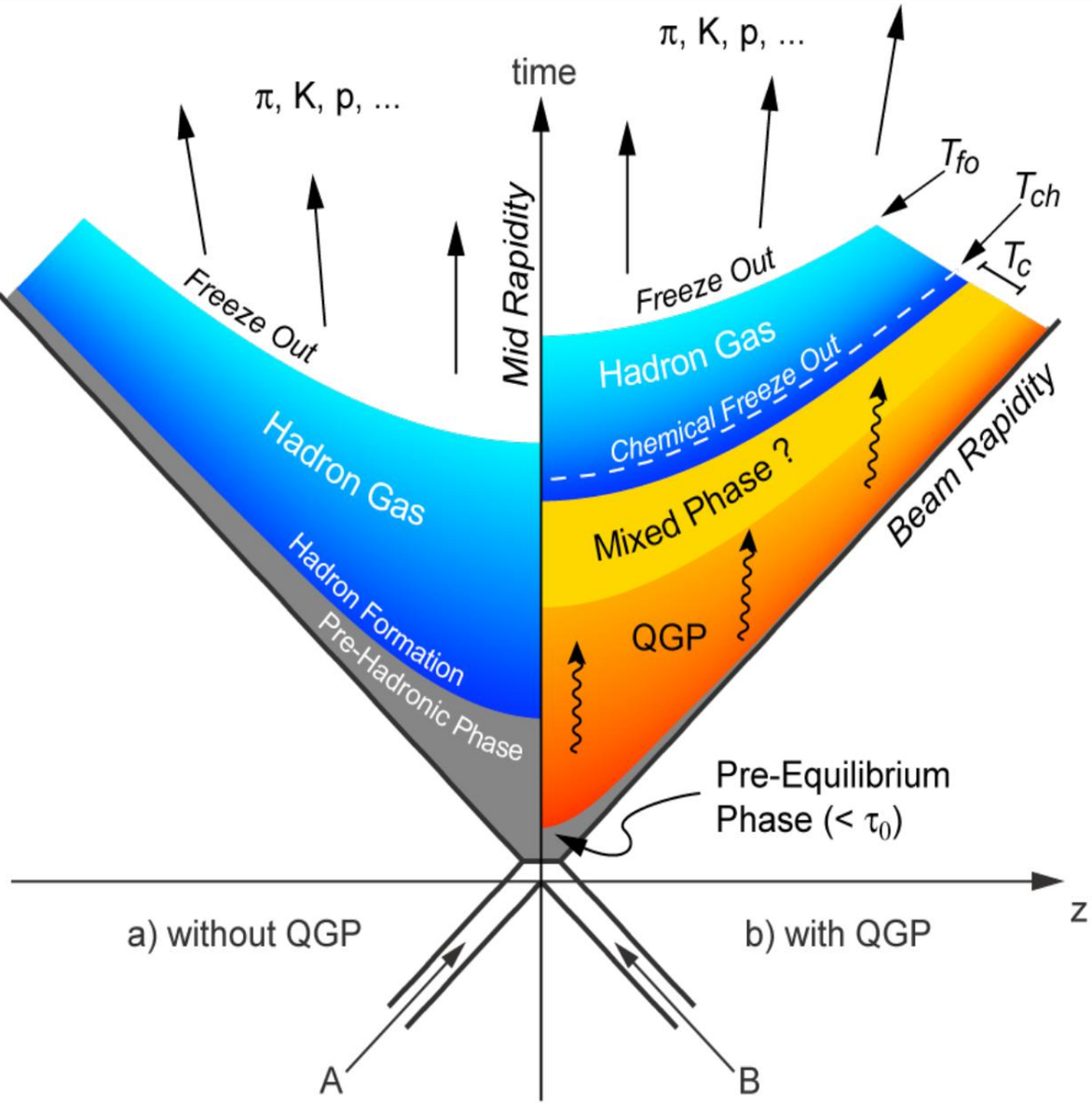

- Chemical freeze-out: ($T_{ch} \leq T_c$):
  - Inelastic scattering stops
  - Particle species abundances become fixed
- Kinetic freeze-out: ($T_{fo} \leq T_{ch}$):
  - Elastic scattering ceases
  - Momentum spectra and flow patterns become fixed

Summary from the Soft Probes

- Heavy-ion collisions create energy densities and temperatures far above the hadronic regime, producing a deconfined QGP.
- The QGP exhibits quark and gluon degrees of freedom and rapidly hydrodynamizes.
- Bulk observables show that the QGP flows like an almost “perfect” liquid with very small η/s.
- Hadronization and hadronic final-state interactions remain essential for connecting the QGP to measured particles.
- From RHIC to LHC energies, bulk QGP signatures evolve smoothly, supporting a consistent picture of QGP formation.
- At lower collision energies, the system becomes increasingly baryon rich and hadron dominated; no conclusive evidence for a QCD Critical Point has been found yet.

Open Questions

What are the initial conditions of the collision?

What is the longitudinal structure of the QGP?

What's the hadronization mechanism with QGP?

nPDF and initial EM field

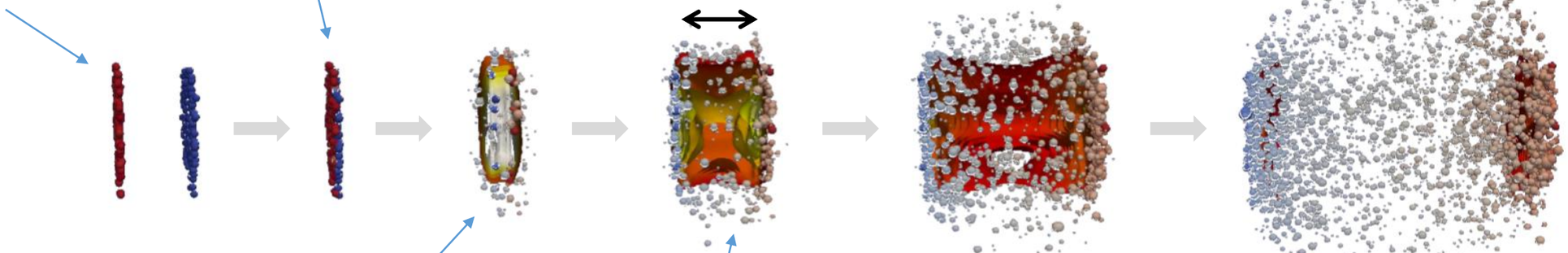

How does the system move toward hydrodynamization?

What are the transport properties of the QGP?
How does QGP respond to hard probes?
What are the inner workings of QGP at various length scales?

What is the in-medium color force?

Visualization taken from Jonah E. Bernhard
arXiv:1804.06469

Probe the Quark Soup!

- How does the strongly interacting medium emerge from an asymptotic free theory?

Start from "un-thermalized" objects and see how they are thermalized in the Quark Soup

- Can we see quasi-particles (at some point, quarks and gluons) in the Quark-Gluon Plasma? What is the structure of QGP probed at different length scales?

"QGP Rutherford Experiment" and HQ Diffusion

- What are the transport properties of the medium?

Study how Colored Probes are modified by QGP
Study how QGP respond to Colored Probes

Hard Probes

Atoms➔Nuclei

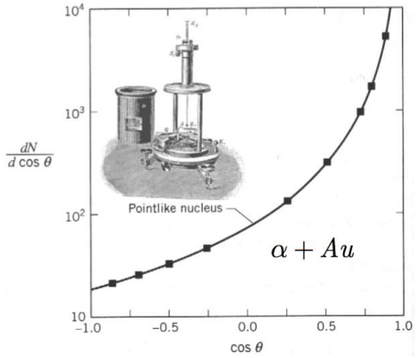

Nuclei➔Nucleons

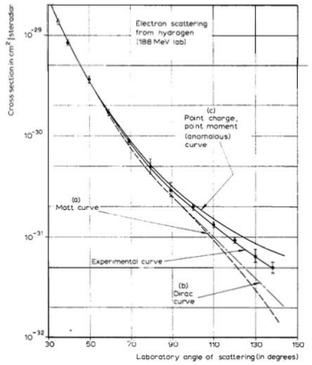

Nucleons➔Quarks

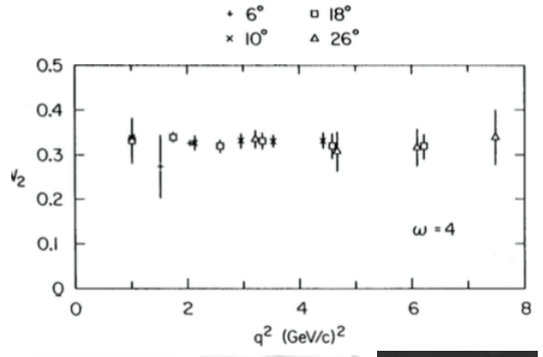

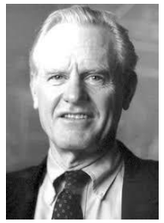

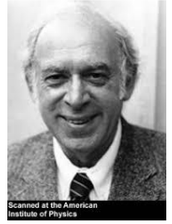

James Bjorken (1982)

FERMILAB-PUB-82-059-T

Jet Quenching

Lifetime O(10^{-24}s)

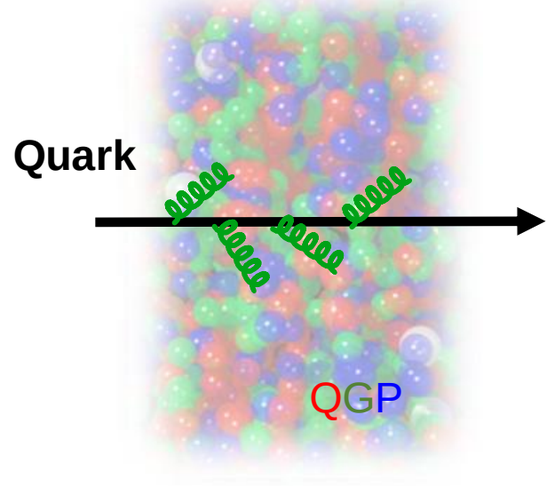

One use **Energetic Quarks** to reveal QGP structure at various length scales

The Advantage of Hard Probes

- Momentum scale is well above QCD scale Λ_{QCD} ~ 200 MeV
  - Described by perturbative methods (pQCD), calculations can be tested with pp scattering
- They are produced early: sensitive to full evolution of QGP
- Sensitive to short wave-length behavior of the medium
  - Transverse resolution of a radiated quanta: $\lambda \sim \frac{1}{Q} \ll 1 \text{ fm}$
  - Example: Q=100 GeV → λ=0.05 fm

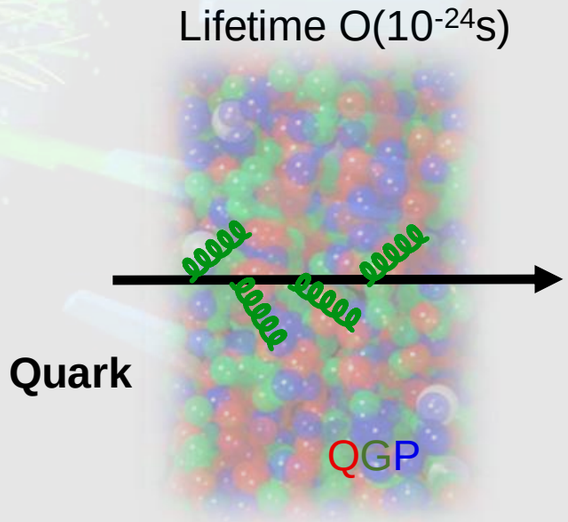

- Long relaxation time: “memory” of their initial conditions at production

Factorization

Factorization

$$\sigma^{AB\to kl} \sim f_i^A(x_1,\mu_F^2) \otimes f_j^B(x_2,\mu_F^2) \otimes \hat{\sigma}^{ij\to kl}$$

Parton Distribution Function (PDF)

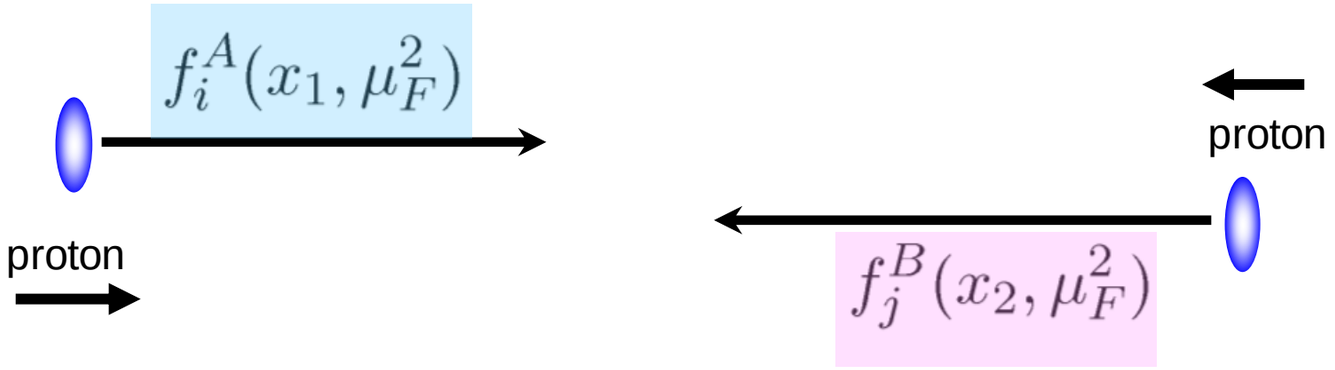

Factorization

$$\sigma^{AB\to kl} \sim f_i^A(x_1,\mu_F^2) \otimes f_j^B(x_2,\mu_F^2) \otimes \hat{\sigma}^{ij\to kl}$$

Parton Distribution Function (PDF) Cross-section of 2→2 process

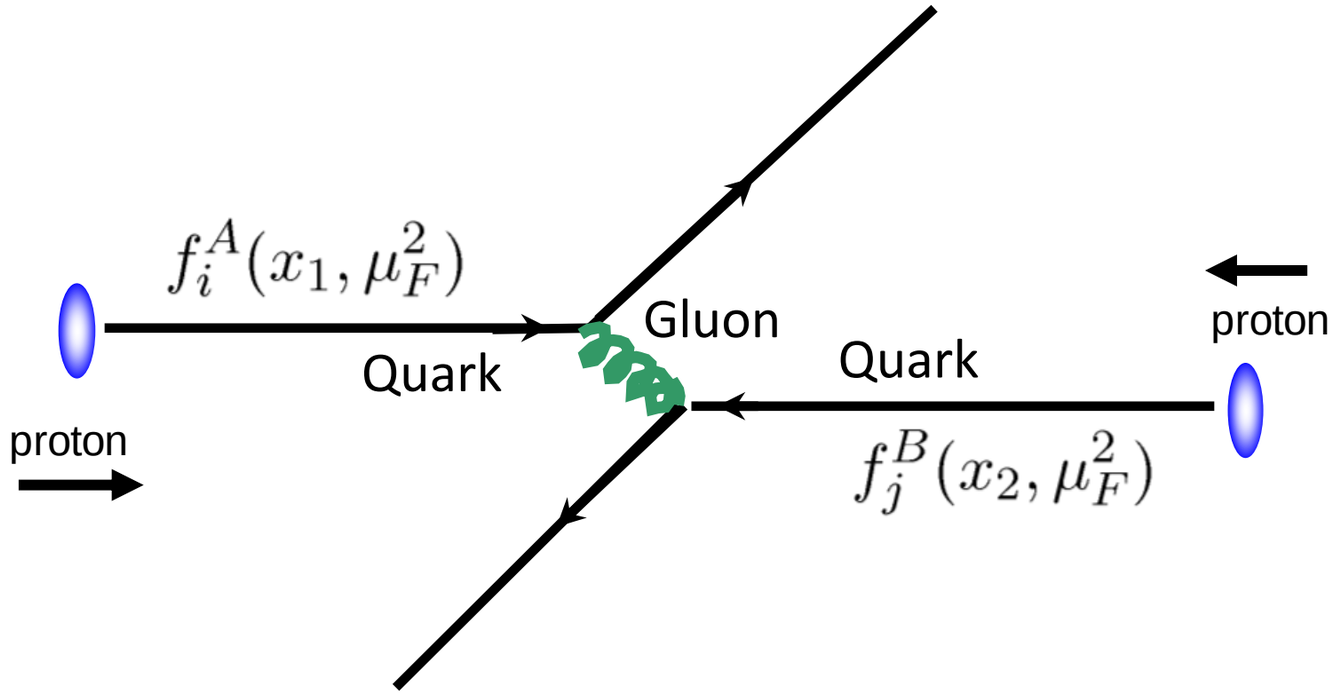

Factorization in AA collisions

$$\sigma^{AB\to kl} \sim f_i^A(x_1,\mu_F^2) \otimes f_j^B(x_2,\mu_F^2) \otimes \hat{\sigma}^{ij\to kl}$$

Nuclear Parton Distribution Function (nPDF) Cross-section of 2→2 process

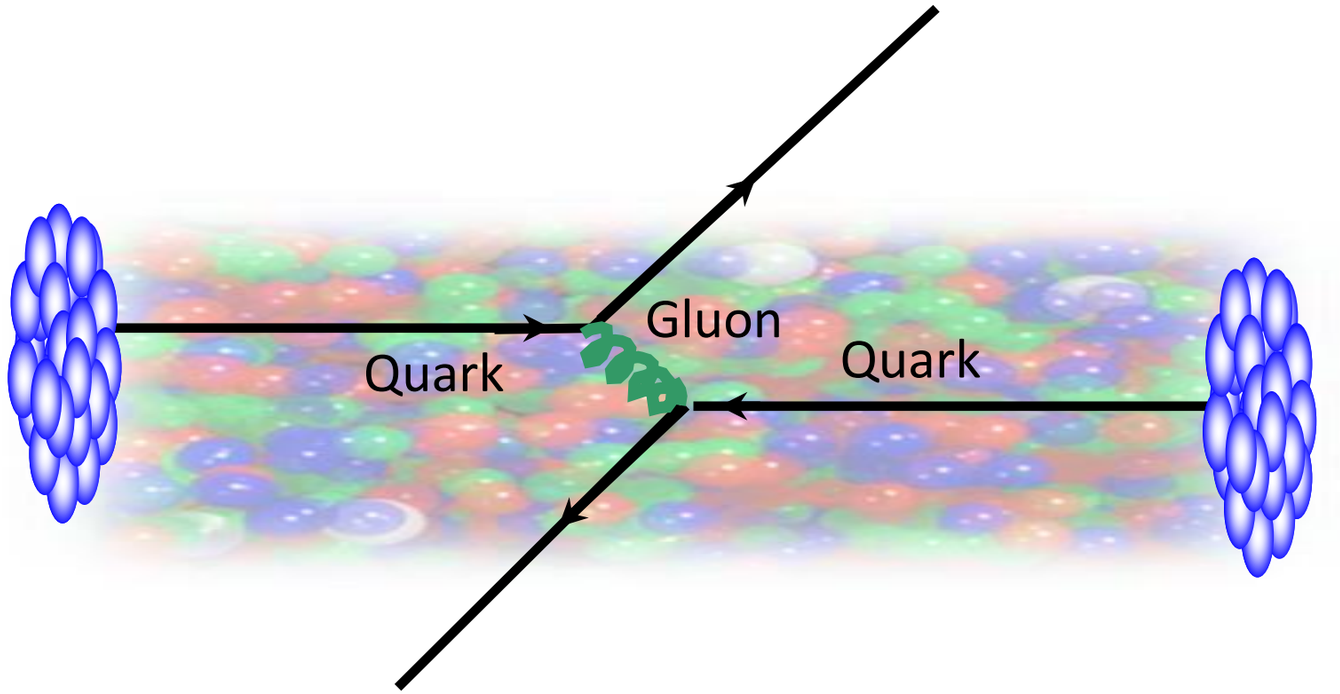

How do we extract the medium effect in A+A collisions?

One typical way is to compare A+A data to pp reference measurement

See for instance review from
D. d'Enterria and C. Loizides
Ann.Rev.Nucl.Part.Sci. 71 (2021) 315-44

A+A measurements

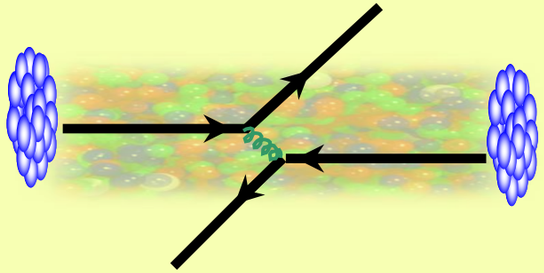

pp reference

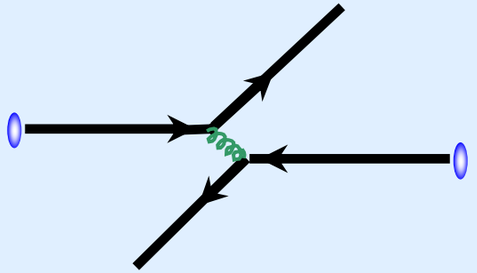

How do we extract the medium effect in A+A collisions?

One typical way is to compare A+A data to pp reference measurement

See for instance review from
D. d'Enterria and C. Loizides
Ann.Rev.Nucl.Part.Sci. 71 (2021) 315-44

A+A measurements

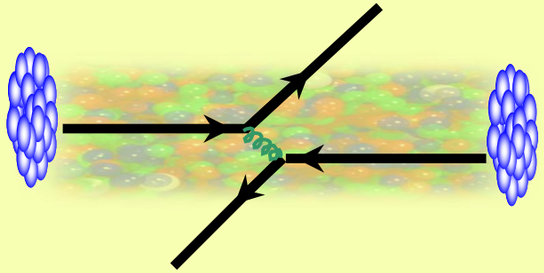

pp reference

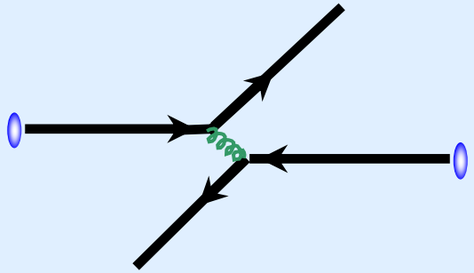

'Nuclear modification factors'

$$R_{AA} = \frac{\sigma_{pp}^{inel}}{N_{coll}} \frac{d^2N_{AA}/dp_T d\eta}{d^2\sigma_{pp}/dp_T d\eta} \sim \frac{\text{"QCD Medium"}}{\text{"QCD Vacuum"}}$$

- $R_{AA} > 1$ (enhancement)
- $R_{AA} = 1$ (no modification)
- $R_{AA} < 1$ (suppression)

N_{coll} → Averaged number of binary scatterings

Can also be written as $1/T_{AA}$

$$T_{AA} = \frac{N_{coll}}{\sigma_{pp}^{inel}}$$

"NN equivalent integrated luminosity per A+A collision"

Reduces the uncertainty from pp inclusive cross-section

How do we extract the medium effect in A+A collisions?

One typical way is to compare A+A data to pp reference measurement

See for instance review from
D. d'Enterria and C. Loizides
Ann.Rev.Nucl.Part.Sci. 71 (2021) 315-44

A+A measurements

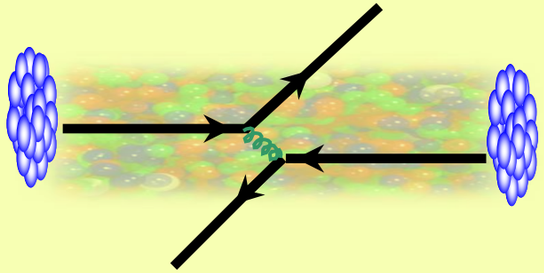

pp reference

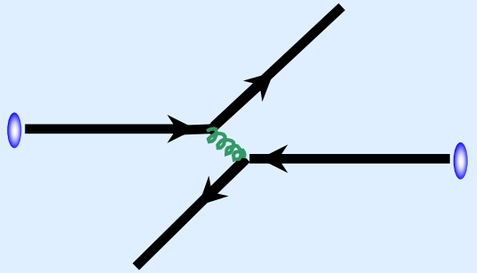

'Nuclear modification factors'

$$R_{AA} = \frac{\sigma_{pp}^{inel}}{N_{coll}} \frac{d^2N_{AA}/dp_T d\eta}{d^2\sigma_{pp}/dp_T d\eta} \sim \frac{\text{"QCD Medium"}}{\text{"QCD Vacuum"}}$$

- $R_{AA} > 1$ (enhancement)
- $R_{AA} = 1$ (no modification)
- $R_{AA} < 1$ (suppression)

N_{coll} → Averaged number of binary scatterings

Questions: How do we know the Glauber model calculation of N_{coll} is correct?

Is the nuclear PDF modified with respect to nucleon PDF?

→ Motivates the studies of electroweak probes and jets in pA

Example: Photon R_{AA}

Z

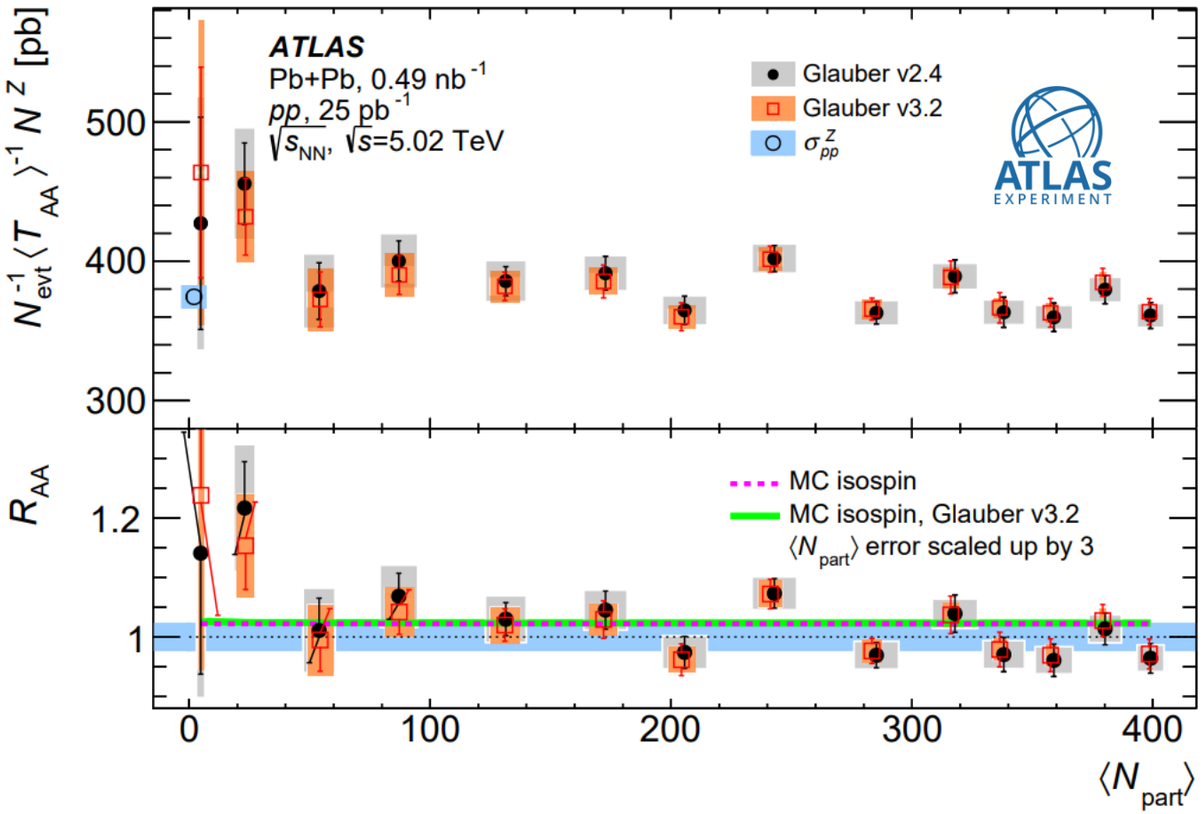

Photons

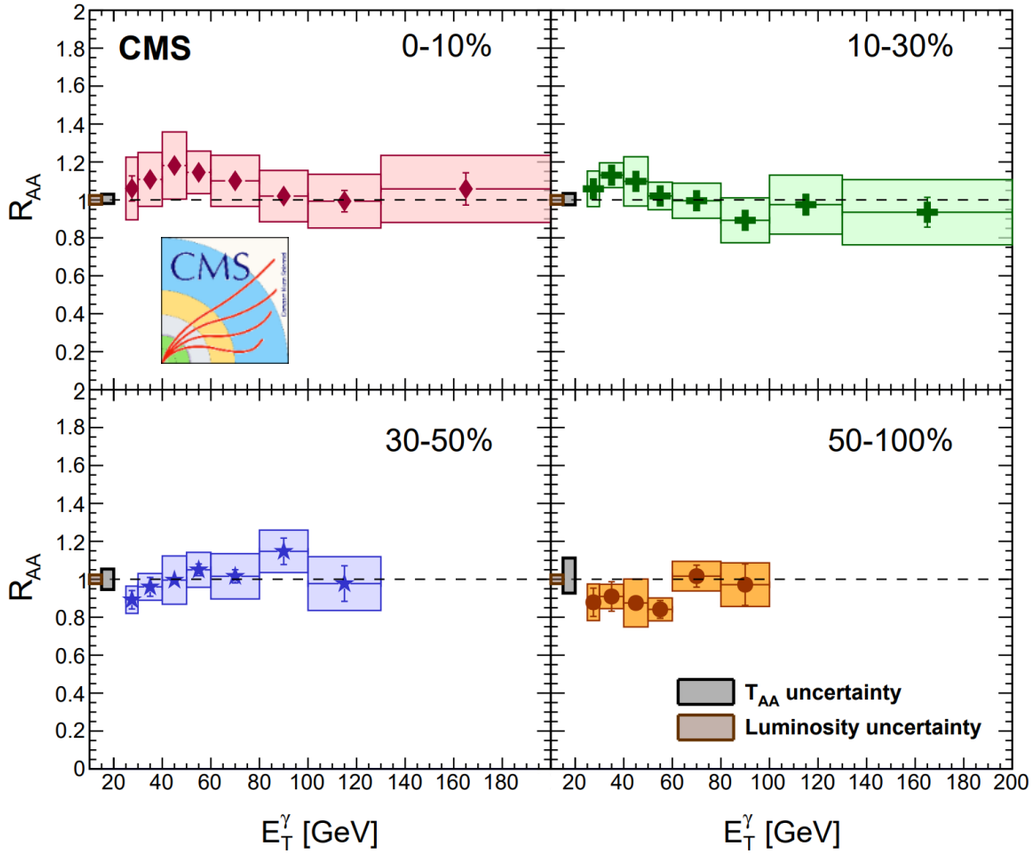

- Electroweak probes do not interact strongly with QGP
- Confirm N_{coll} scaling of hard scattering
- High precision W, Z and isolated photon measurements: constraint nPDF

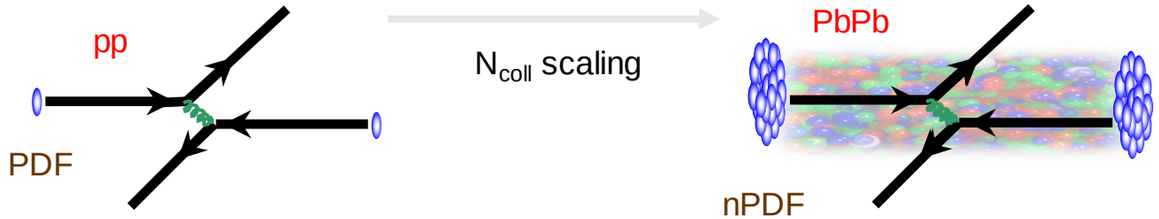

Nuclear Parton Distribution Function

Jet and Heavy Quark for constraining the nuclear parton distribution function

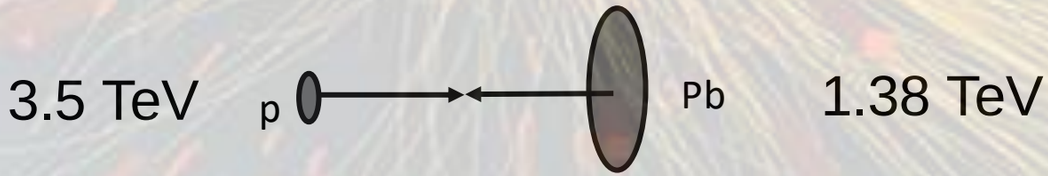

nPDF modification at large Q^2

$$R = \frac{nPDF}{PDF}$$

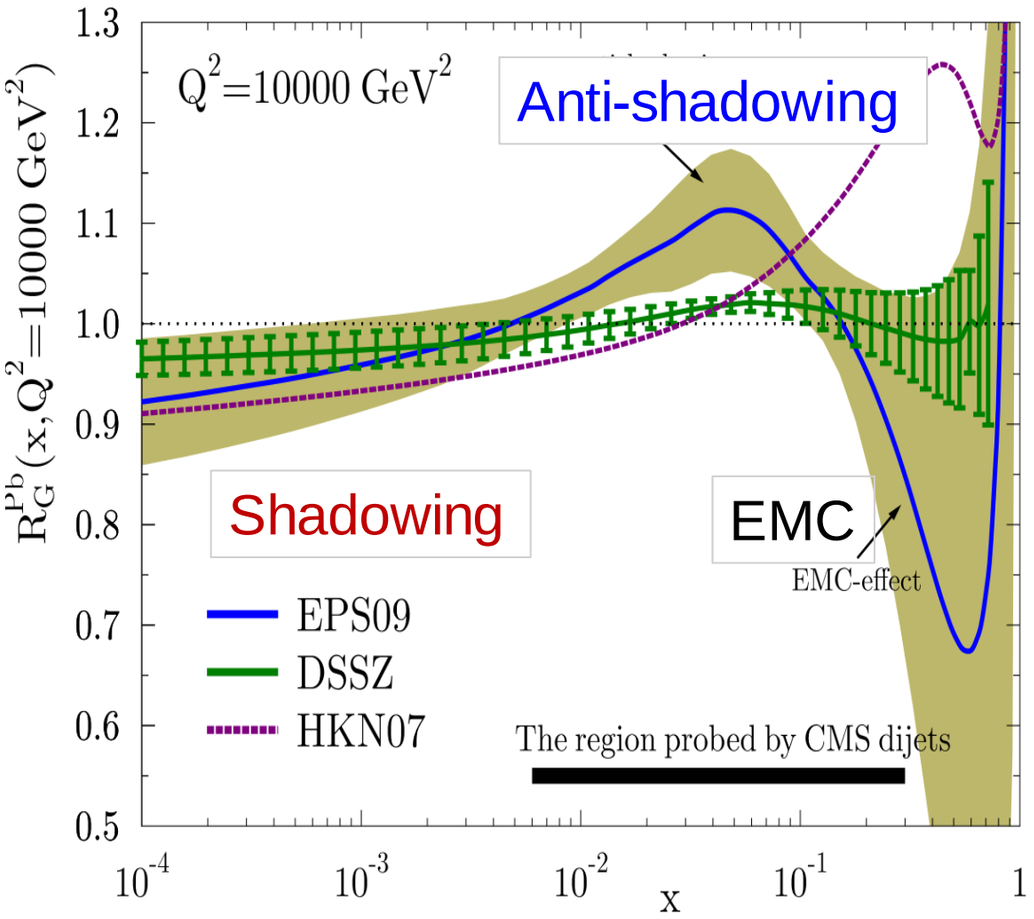

Nuclear modification of hard scattering involving large momentum transfer due to PDF is small (at the order of 10%)

Initial Production Nuclear PDF with D^0 R_{pPb}

Forward D^0 R_{pPb}

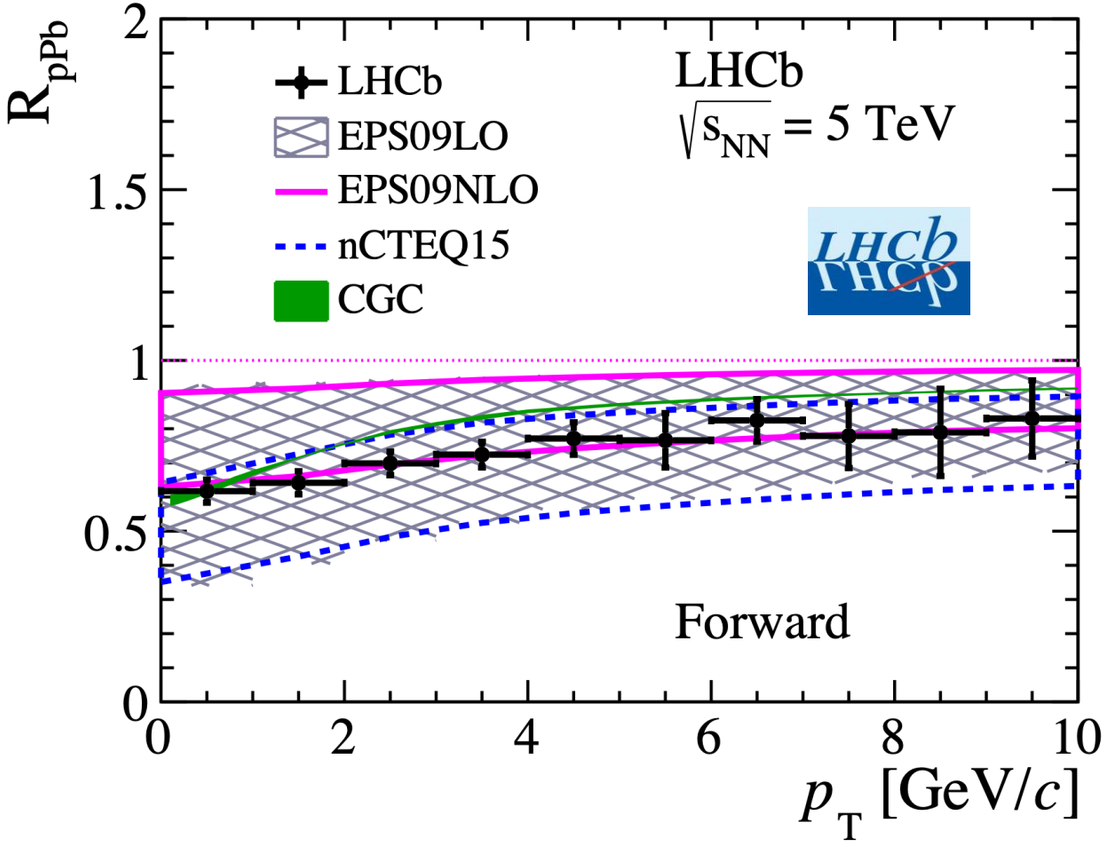

[JHEP 10 (2017) 090]

Midrapidity D R_{pPb}

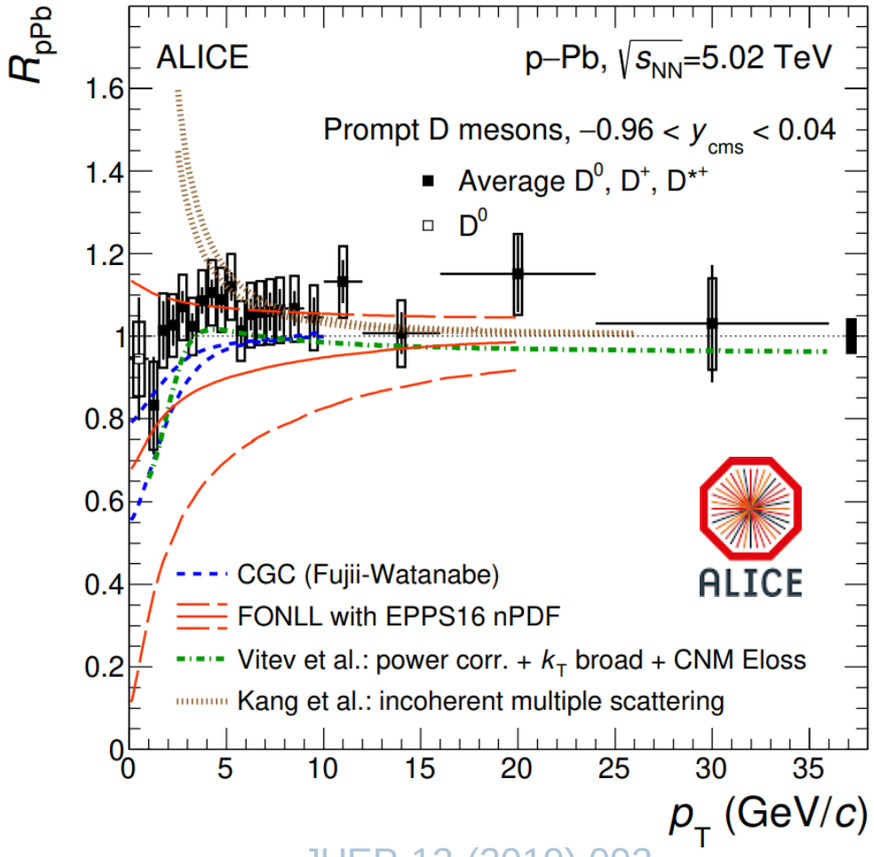

JHEP 12 (2019) 092

Significant suppression of D^0 in the forward region
Larger suppression at low D^0 p_T from LHCb

Prompt D in the mid-rapidity:
Consistent with unity within uncertainty

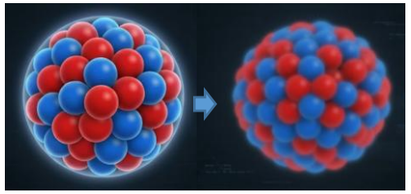

Initial Production Nuclear PDF with D^0 R_{pPb}

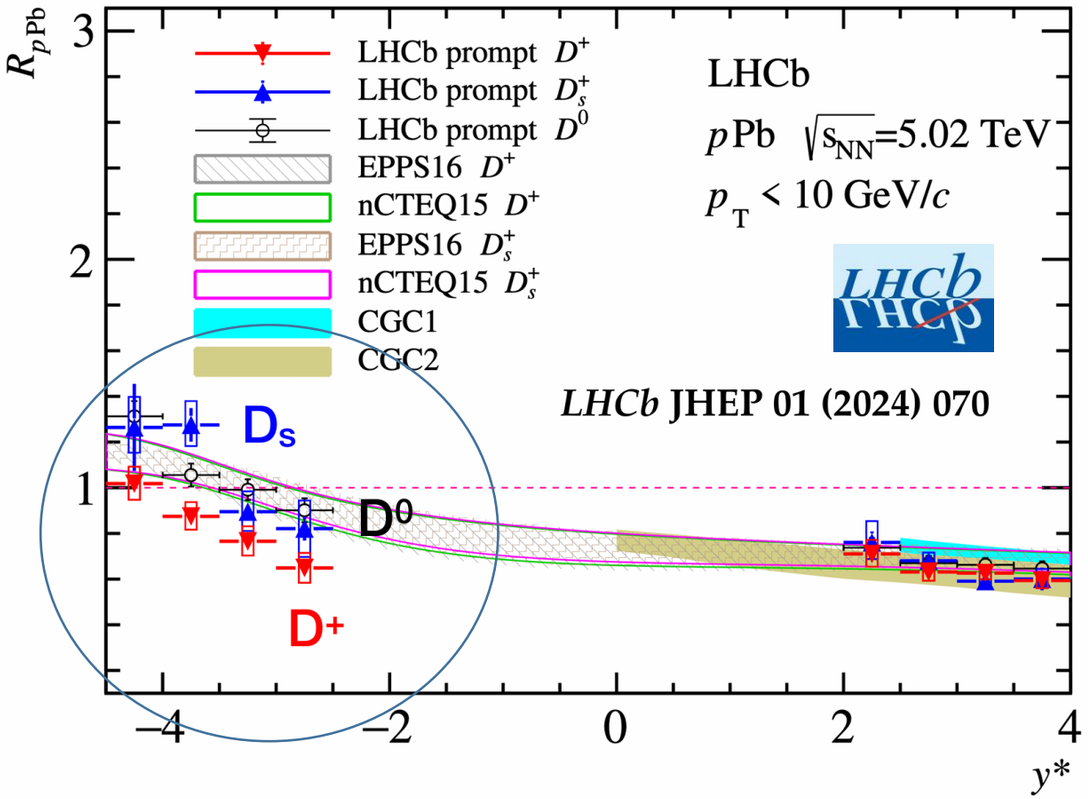

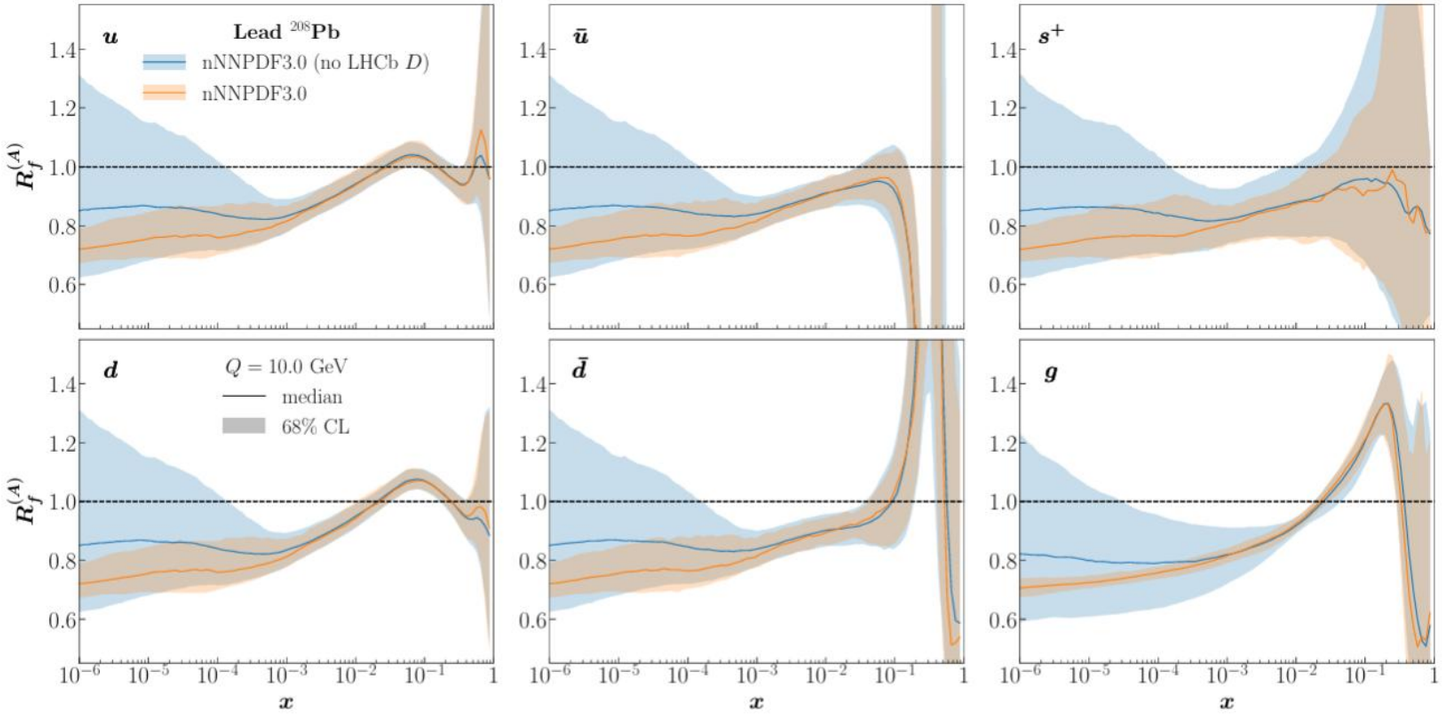

Significant **hadronization effects** may present in the experimental data

Backward region R_{pPb}: (**high x** region)

$D_s \geq D^0 \geq D^+$

Strong constraints on gluon PDF at **low x** from **LHCb D^0** and CMS dijet at intermediate to high x in pPb collisions in NNPDF3.0 (shown), EPPS21 and nCTEQ25

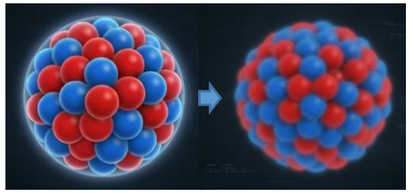

nPDF analyses should proceed with caution!

Different Interpretation of the Pion Data

Hadron observables: sensitive to possible modifications of **fragmentation function** and **hadronization** → Different interpretation of the data!

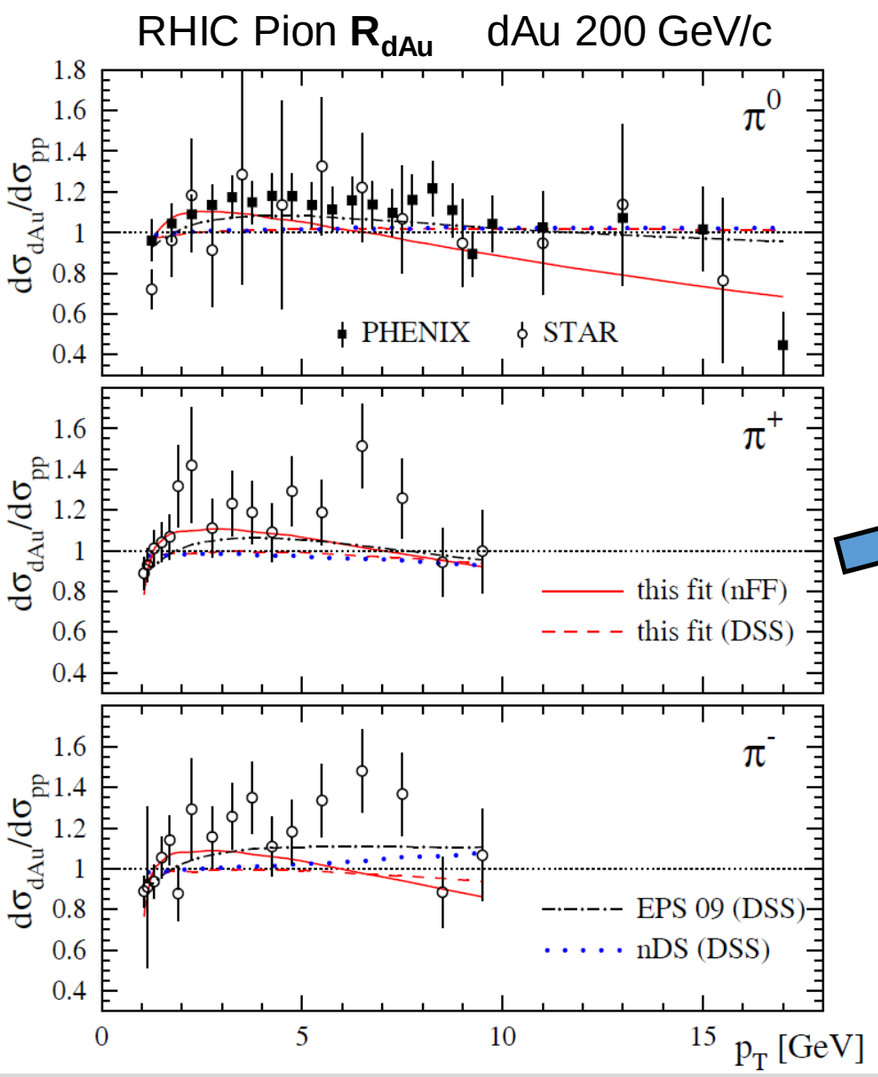

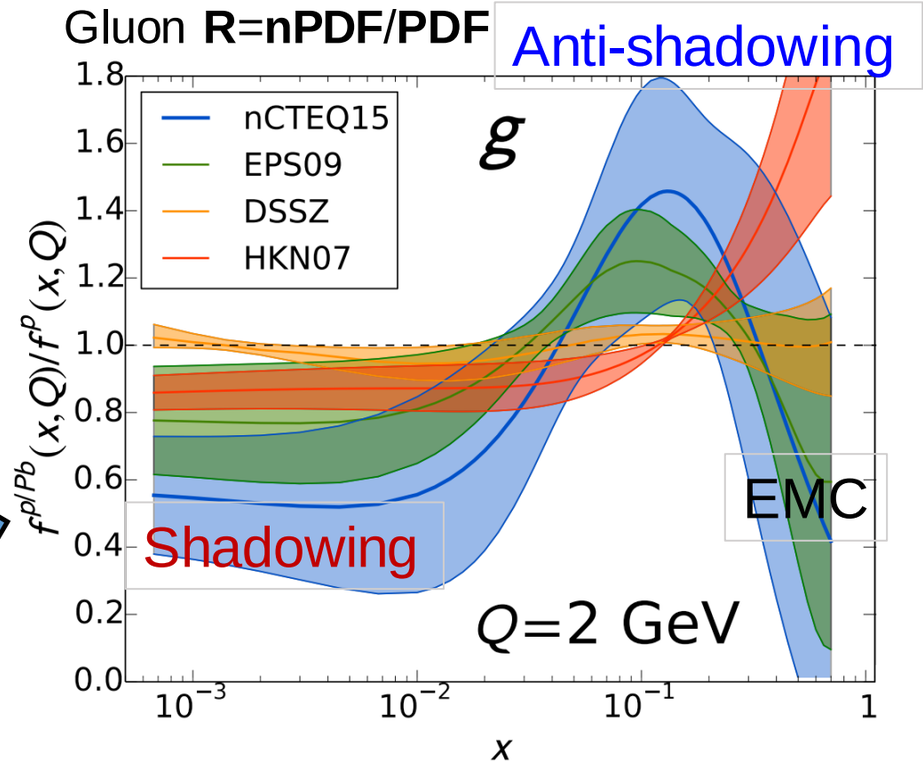

- **EPS09** & **nCTEQ15**: hint of **anti-shadowing** and **EMC effect** of gluon nPDF
- **DSSZ**: modification of parton-to-pion fragmentation function in heavy ion collisions and no gluon anti-shadowing

Detecting Quarks and Gluons in e^+e^- collisions

Dijet event

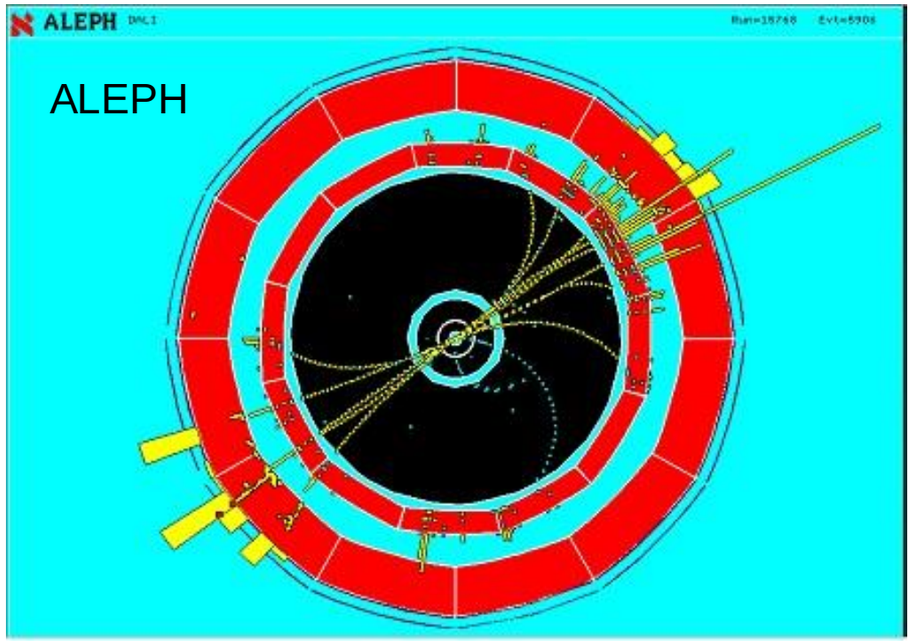

$$e^+ + e^- \rightarrow q + \bar{q}$$

Trijet event

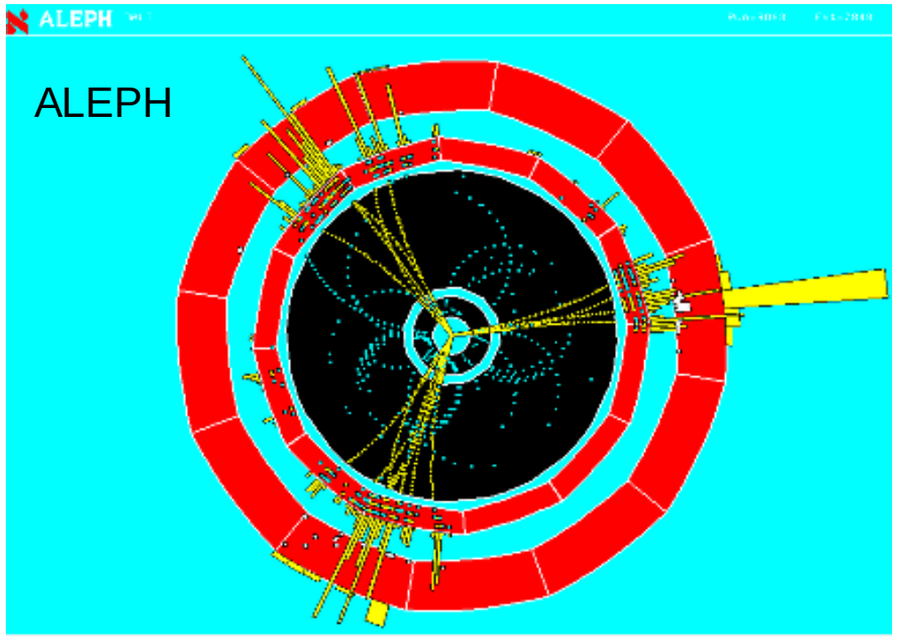

$$e^+ + e^- \rightarrow q + \bar{q} + g$$

Jets (defined by jet clustering algorithm) are used as a proxy of quarks and gluons

Anti-k_T algorithm

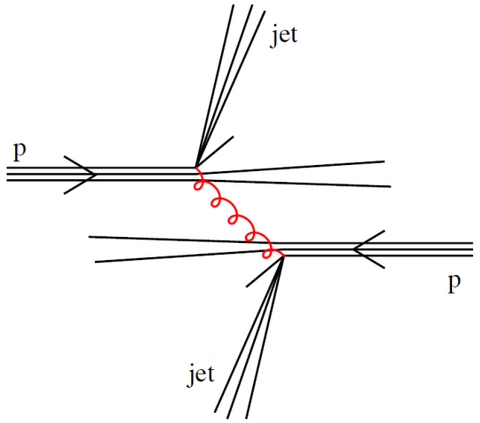

From Gavin Salam

$$d_{ij} = \min\left(\frac{1}{k_{ti}^2}, \frac{1}{k_{tj}^2}\right)\frac{\Delta R_{ij}^2}{R^2}, \qquad d_{iB} = \frac{1}{k_{ti}^2}$$

PP event

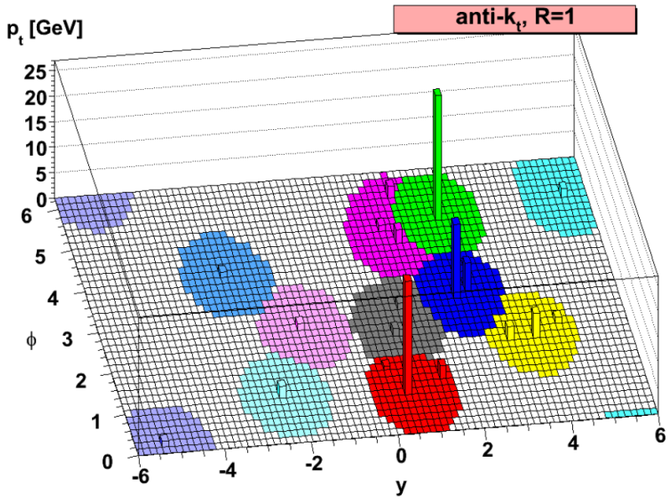

$$\Delta R_{ij}^2 = (y_i - y_j)^2 + (\phi_i - \phi_j)^2$$

1. Find smallest of d_{ij}, d_{iB}
2. if ij, recombine them
3. if iB, call i a jet and remove from list of particles
4. repeat from step 1 until no particles left.

Cacciari, GPS & Soyez, '08

Clustering start from high p_T particles. Clustered shape has circular shape.
Now commonly used in the analysis of heavy ion collision

Jet Composition

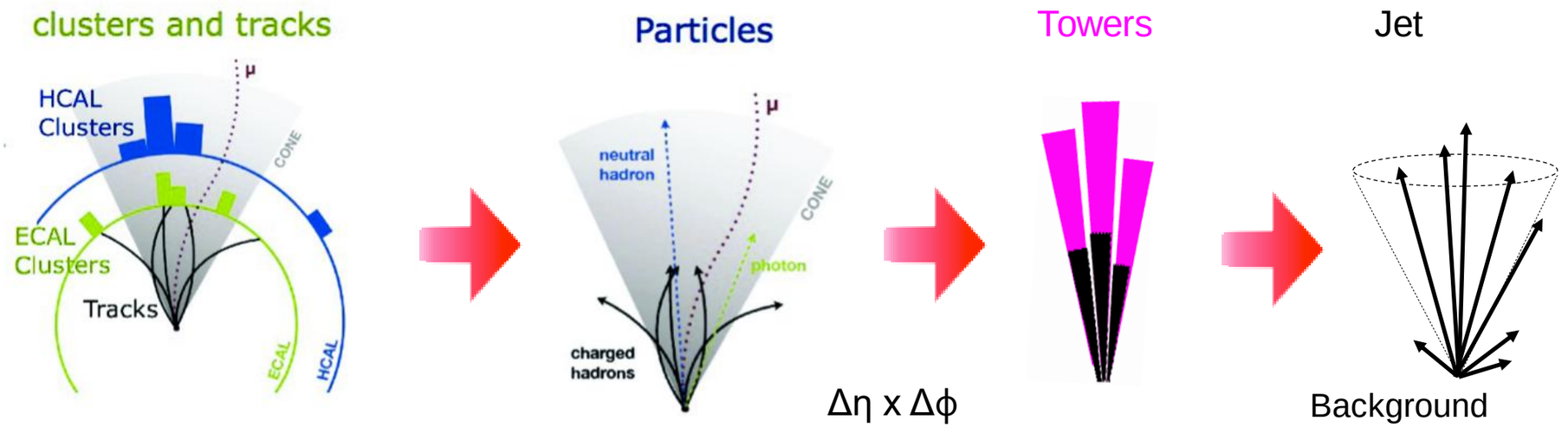

$\Delta\eta \times \Delta\phi$
0.076 x 0.076 in barrel

Background subtraction and jet clustering

Anti-k_T algorithm is used in most CMS publication

On average, charged hadrons carry 65% of the jet momentum

Measure the known part
Correct the rest by MC simulation

Optimize the use of calorimeter and tracker
Example: “Particle Flow” in CMS

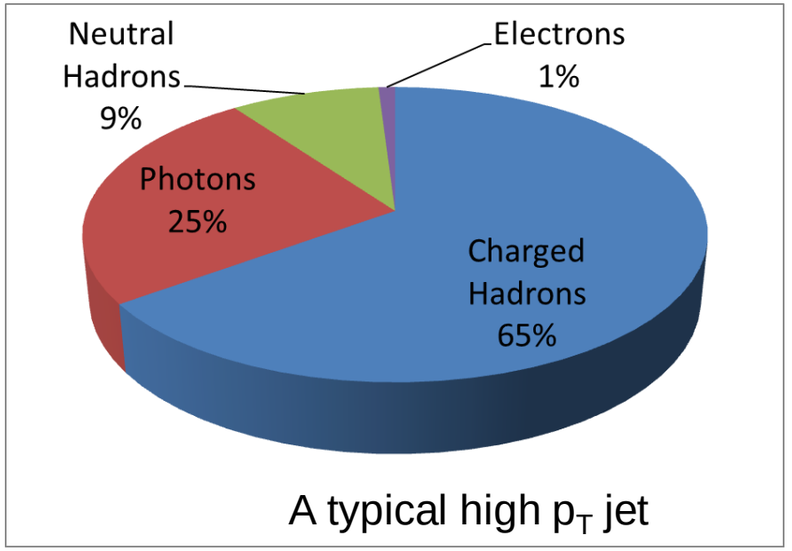

A typical high p_T jet

Inclusive Jet Spectra: Scanning the Parton Shower

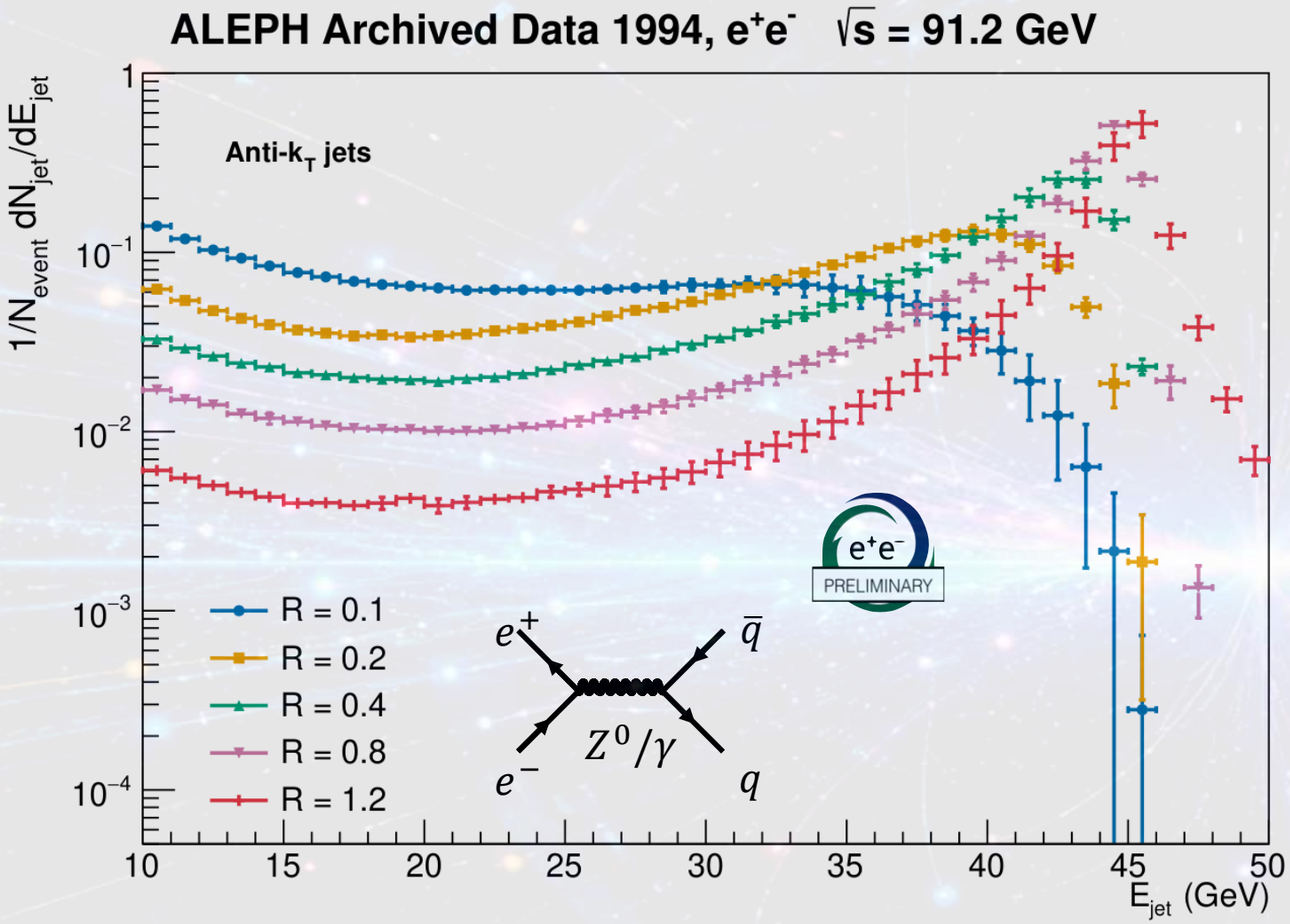

- **New preliminary radius scan:** fully corrected energy spectra for R values from 0.1 to 1.2
- **Small R resolves the shower:** radiation is split into many narrow, lower-energy jets; the 45.6 GeV peak softens and moves to lower energy.
- **Large R captures the hemisphere:** radiation recombines into one jet near $E_{jet} \approx m_Z/2 \approx 45.6$ GeV.

R↓ resolves radiation → R↑ rebuilds the $m_Z/2$ peak

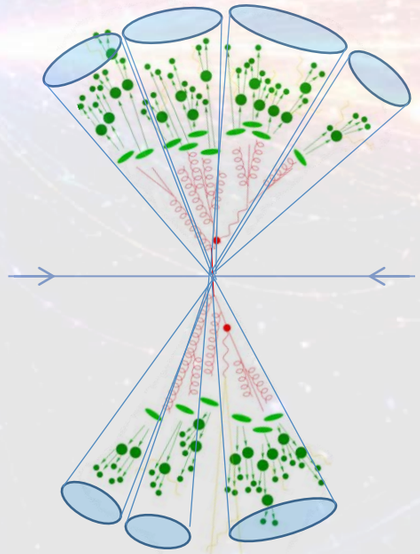

vs.

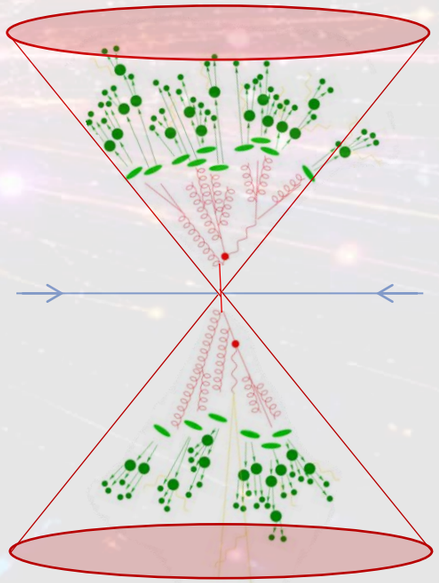

Jet Spectra in pp(bar) collisions

ppbar 1.96 TeV

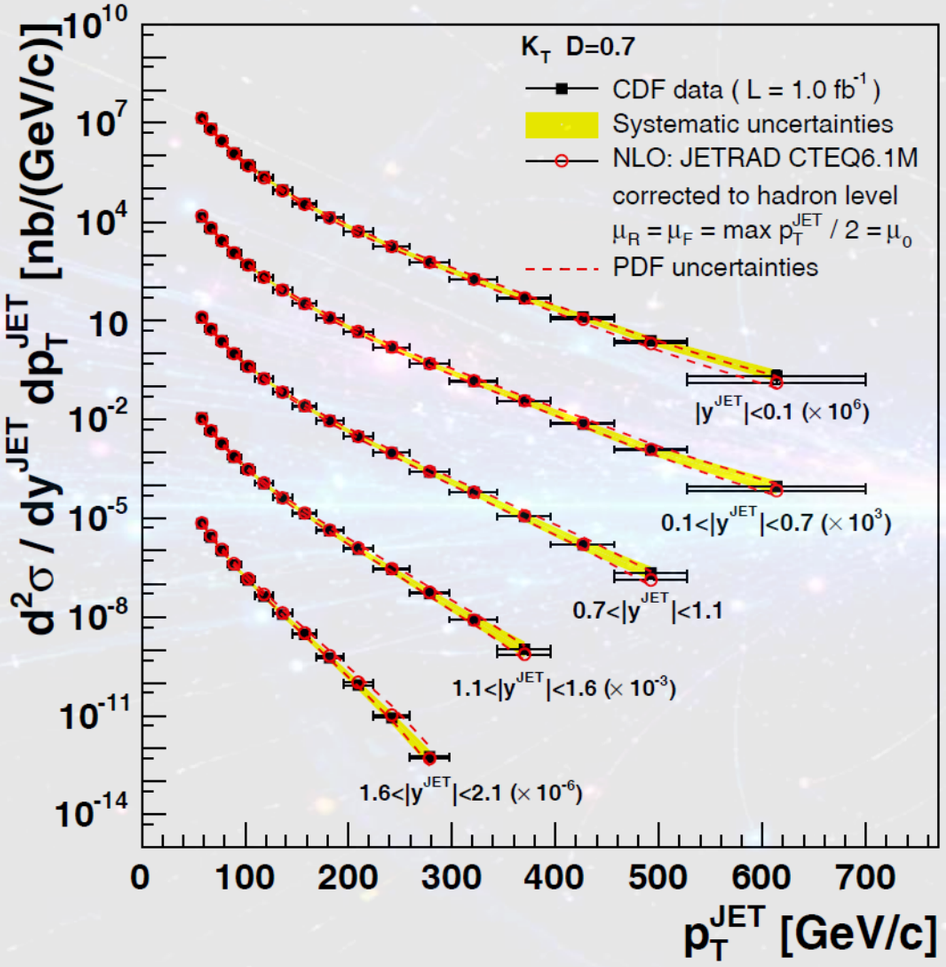

pp 13TeV

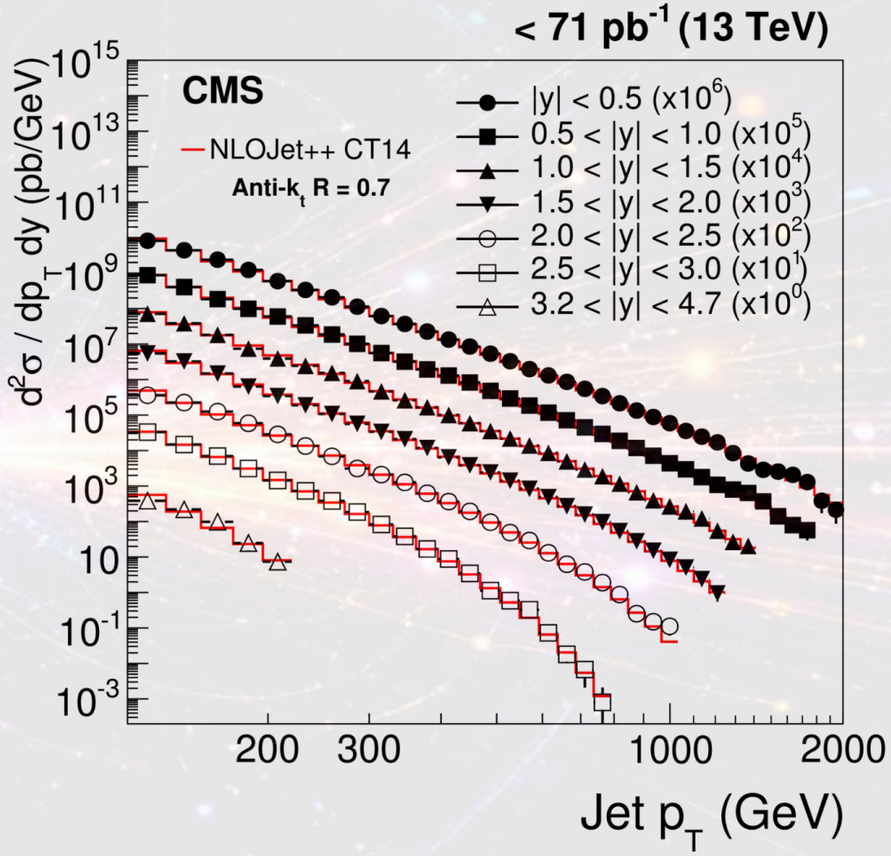

Jet spectra with large R parameter from proton-(anti-)proton collisions are well understood. Consistent with NLO calculations.

Dijet pseudorapidity in the LAB Frame

Idea: Angular distributions of high p_T dijets

CMS pPb 35 nb^{-1}

$\sqrt{s_{NN}}$ = 5.02 TeV

$p_{T,1}$ > 120 GeV/c

$p_{T,2}$ > 30 GeV/c

$\Delta\phi_{1,2} > 2\pi/3$

All $E_T^{4<|\eta|<5.2}$

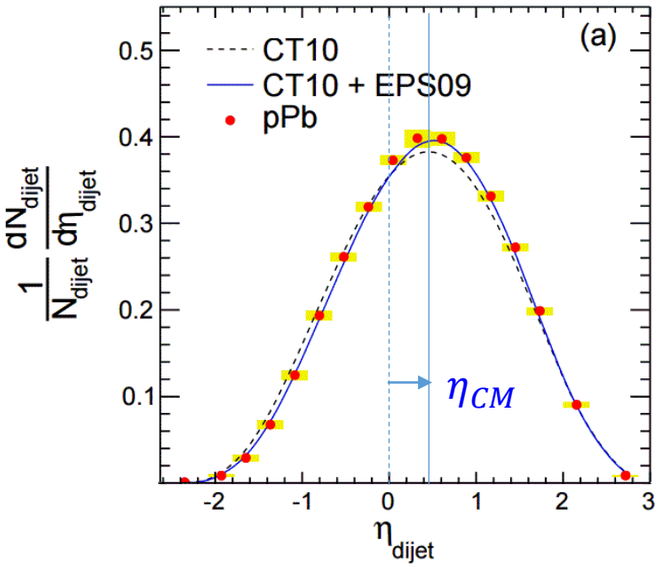

$$\eta_{dijet} = \frac{\eta_1 + \eta_2}{2}$$

$$\propto 0.5 \log\left(\frac{x_p}{x_{Pb}}\right) + \eta_{CM}$$

- Jets: Less sensitive to fragmentation functions and hadronization effects
- Can be calculated with pQCD with small theoretical uncertainties
- Normalized distribution: lead to smaller theoretical and experimental uncertainties

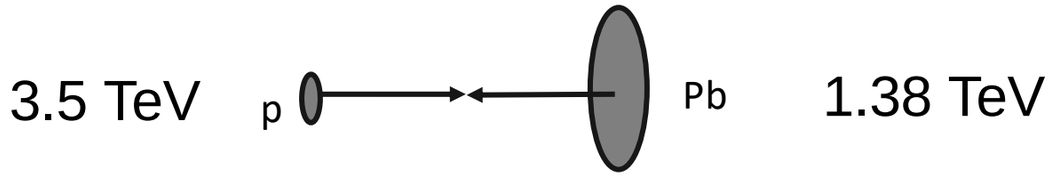

Distribution shift to positive value due to asymmetric proton and lead ion beam energy

EPJC 74 (2014) 2951

Dijet pseudorapidity in the LAB Frame

Idea: Angular distributions of high p_T dijets

CMS pPb 35 nb^{-1}

$\sqrt{s_{NN}}$ = 5.02 TeV

$p_{T,1}$ > 120 GeV/c

$p_{T,2}$ > 30 GeV/c

$\Delta\phi_{1,2} > 2\pi/3$

All $E_T^{4<|\eta|<5.2}$

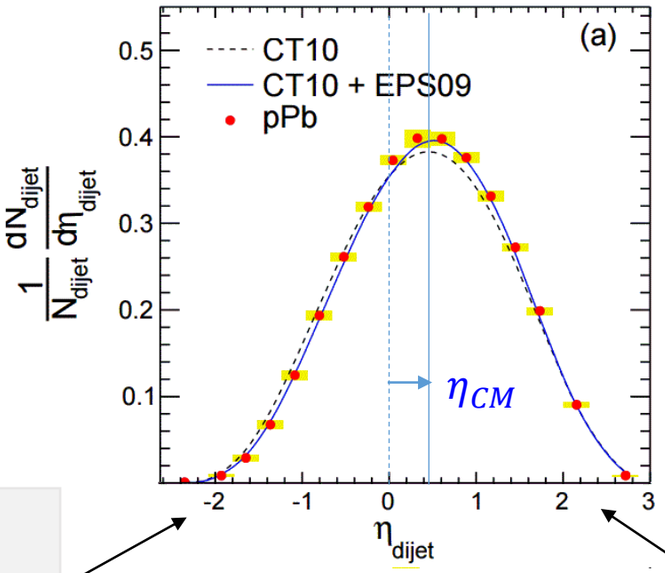

$$\eta_{dijet} = \frac{\eta_1 + \eta_2}{2} \propto 0.5 \log\left(\frac{x_p}{x_{Pb}}\right) + \eta_{CM}$$

$x_p < x_{Pb}$

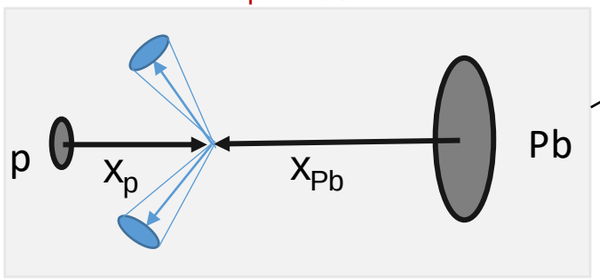

Sensitive to EMC effect

$x_p \sim x_{Pb}$

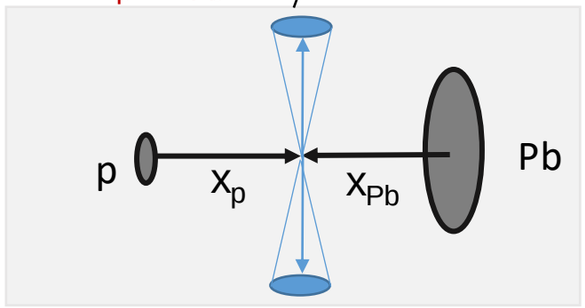

Sensitive to anti-shadowing

$x_p > x_{Pb}$

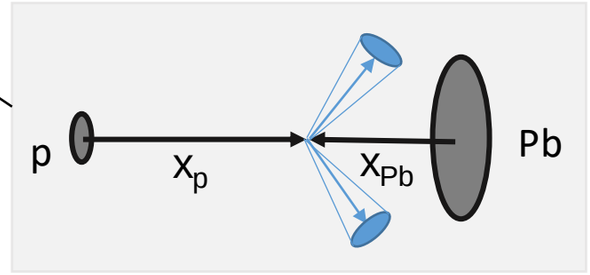

Sensitive to shadowing

EPJC 74 (2014) 2951

Dijet Pseudorapidity in pPb vs. pp

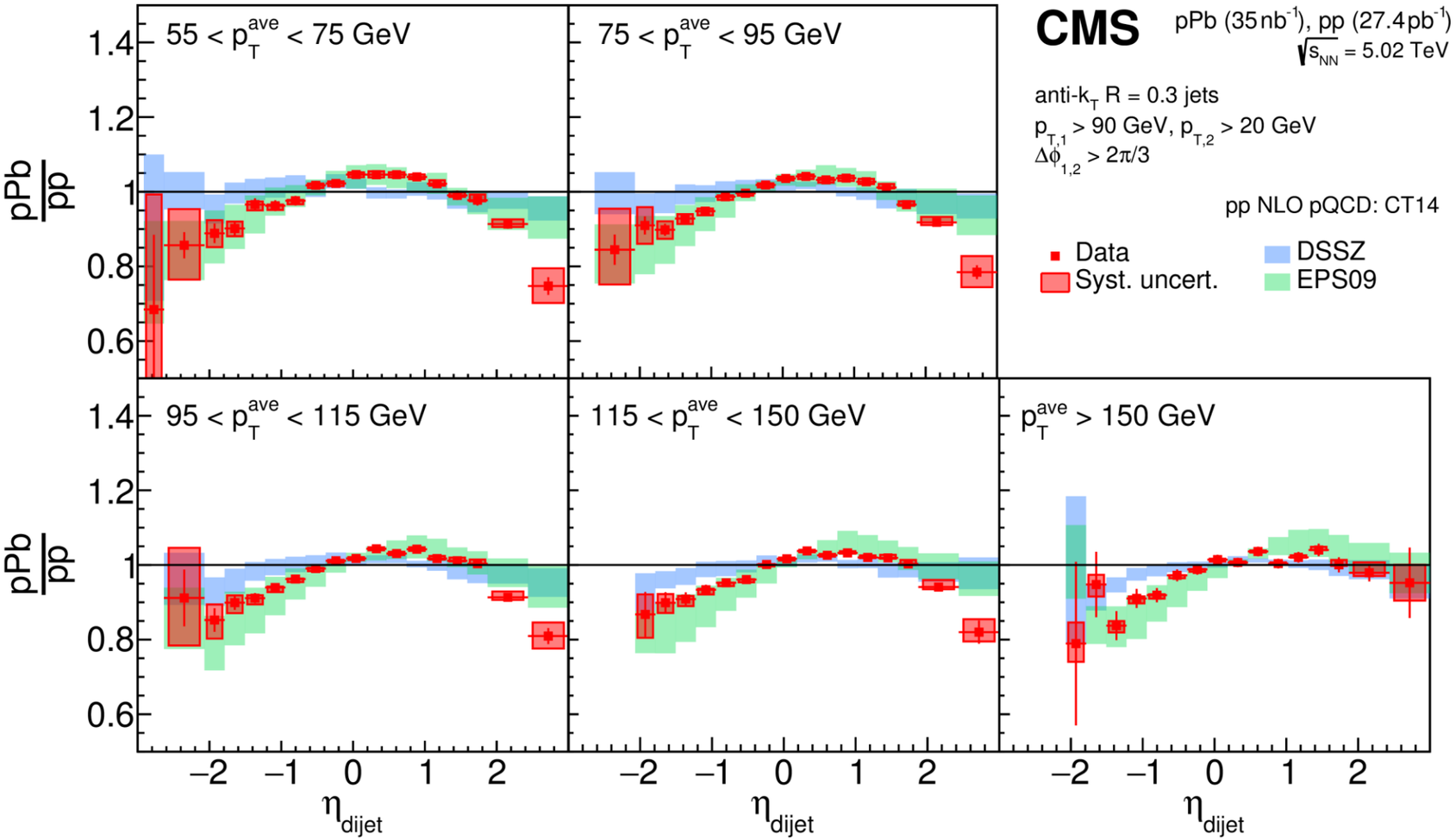

- **EPS09**: hint of **anti-shadowing** and **EMC effect** of gluon nPDF
- **DSSZ**: modification of parton-to-pion fragmentation function in heavy ion collisions and no gluon anti-shadowing

Summary: Vacuum Baseline

- Electroweak boson data and proton-lead data were used to provide additional constraints on the nuclear parton distribution function
- Dijet reduce fragmentation ambiguity and provide sensitivity to nuclear gluon PDFs
- We have learned a lot about the QGP and the initial state of the heavy ion collisions from the Soft Probes
- Next: We will probe the Quark Gluon Plasma with fast moving hard probes.

Backup Slides

Relativistic Heavy Ion Collisions (Simulation)

MIT Heavy Ion Event Display: Pb+Pb 5.02 TeV

Quark Gluon Plasma

Baryons 

Mesons 

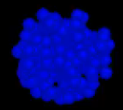

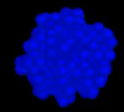

Yen-Jie Lee, Andre S. Yoon and Wit Busza

Acceleration

Relativistic Heavy Ion Collisions

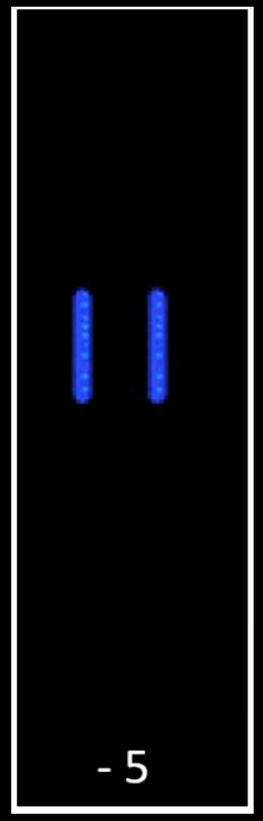

Two Lorentz-Contracted Nuclei, described at high energy as dense sheets of quarks, gluons and color fields

Relativistic Heavy Ion Collisions

Collision! Highest energy density state. A huge number of soft (low momentum transfer) scatterings/interaction.

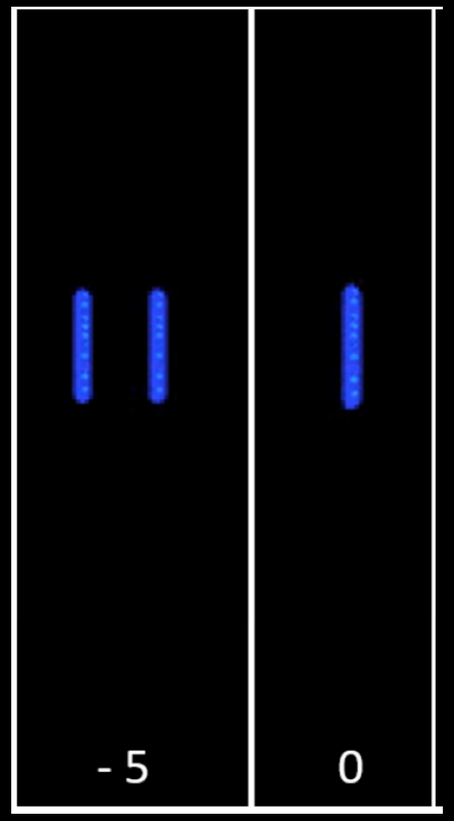

Two Lorentz-Contracted Nuclei, described at high energy as dense sheets of quarks, gluons and color fields

Relativistic Heavy Ion Collisions

Collision! Highest energy density state. A huge number of soft (low momentum transfer) scatterings/interaction.

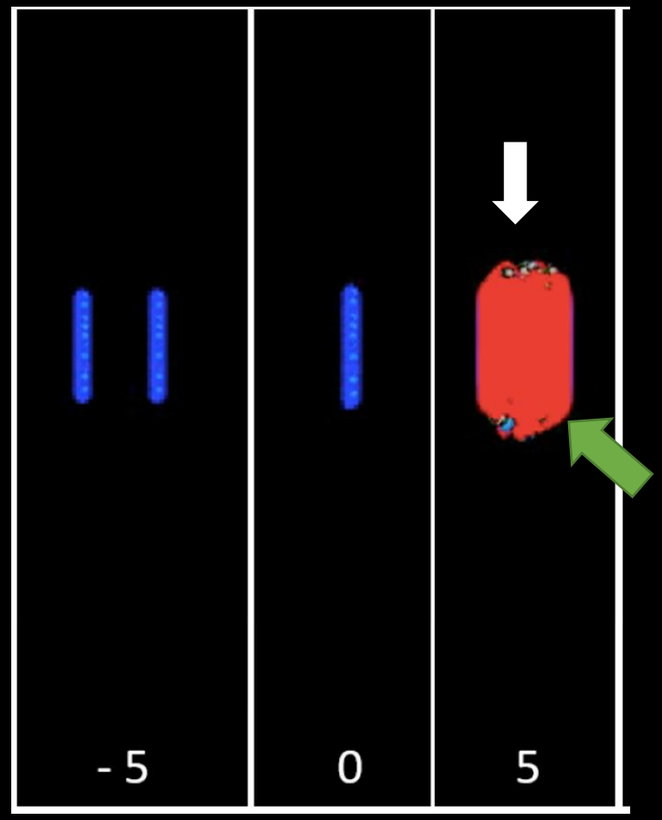

Two Lorentz-Contracted Nuclei, described at high energy as dense sheets of quarks, gluons and color fields

Midrapidity: hydrodynamized QGP with very small baryon doping (μ_B)
Forward: newly produced baryon-rich matter with larger μ_B and less equilibration

Relativistic Heavy Ion Collisions

Collision! Highest energy density state. A huge number of soft (low momentum transfer) scatterings/interaction.

Bulk QGP hadronization differs from fragmentation-dominated hadronization in e^+e^- or pp collisions

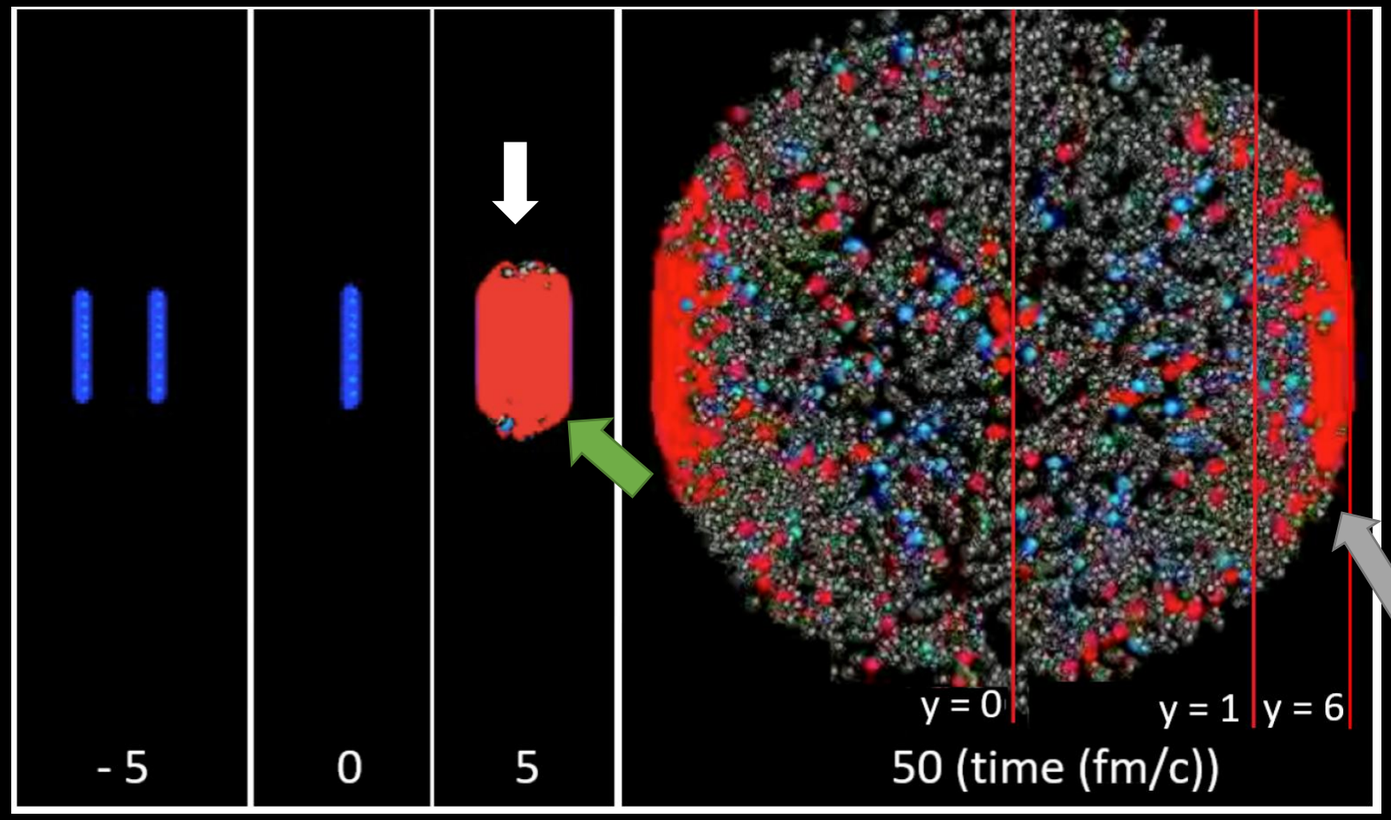

Two Lorentz-Contracted Nuclei, described at high energy as dense sheets of quarks, gluons and color fields

Midrapidity: hydrodynamized QGP with very small baryon doping (μ_B)
Forward: newly produced baryon-rich matter with larger μ_B and less equilibration

Participant baryons can lose ~ 85% of the momentum and appear at forward rapidity, creating a baryon-rich matter with larger μ_B.

Parton Distribution Function

Nuclear Parton Distribution Functions (nPDF)

Deep Inelastic Scattering Data

Drell-Yan Data

RHIC Pion Data

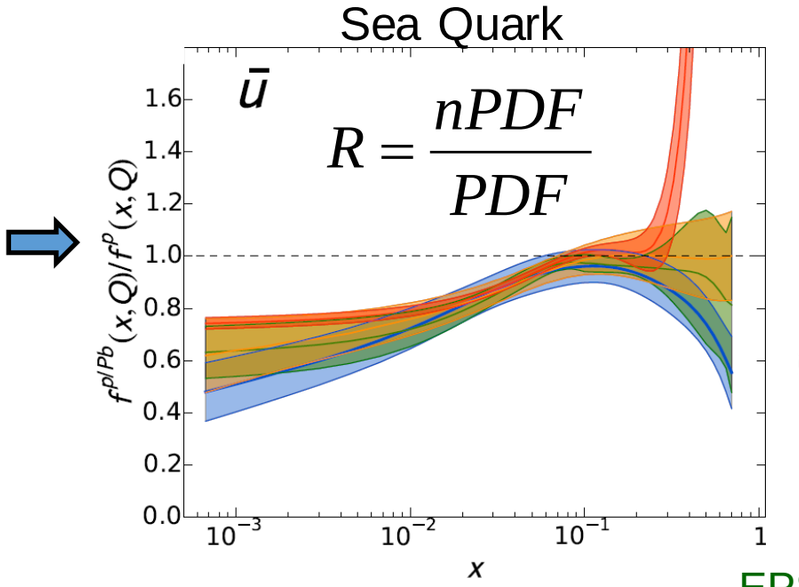

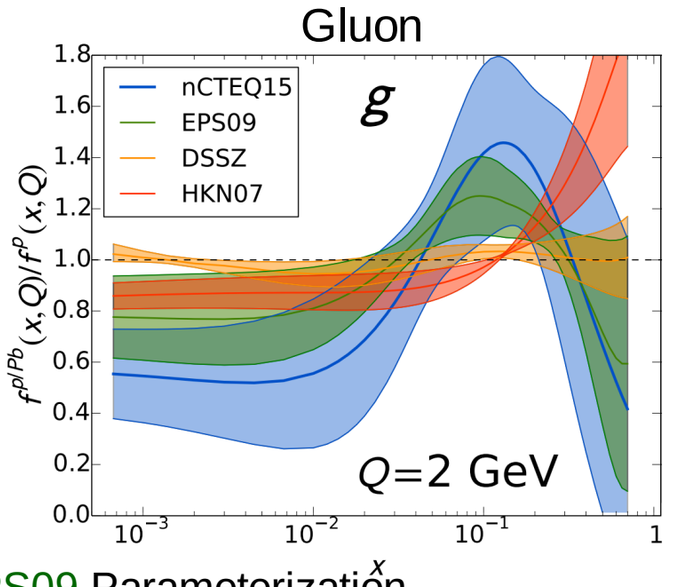

	Q^2 cutoff	DIS	DY	PHENIX Pion	STAR Pion
HKN07	1	V	V		
EPS09	1.69	V	V	V	
DSSZ	1	V	V	V	V
nCTEQ15	4	V	V	V	V

EPS09 Parameterization

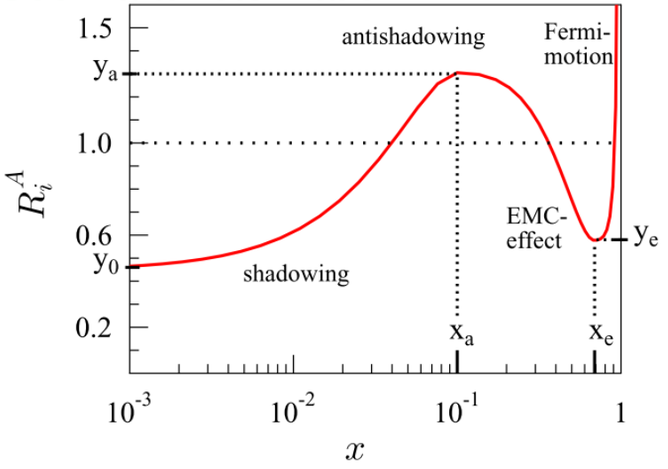

EPPS16: with LHC pPb data (W,Z, jets)

Initial Production Nuclear Modification

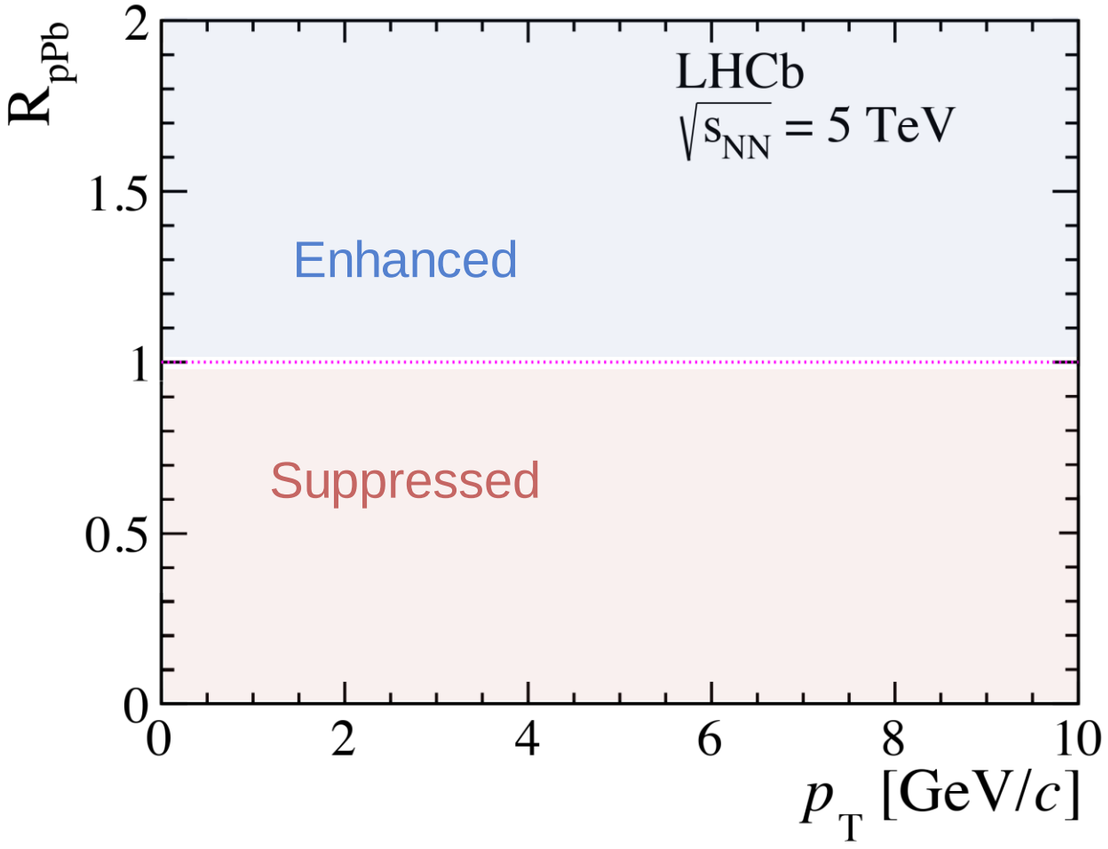

Is initial production in A-A collisions just superposition of nucleon-nucleon collisions?

- p-A collisions to test these kind of effects
  - Ion as collision particles
  - No medium effect expected

- Observable of particle yield modification in pA collisions compared to pp

$$R_{pA} = \frac{\mathrm{d}\sigma_{pA}/\mathrm{d}p_T}{A\mathrm{d}\sigma_{pp}/\mathrm{d}p_T} \quad \begin{matrix} \leftarrow \text{pA} \\ \leftarrow \text{pp} \end{matrix}$$

  - R_{pA} should be 1 in the naive picture above

Phases of QED (Electrons and Nuclei) Matter

Vapor

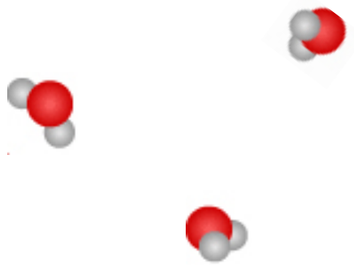

Water

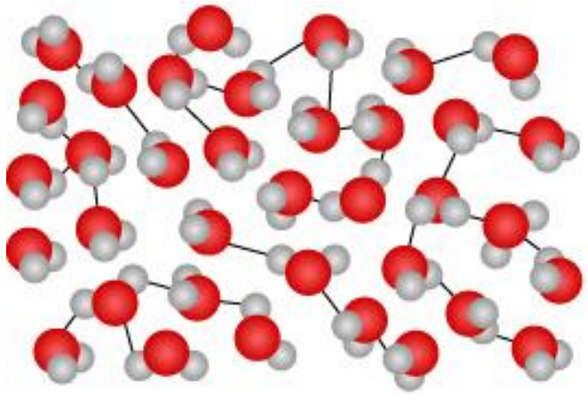

Ice

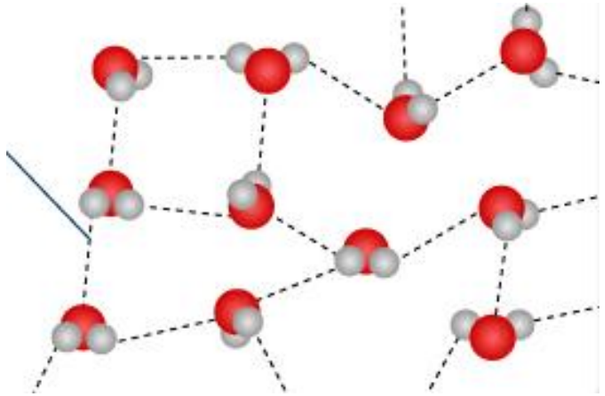

Lattice QCD Equation of State

- Solve the QCD equation of state on a discrete space-time lattice
- Reliable for zero net baryon density!
- Indeed, we see a rapid increase in the degrees of freedom!!!
- Predicts a speed of sound $c_s \approx 0.4 - 0.55$

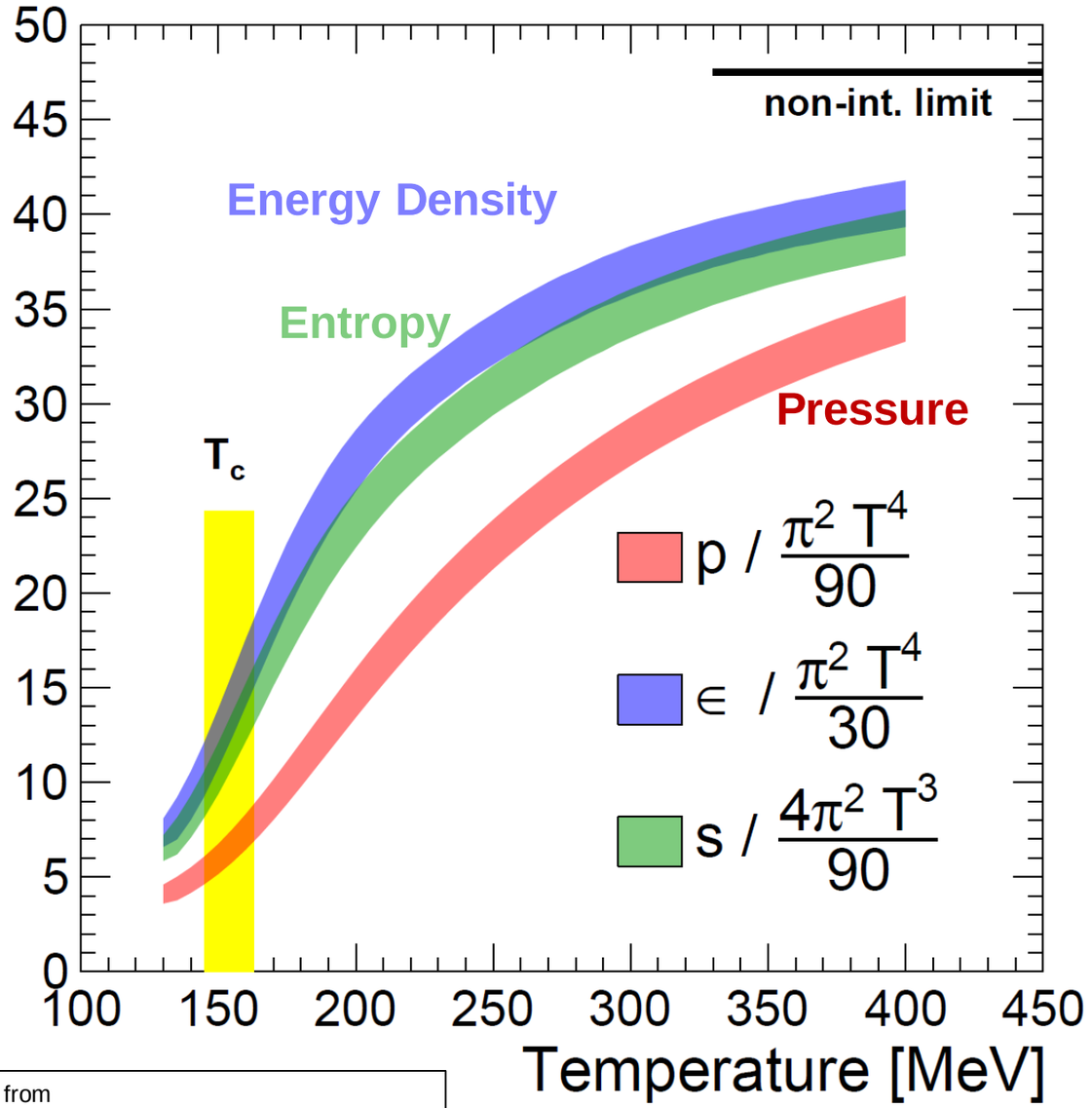

Replotted from
HotQCD Collaboration PRD90 (2014) 094503

How do we extract the medium effect in A+A collisions?

One typical way is to compare A+A data to pp reference measurement

See for instance review from
D. d'Enterria and C. Loizides
Ann.Rev.Nucl.Part.Sci. 71 (2021) 315-44

A+A measurements

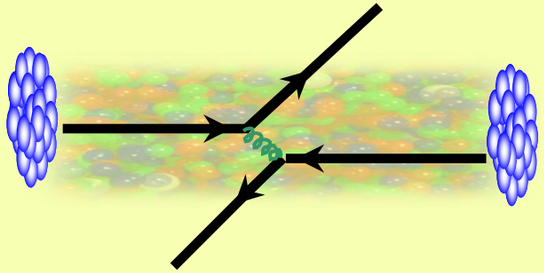

pp reference

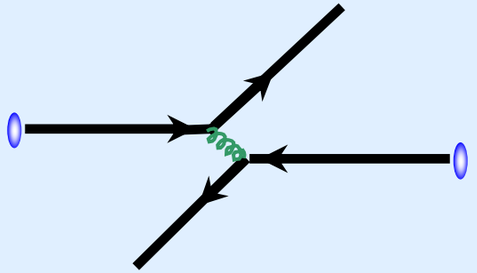

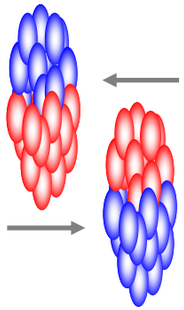

N_{part} → Number of participating nucleons

N_{coll} → Number of binary scatterings

Example:

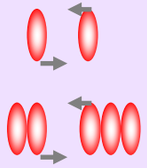

$N_{part} = 2$ $N_{coll} = 1$

$N_{part} = 5$ $N_{coll} = 6$

Evolution of the Early Universe

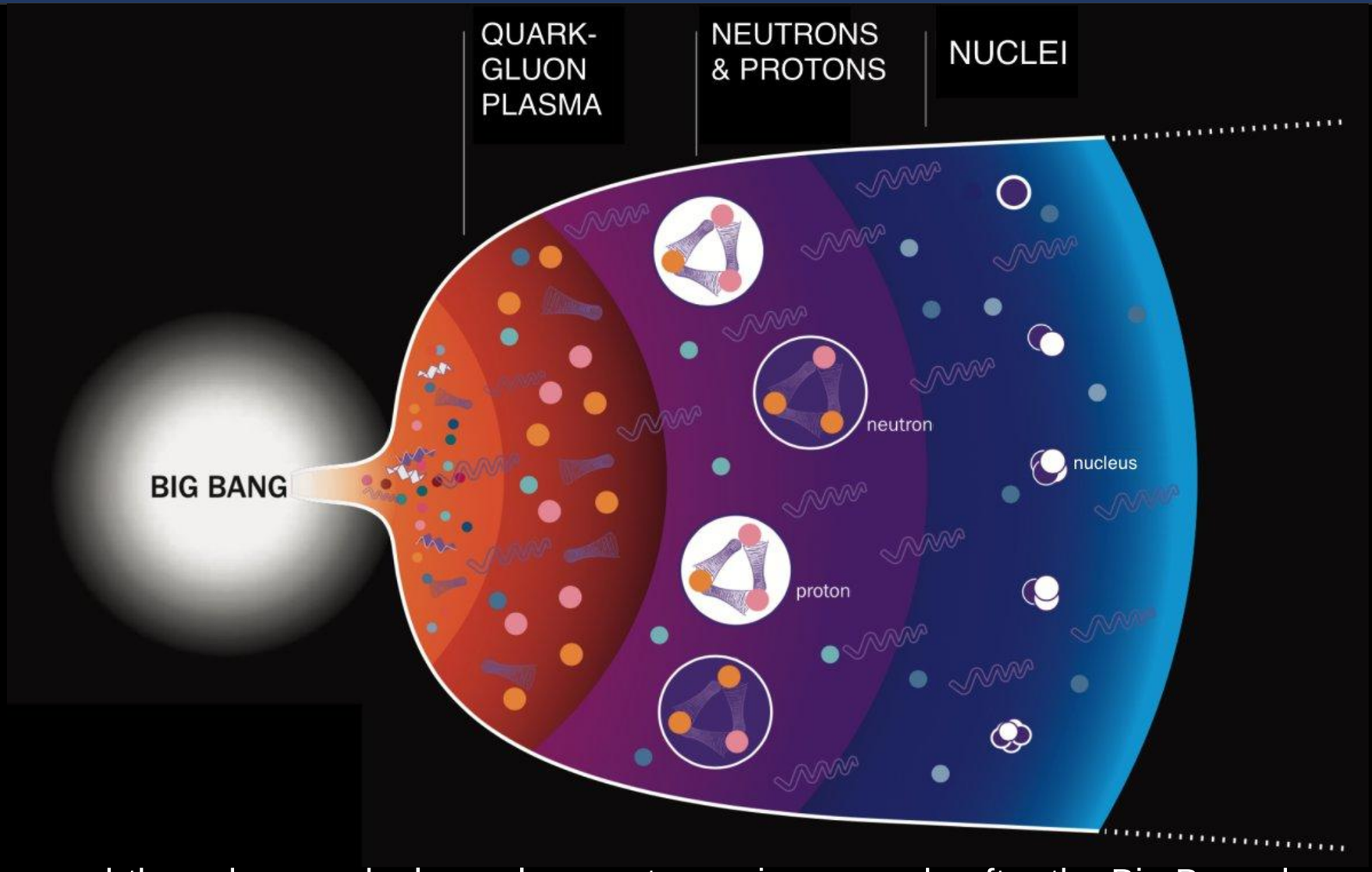

The early universe passed through a quark-gluon plasma stage microseconds after the Big Bang; heavy ion collisions recreate tiny versions of that epoch.

First Order Transition in Matter

Frozen Soap Bubble

https://www.youtube.com/watch?v=_nKxYMlHZoE&feature=youtu.be

High Density Quantum Chromodynamics in Cosmology

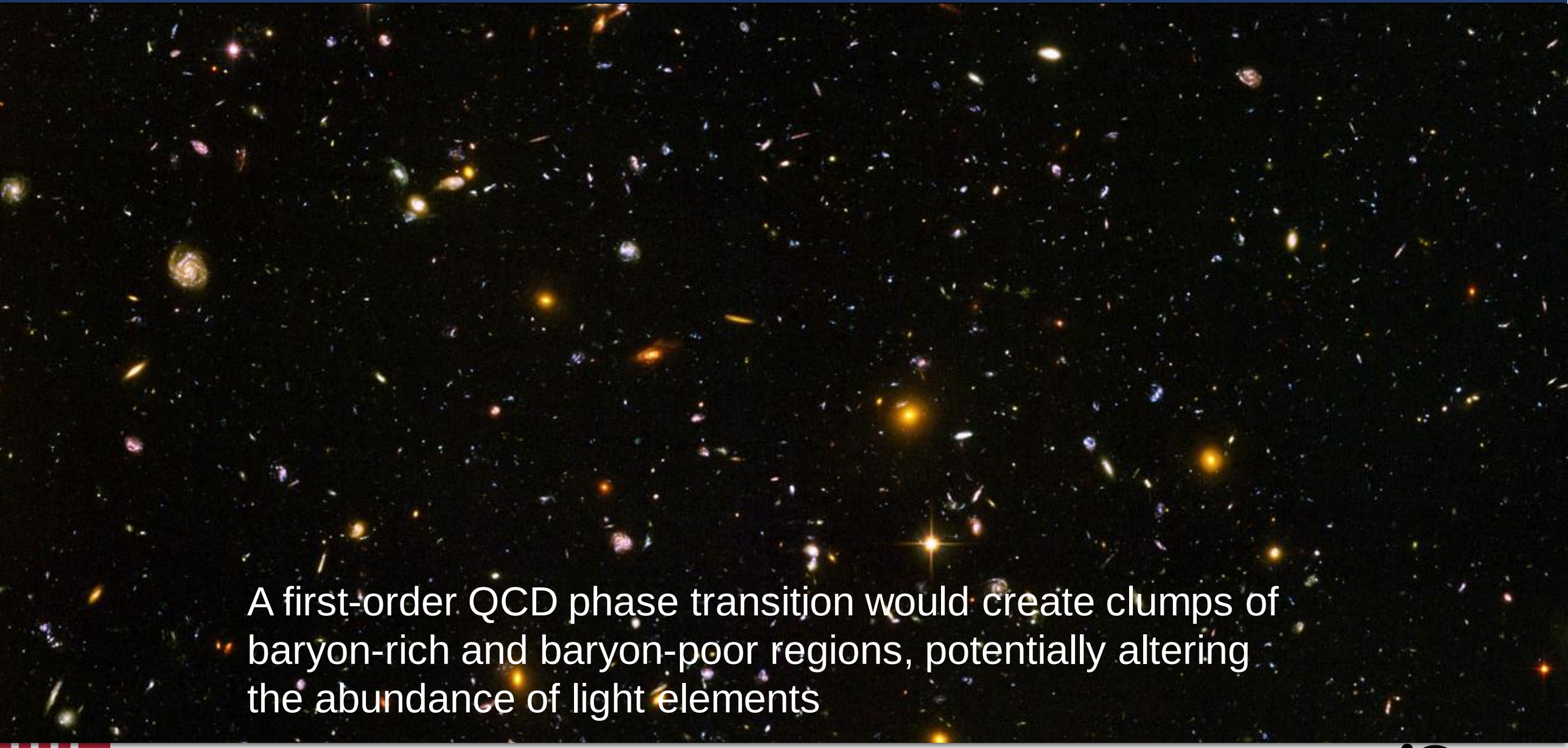

A first-order QCD phase transition would create clumps of baryon-rich and baryon-poor regions, potentially altering the abundance of light elements